Chem Soc Rev

REVIEW ARTICLE

View Article Online
View Journal | View Issue

Surface modification and endothelialization of biomaterials as potential scaffolds for vascular tissue engineering applications

Xiangkui Ren,[abc] Yakai Feng,*[abcd] Jintang Guo,[abc] Haixia Wang,[a] Qian Li,[a] Jing Yang,[a] Xuefang Hao,[a] Juan Lv,[a] Nan Ma*[e] and Wenzhong Li[f]

Surface modification and endothelialization of vascular biomaterials are common approaches that are used to both resist the nonspecific adhesion of proteins and improve the hemocompatibility and long-term patency of artificial vascular grafts. Surface modification of vascular grafts using hydrophilic poly(ethylene glycol), zwitterionic polymers, heparin or other bioactive molecules can efficiently enhance hemocompatibility, and consequently prevent thrombosis on artificial vascular grafts. However, these modified surfaces may be excessively hydrophilic, which limits initial vascular endothelial cell adhesion and formation of a confluent endothelial lining. Therefore, the improvement of endothelialization on these grafts by chemical modification with specific peptides and genes is now arousing more and more interest. Several active peptides, such as RGD, CAG, REDV and YIGSR, can be specifically recognized by endothelial cells. Consequently, graft surfaces that are modified by these peptides can exhibit targeting selectivity for the adhesion of endothelial cells, and genes can be delivered by targeting carriers to specific tissues to enhance the promotion and regeneration of blood vessels. These methods could effectively accelerate selective endothelial cell recruitment and functional endothelialization. In this review, recent developments in the surface modification and endothelialization of biomaterials in vascular tissue engineering are summarized. Both gene engineering and targeting ligand immobilization are promising methods to improve the clinical outcome of artificial vascular grafts.

1. Introduction

Cardiovascular diseases are considered to be one of the serious leading killers in developed countries.[1–3] In the treatment of occluded coronary arteries, coronary artery bypass graft surgery (CABG) is one of the most commonly performed surgeries. Currently, native vein and artery segments remain the best option for peripheral and coronary bypass procedures as they are both compliant and non-thrombogenic. However, their availability is very limited sometimes, which seriously limits traditional transplantation surgeries. Because autologous blood vessels could be occluded or diseased, especially if the patients already suffer from some sort of peripheral vascular disease, these vessels from their own tissues often cannot meet the actual demand for clinical application of small-diameter vascular grafts.

To date, several commercial artificial vascular grafts have been approved by the U.S. Food and Drug Administration (FDA), and millions of patients have benefited from these products. However, low long-term patency and restenosis may occur after bypass surgery and usually lead to implant failure. In particular, small-diameter vascular grafts (diameter < 4 mm) are so far associated with an increased risk of thrombosis and occlusion.[4] Therefore, strategies are highly demanded for the improvement of their compliance and hemocompatibility.[5] Surface modification and endothelialization of vascular biomaterials are two common approaches that are used to resist the nonspecific adhesion of proteins, to improve hemocompatibility and hence to enhance the long-term patency of artificial vascular grafts. Therefore, this review will focus on the recent developments in surface modification and endothelialization of biomaterials in vascular tissue engineering applications.

In the first part of this review, we will introduce various biomaterials for artificial vascular grafts; these biomaterials include biostable polymers, such as expanded polytetrafluoroethylene

[a] School of Chemical Engineering and Technology, Tianjin University, Weijin Road 92, Tianjin 300072, China. E-mail: yakaifeng@tju.edu.cn

[b] Collaborative Innovation Center of Chemical Science and Chemical Engineering (Tianjin), Weijin Road 92, Tianjin 300072, China

[c] Tianjin University-Helmholtz-Zentrum Geesthacht, Joint Laboratory for Biomaterials and Regenerative Medicine, Weijin Road 92, Tianjin 300072, China

[d] Key Laboratory of Systems Bioengineering of Ministry of Education, Tianjin University, Weijin Road 92, Tianjin 300072, China

[e] Institute of Chemistry and Biochemistry, Free University of Berlin, Takustr. 3, D-14195 Berlin, Germany

[f] Department of Cardiac Surgery, University of Rostock, Schillingallee 69, D-18057 Rostock, Germany

5680 | Chem. Soc. Rev., 2015, 44, 5680–5742

This journal is © The Royal Society of Chemistry 2015

(ePTFE), poly(ethylene terephthalate) (PET) and polyurethanes (PU), and biodegradable polymers such as poly(lactide-co-glycolide), poly(ε-caprolactone) (PCL), poly(ethylene glycol)-b-poly(ʟ-lactide-co-ε-caprolactone) and polydepsipeptides. The following part will review the surface modification methods of artificial vascular grafts to improve their hemocompatibility. Surface modifications involve grafting hydrophilic poly(ethylene glycol) (PEG) and zwitterionic polymers or groups, and the immobilization of heparin, gelatin, peptides and other bioactive macromolecules. The last part will introduce the newly developed endothelialization on biomaterial surfaces by special peptides and gene delivery technology (Fig. 1).

1.1 Artificial vascular grafts

For many years, adequate and suitable native vessel segments for revascularization are usually not available in many patients. Tissue engineering holds great promise as a new approach to create replacement tissues such as vascular grafts and heart valves.[6,7] In the twenty-first century, the use of tissue engineering technology to develop complex tissues and organs, such as heart, muscle, kidney, liver and lungs, is still a distant milestone. In tissue engineering, it is highly expected that the biological complexity of the native extracellular matrix (ECM) is fully mimicked in tissue-engineered constructs to which cells can attach, grow, proliferate, migrate, and/or differentiate and further perform diverse biological

Xiangkui Ren

Xiangkui Ren received his PhD degree from Nankai University in 2010. He spent the period of 2007–2009 as an exchange student at The University of Akron in USA under the supervision of S. Z. D. Cheng. In July 2010, He joined Prof. Er-Qiang Chen's group as a postdoctoral researcher in Peking University. He joined Tianjin University as a Lecturer of polymer physics in December 2012. His research focuses on the self-assembly and structures of functional polymers.

Yakai Feng

Yakai Feng received his BSc degree in Chemistry and MSc degree in Polymer Chemistry from Nankai University, his EngD in Organic Chemical Engineering from Tianjin University in 1997, and his PhD at RWTH Aachen University in 2000. He worked as a chemist in ADIAM life science AG and then in the Institute of Polymer Research, GKSS Research Center. Now, he is a professor in the Department of Polymer Engineering and Science, School of Chemical Engineering and Technology, Tianjin University. He is the director of Tianjin University-HZG Joint Laboratory for Biomaterials and Regenerative Medicine. His current research interests focus on surface modification, multifunctional materials and gene delivery.

Jintang Guo

Jintang Guo received her PhD degree from Tianjin University in 1998. She is a Professor at Tianjin University. Her research focuses on functional biomaterials and gene delivery.
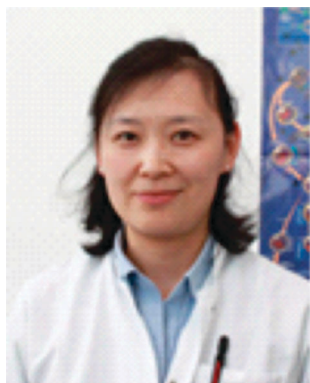
Nan Ma

Nan Ma obtained a BS degree from the Medical School, Jilin University, China, in 1994, MS degree from Peking Union Medical College, China in 1998, and PhD degree from the National University of Singapore, Singapore, in 2003. Her research interests include stem cells for cardiac regeneration and polymer materials for tissue engineering applications.

Wenzhong Li

Wenzhong Li obtained BS and MS degrees from Nanjing University of Aeronautics and Astronautics, Nanjing, China, in 1991 and 1994, respectively, and his PhD degree from the National University of Singapore, Singapore, in 2005. His current research focuses on biomaterials for gene delivery and cardiovascular tissue engineering applications.
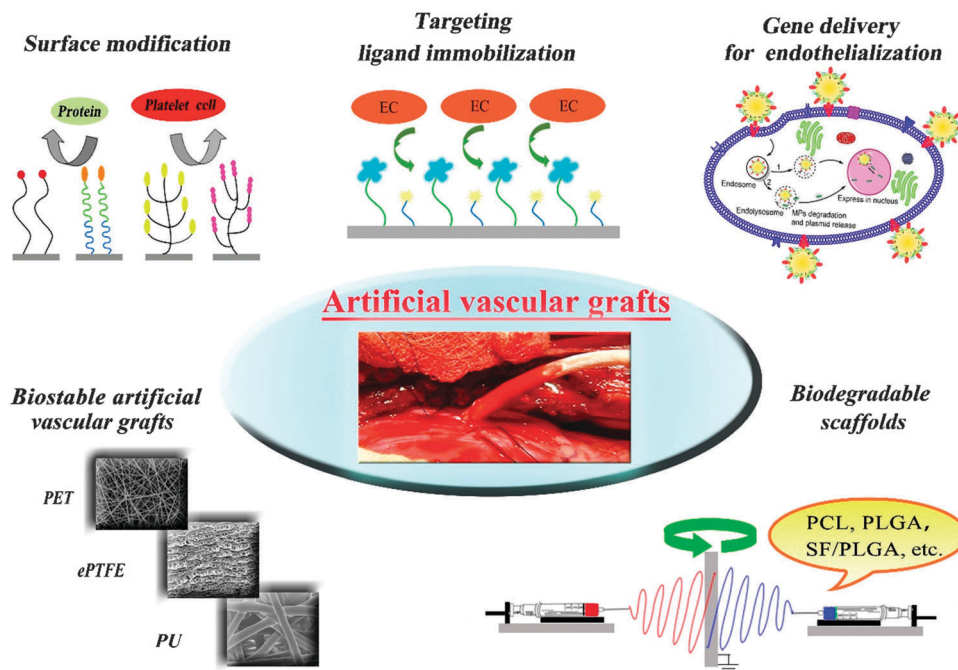
Fig. 1 Surface modification and endothelialization of biomaterials for vascular tissue engineering applications.

functions as living tissues.[8,9] In this way, either biodegradable synthetic scaffolds or biological scaffolds are required to enhance the adhesion and proliferation of cells.

Autologous blood vessels harvested from a patient's own tissues are not often suitable for the clinical application of small-diameter blood vessels. Therefore, various artificial vascular grafts have been widely developed and used clinically, which benefit from novel biomaterials, fabrication technologies, surface modifications, as well as their biomimetic structures and mechanical properties, similar to autologous blood vessels. With the development of biomedical materials, it is an ideal choice to use artificial vascular grafts with a patency rate comparable to that of natural blood vessels. ePTFE, PET and PU, as biostable synthetic materials, have been widely used with great success for bypass conduits with diameters larger than 6 mm.[10] However, they are limited to grafts with inside diameters smaller than 6 mm, especially smaller than 4 mm because of the frequent thrombosis and occlusion in these small-diameter artificial grafts.[11,12] Thus, these grafts face a challenge to oppose the natural coagulation process when they come in contact with blood. Many problems such as thrombogenicity, poor vasoactivity, and inappropriate mechanical properties need to be solved. Artificial scaffolds should be applied to generate small-diameter vascular grafts. The inner layer of such vascular scaffold is designed to create a continuous layer of endothelium to prevent thrombosis and consecutive clogging. Furthermore, bioengineered artificial scaffolds should have adequate mechanical properties approximating to those of autologous blood vessels.

Artificial vascular grafts and scaffolds are usually treated by surface modification such as physicochemical modification and biological modification.[13] The purpose of these modifications is

to modulate platelet responses directly through the modulation of thrombogenic proteins, or by inducing an active endothelium, or through immobilizing antithrombogenic biomolecules onto the surface of artificial vascular grafts. Nanotechnology plays a significant role in the surface modification of cardiovascular implants through biofunctionalization and nanofabrication of biomaterials. This will pave the way for the development of ideal artificial vascular grafts to achieve high long-term patency.[14]

1.2 Hemocompatibility of artificial vascular grafts

Thrombus formation in implanted artificial vascular grafts depends primarily on three factors, namely, the surface properties of the artificial vascular materials, implantation site and blood flow. Artificial vascular grafts act as permanent body implants, which directly contact with blood, and blood flows through their lumen; thus, it is a requirement for them to have and maintain a highly hemocompatible surface throughout their lifetime. Although a large number of anticoagulation treatments have been investigated to design hemocompatible vascular surfaces and adjuvant therapies have been used during angioplastic procedures, thrombosis usually occurs after the implantation of artificial vascular grafts. Because artificial vascular grafts are recognized as foreign by the human body, they can induce the activation of blood coagulation systems and inflammatory reactions. These blood responses are caused by the natural response of the host defense mechanism against the foreign surface of artificial vascular grafts.[15] Pathological processes such as microthrombi generation or thrombosis, hemodynamic instability, bleeding complications and organ damage, are caused by the inadequate control of natural inhibitors.

In general, the primary interaction that occurs at the interface between human blood and biomaterials is nonspecific protein adsorption. Multistep and interlinked processes, which include platelet adhesion, activation and clot formation, may be initiated by a small amount of fibrinogen adsorbed on a biomaterial surface. When foreign materials, such as vascular implants, are in contact with human blood for a long time, these disadvantages are seriously aggravated.[16,17] Therefore, high resistance to non-specific protein adsorption is one of the crucial requirements for synthetic artificial vascular grafts. Thus far, small-diameter vascular grafts often cause failure in clinical applications, which is mainly due to the early thrombotic occlusion of these vascular grafts. Hence, it is necessary to develop artificial vascular grafts that adsorb minimally or do not adsorb thrombogenic blood proteins on their surface.[5] Furthermore, their surfaces should not interact with coagulation factors. Based on these considerations, various approaches have been developed to modify the surface of artificial vascular grafts such as covalently linking heparin, antiplatelet agents, thrombolytic agents and hydrophilic polymers.[18] A great number of investigations are attributed towards the construction of hemocompatible surfaces using many surface modification techniques. As a general rule, surface modification is considered to be an effective way to combine hydrophilic, non-fouling materials onto the surfaces of a wide range of hydrophobic substrates in order to improve hemocompatibility.

To date, many surface modification methods have been used to enhance the hemocompatibility of artificial vascular grafts. One of the most significant methods is anticoagulant surface modification by incorporating anticoagulants onto biomaterial surfaces to inhibit intrinsic thrombogenicity. For example, heparin has been coated on several types of medical devices, including extracorporeal circuits for cardiopulmonary bypass[19,20] and stents.[21] It has been proven that heparin can successfully enhance surface hemocompatibility and improve patient outcome.[22–24] In addition to incorporating anticoagulants, gelatin is also usually used in surface modification because it is a natural degradable polymer that is derived from collagen. Gelatin has many advantages such as biodegradability, biocompatibility and its commercial availability because of its low cost. Furthermore, gelatin is non-immunogenic compared to its precursor and can promote cell adhesion, migration, differentiation and proliferation.[25] Therefore, gelatin scaffolds and microspheres have been widely explored for medical applications such as tissue engineering and drug delivery systems.[26] Additionally, zwitterionic polymers have also attracted much attention for use in the new generation of blood inert materials due to their good plasma protein resistance.[27–30] It is well known that hydrophilic zwitterionic polymers have both a positively and a negatively charged moiety in the same segment side chain, which could bind a significant amount of water and lead to a strong repulsive force to proteins. Therefore, as one of the most used surface modification methods, the immobilization of zwitterionic functionalities onto artificial vascular grafts is considered to have a perfect promising future in improving surface hemocompatibility.[31] Another hydrophilic surface modification method involves the covalent grafting of PEG to improve surface hemocompatibility.

Hydrophilic PEG has the ability to bind many water molecules to form a surface hydration layer, which can effectively resist nonspecific protein adsorption.[32]

Hydrophilic surface modification can improve surface hemocompatibility and benefits from anti-nonspecific protein adsorption, but it should be noted that highly hydrophilic surfaces can also limit or completely disable cell attachment and spreading. Because highly hydrophilic surfaces bind cell adhesion-mediating molecules with relatively weak forces, this could lead to the detachment of these molecules especially when they bind a large number of cells. On the other hand, highly hydrophobic surfaces adsorb proteins in rigid and denatured forms, thus hampering cell adhesion. Therefore, a moderately hydrophilic surface is beneficial for optimal cell adhesion because of the adsorption of cell adhesion mediating molecules in an advantageous geometrical conformation, which enables specific sites on these molecules to be accessible to cell adhesion receptors.[33–35]

1.3 Endothelialization of artificial vascular grafts

As mentioned above, artificial vascular grafts (>6 mm) have been widely used in clinical treatments; however, small-diameter artificial grafts still remain a great challenge. Native blood vessels are usually composed of three layers: the tunica intima, tunica media, and tunica adventitia. The tunica intima consists of monolayer endothelial cells lining the lumen of the vessel, as well as a subendothelial layer made up of mostly loose connective tissue. As the inner lining of natural blood vessels, endothelial cells (ECs) represent a physical interface between blood and surrounding tissue, and they also maintain the hemostatic–thrombotic balance that regulates inflammation and angiogenesis. It is proposed that the endothelialization of artificial vascular grafts that are seeded with autologous vascular endothelial cells should help in improving the patency rates of these grafts. Unfortunately, artificial vascular grafts cannot spontaneously endothelialize *in situ* due to low endothelial cell initial attachment, cell spreading and growth. Therefore, biomaterials as well as artificial vascular grafts that are endothelialized before implantation are recommended as the most practical and potential approach for creating a continuous endothelial layer on material surfaces.

For several decades, the use of endothelialized biomaterials for tissue engineering and regenerative medicine has been paid extensive attention. Endothelialized biomaterials involve various materials including ECM-based proteins, surface modified synthetic polymers, biodegradable scaffolds and synthetic peptides. Both ECs adhered to artificial vascular grafts and rapid endothelialization are intended to address the serious problems associated with thrombosis and low long-term patency.[36] In order to treat injuries and defects in blood vessels, ePTFE and PET bypass grafts have been developed and used in clinical applications. However, graft patency is limited for small-diameter (<4 mm) artificial vascular grafts due to thrombosis and the lack of endothelialization. Adhesion and agglomeration of platelets occur followed by EC detachment from endothelialized grafts when exposed to circulating blood, which is the main reason for thrombosis. Thus, it is

This journal is © The Royal Society of Chemistry 2015

Chem. Soc. Rev., 2015, **44**, 5680–5742 | **5683**

necessary to accelerate EC attachment and proliferation on the internal surface, especially, under blood flow, to keep good long-term patency. Actually, the endothelialization of artificial vascular grafts has been extensively investigated as an ideal way to enhance their biocompatibility. Hydrophilic surfaces tend to enhance the early stages of cell adhesion, proliferation and differentiation compared with hydrophobic surfaces. Moreover, extremely high surface energy promotes cell adhesion but hinders cell motility and functions.[37,38] Therefore, the comprehensive design of surface hydrophilicity plays a significant role in EC adhesion, proliferation, migration and endothelialization. Furthermore, endothelialized surfaces with non-thrombogenic and non-adhesive interfaces can effectively prevent occlusion.[39–41] Consequently, rapid endothelialization is a prerequisite for artificial vascular grafts.

In order to induce the rapid and complete endothelialization of vascular graft surfaces, many bioengineering approaches have been developed, either prior to implantation or by accelerating the *in situ* endothelialization of vascular grafts. In particular, a number of capturing ligands, including peptides, antibodies, magnetic molecules, oligosaccharides and aptamers, have been investigated to modulate cell attachment and proliferation on artificial vascular grafts.[42–44] Usually, these artificial vascular grafts are pretreated with endothelial cell-specific binding molecules, so that the attachment and retention of ECs on them are significantly enhanced.[45,46] In order to improve the biocompatibility and EC adhesion of biomaterials, many peptide sequences have been discovered and grafted onto artificial vascular grafts such as REDV,[47] RGD[48] and GRGDSP from fibronectin, IKLLI, IKVAV,[49] PDSGR and YIGSR[50,51] as laminin-derived recognition sequences, and DGEA as a collagen type I derived sequence. It has been proven that these peptide ligands have the ability to interact with cell receptors directly. Among these peptides, the RGD peptide has been widely used in the modification of biomaterials to enhance the cell adhesion. For instance, RGD-containing ligands promote cell adhesion on the surface of RGD-modified materials *via* cell-specific combination with integrin receptors in the plasma membrane.[52] Unlike the general adhesive property of the RGD peptide, another kind of peptide, *i.e.* REDV, is well known for its ability to initiate cell-specific binding to ECs. Ji *et al.* have already demonstrated that a surface coating of carboxybetaine-REDV could enhance the competitive growth of ECs while inhibiting the adhesion, proliferation and migration behavior of smooth muscle cells (SMCs).[53] Moreover, a variety of angiogenic factors, such as vascular endothelial growth factors (VEGFs),[54] fibroblast growth factors (FGFs), hepatocyte growth factors (HGFs), angiopoietin-1 and matrix metalloproteinase (MMP),[55] have been proven to play a critical role in angiogenesis by stimulating the migration and proliferation of ECs. Among all these pro-angiogenic factors, VEGF is the most powerful growth factor to promote angiogenesis. However, a high dose of VEGF tends to produce highly fenestrated, immature capillaries that are similar to capillaries in tumor tissue.[56] Compared with VEGF, the basic fibroblast growth factor (bFGF) is not a strong pro-angiogenic factor, and it tends to produce more mature vessels.[57] Yuan *et al.* have already demonstrated that the dual-release of VEGF and platelet-derived growth factor (PDGF) is a feasible approach for small-diameter vascular regeneration.[58] In addition, gene delivery technology has been used to promote the endothelialization of artificial vascular grafts. In addition to the VEGF gene, a human C2H2-zinc finger gene, *i.e.* the ZNF580 gene, has already been proven to play an important role in the intervention of atherosclerosis and the process of migration and proliferation of ECs.[59] The gene complexes of ZNF580 can enhance the proliferation and migration of ECs *in vitro*, which might induce rapid endothelialization on tissue engineering scaffolds and vascular grafts.[60,61]

2. Biomaterials for artificial vascular grafts

Many types of natural polymers and synthetic polymers that function as biomaterials have been investigated and used to prepare artificial vascular grafts. Natural polymers including collagen, fibroin, gelatin, and decellularized vessels and tissues usually suffer from different properties from different sources and different batches. Besides, they may be contaminated with bacteria or viruses and might cause antigenicity. In contrast, synthetic polymers can be easily controlled from batch to batch. They have exact chemical structures and adjustable mechanical properties. Especially, some synthetic biomaterials exhibit high hemocompatibility and processability. For example, PET, poly(tetrafluoroethylene) (PTFE), PU, biodegradable polyesters and poly(ester amide)s have been used to prepare artificial vascular grafts and scaffolds as shown in Fig. 2. For this application, a certain level of porosity is necessary; moreover, the wall of artificial vascular grafts should prevent the leakage of blood. Furthermore, the inner lumen surface of artificial vascular grafts should have high hemocompatibility and the ability to enhance rapid endothelialization.[62]

2.1 Polyethylene terephthalate

Dacron® (poly(ethylene terephthalate), PET) was first produced industrially worldwide in 1957 by DuPont. PET exhibits many intrinsic properties such as transparency, solvency, crease resistance, good barrier properties, resistance to fatigue, and high tenacity. It has been commonly used in various fields, especially in artificial vascular grafts.

PET has been used to manufacture large-diameter artificial vascular grafts, usually by the knitting or weaving technology (Fig. 3). In order to control the degree of porosity, the effect of various knitting parameters on different properties has been investigated. PET artificial vascular grafts need to be treated with an autologous thrombotic matrix before implantation, which is known as preclotting. They have already been proven to exhibit good performance in large-diameter blood vessel (≥6 mm) applications.

More recently, electrospun PET nanofibers have been prepared using the electrospinning technology and applied to blood vessel engineering (Fig. 3).[63] Catalani *et al.*[64] electrospun a co-solution of PET and collagen to obtain artificial vascular grafts with excellent mechanical and biological properties. In addition to the electrospinning technology, the melt blowing
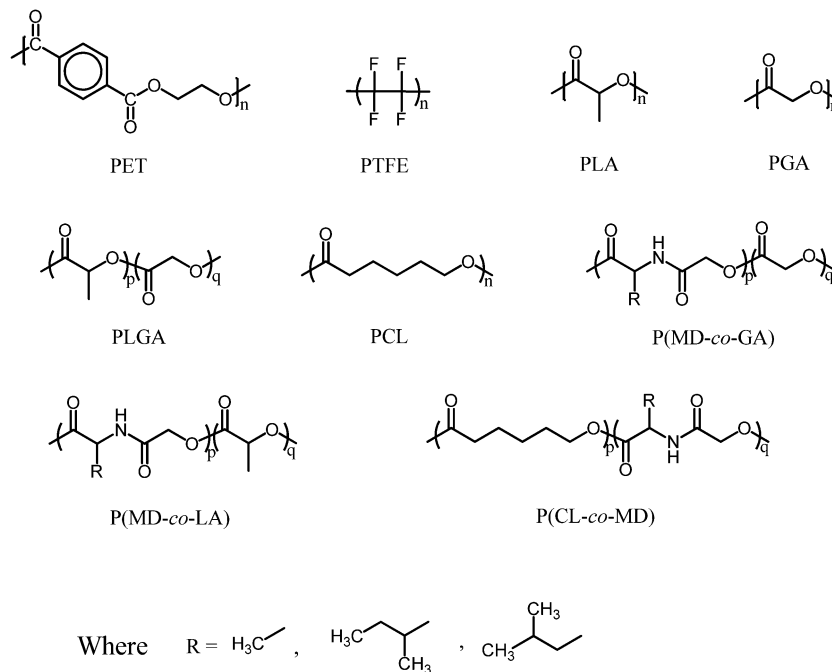
Fig. 2 Chemical structures of biomaterials for artificial vascular grafts and scaffolds.
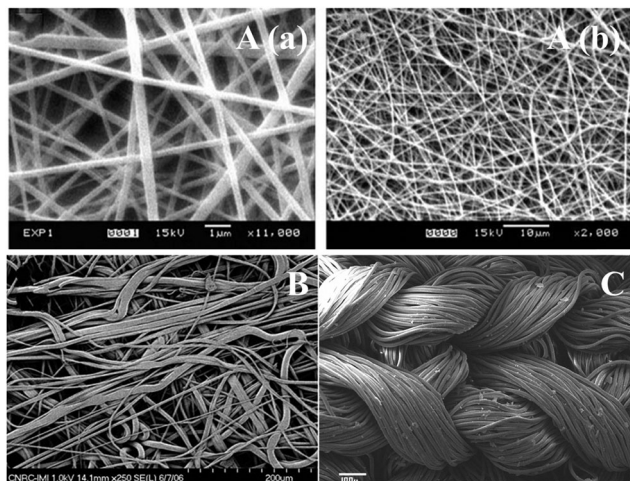

Fig. 3 SEM micrographs of PET grafts prepared by different technologies. (A) Electrospinning technology. Reproduced with permission from ref. 63. Copyright 2005, Elsevier. (B) Melt blowing method. Reproduced with permission from ref. 65. Copyright 2011, John Wiley and Sons. (C) Weaving technology.

method has also been developed as another technology to produce non-woven PET fibers. These PET fibrous webs can be stacked by means of a consolidation technique through the variation of fiber-diameter distribution and number of consolidated web stacks (Fig. 3).[65] The fibrous webs show burst pressure and compliance, which are very similar to those of native arteries. Web-scaffolds with the fiber diameter range of 1–5 μm and pore size range of 1–20 μm are suitable for the growth of human brain ECs and aortic SMCs. Note that one of the essential pre-conditions for further clinical application is

the ability of these non-woven PET scaffolds to withstand sterilization. Low temperature plasma sterilization has been found to be more suitable for non-woven PET fibers than the ethylene oxide method.[66]

The successful application of PET as large-diameter artificial vascular grafts mainly benefits from its high reliability and good long-term performance. However, some structural defects may lead to blood leakage and even the formation of a graft rupture or false aneurysm. Moreover, surface thrombogenicity can be caused by an unfavorable healing process due to the lack of ECs and anastomotic intimal hyperplasia, which is induced by hemodynamic disturbances.[67] In order to address these problems, coating and surface modification are usually used to modify PET grafts by using adhesion proteins,[68] dermatan sulfate,[69] FGFs,[70] carboxymethyl dextran,[71] amine-rich thin plasma-polymerized coating,[72–74] polysaccharides[10,75,76] or polysaccharide sulfates,[77,78] O-carboxymethylchitosan,[79] functionalized carbon nano-particles[80] and chondroitin sulfate.[81] Plasma and NaOH treatments[82] are usually performed as pretreatment methods to modify the surface of PET grafts with functional groups for linking or crosslinking bioactive molecules. For example, PET is first treated by an amine-rich plasma method and then coated by chondroitin sulfate to enhance the adhesion of ECs while decreasing platelet adhesion.[81] It is important to note that the aminolysis reaction induces chain scissions, which may reach the bulk PET and sometimes strongly impact its mechanical properties. To reduce these negative effects, an aminated long-chain polymer, i.e. polyvinylamine, is used as an aminolysis reagent to introduce amine (–NH$_2$) moieties only on the top surface of PET. Thus, the surface reactive moieties on PET can be obtained for further functionalization of PET grafts with bioactive molecules. Their bulk mechanical properties

can be preserved, which is beneficial for artificial vessel graft application.[83]

Except for surface thrombogenicity, the aging of PET vascular grafts is another unavoidable problem, and it is deservedly related to human metabolism.[84] Furthermore, it depends not only directly on the duration of the *in vivo* implantation but also on storage conditions.[85]

2.2 Expanded poly(tetrafluoroethene)

PTFE is a fully fluorinated polymer, which is prepared from tetrafluoroethylene (CF_2=CF_2), and was discovered in 1938 by Plunkett.[86] PTFE shows non-adhesive characteristics due to its low surface energy (20 mN m^{-1}). It has been reported to be used as an artificial heart valve because of its good performance and long-term biostability during implantation.

A type of porous microstructure, which is composed of nodes interconnected by fibrils, can be manufactured from PTFE by an expansion process at temperatures above its melting point (Fig. 4) and this product is well known as expanded PTFE (ePTFE). Since an ePTFE graft was introduced in the early 1970s for peripheral surgery, it has been widely used as vascular grafts by several commercial companies worldwide such as W. L. Gore and Associates, Atrium Medical Corporation, C. R. Bard, Inc. and ZEUS®.[87] The surface of ePTFE vascular grafts is highly thromboresistant and biostable at implantation, and *in vivo* results have demonstrated that these grafts can keep their structures and functions for up to 6.5 years after implantation.[86] More importantly, no major tissue inflammatory responses have been found. Both PET grafts and ePTFE grafts have been implanted in femoropopliteal bypass with no significant differences in midterm graft patency at 5 years (49.2% *vs.* 38.4%).[88] For the treatment of critical limb ischemia and nonhealing foot wounds, ePTFE bypass has been proven to be a cost-effective option when a good-quality great saphenous vein is not available.[89] Although these grafts have been successfully implanted as large-diameter vascular grafts in clinic applications, they are not very good as small-diameter grafts because of the foreign surface and compliance mismatches that usually lead to re-occlusion *in vivo*, as well as low patency in long-term applications. Thus, the development of novel small-diameter vascular grafts (2–5 mm diameter) still remains a big clinical challenge.[90] The lack of sufficient and continuous endothelialization of artificial vascular grafts becomes the main barrier for the success of the implantation of vascular grafts. Many a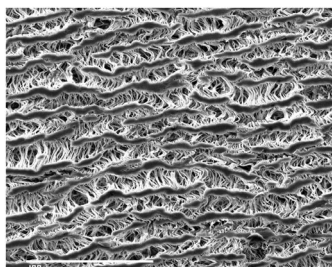ttempts to address this problem have been made. For example, carbon coating[91] and fibrin glue with growth factors[92] are not fully successful to improve patency rates, but the carbon coating for ePTFE positively affects its surface biocompatibility and increases the adhesion and proliferation of vascular smooth muscle cells (VSMCs) compared with pristine polymer foils.[93] Moreover, laminin type 1 modified surfaces can accelerate both the neovascularization and endothelialization of porous ePTFE vascular grafts.[94] With the reactive plasma treatment, the hydrophobic surface of bare PTFE changes to a hydrophilic surface due to the formation of carbonyl groups on its surface.[95]

There has been a controversy over the past decades about whether ePTFE is better than PET or not for the choice of prosthetic graft materials. However, it is really difficult to interpret these studies due to a number of problems in the design of the investigations, which include short follow-up time, the inclusion of both supra- and infra-geniculate bypasses and the inclusion of different graft diameters.[62,96] For the supra-geniculate femoro-popliteal allograft bypass grafting, the question about whether an ePTFE or a PET graft should be used has been answered. During prolonged follow-up (10 years), PET femoro-popliteal bypass grafts have superior patency compared with those of ePTFE grafts.[96] In order to combine the advantages of PET and ePTFE, fluoropassivation and gelatin coating have been applied to PET vascular grafts. The fluoropassivation increases the surface fluorine content to 28–32% and decreases the hydrophilicity; however, this fluoropolymer cover-layer is not stable under the hostile biological environment.[97]

2.3 Polyurethanes

Polyurethanes (PUs) are well known as a type of commercial biomaterial due to their favorable biocompatibility and excellent mechanical properties. Although polyether-based polyurethanes are more stable than polyester-based polyurethanes (PEU) and poly(carbonate urethanes) (PCUs) in hydrolytic degradation tests *in vitro*, they degrade significantly faster under enzymatic attack and oxidative environments *in vivo*, and especially under high stress. Thus polyether-based polyurethanes cannot be used to prepare medical devices for long-term implantation; however, PEU and PCUs are widely applied as biomaterials for applications in drug release systems, scaffolds, catheters and artificial vascular grafts.[98–102] Though the initial animal trials of PEU are very attractive, the hydrolytic instability of PEU has proven to be a drawback.[62]

PCUs have been developed to address the instability problem of PUs. Compared with PEU, PCUs are relatively stable *in vivo*. Furthermore, PCUs can provide relatively beneficial hemocompatibility and excellent mechanical properties. Accordingly, PCUs have been used in various biomedical applications such as catheters, vascular grafts, blood bags and artificial hearts. Importantly, PCU artificial vascular grafts exhibit approximately similar mechanical properties and compliance of natural blood vessels. Both the spraying and electrospinning technologies have been used to make PCU artificial vascular grafts. As shown in Fig. 5A, their fibers are non-uniform, and many islands are found in the inner surface of PCU artificial vascular grafts that were prepared by the spraying method. Although the fiber diameter can be controlled by the spraying parameters, this
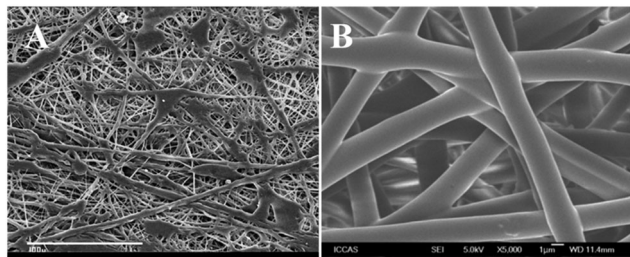

Fig. 4 SEM micrograph of an ePTFE graft.

5686 | *Chem. Soc. Rev.*, 2015, **44**, 5680–5742

This journal is © The Royal Society of Chemistry 2015

Fig. 5 SEM micrographs of PCU artificial vascular grafts prepared by the spraying technology (A) and electrospinning technology (B).

non-uniformity and islands cannot completely be avoided. The large-diameter fibers and islands provide the PCU artificial vascular grafts with high mechanical properties. Moreover, Khorasani et al. fabricated small-diameter vascular grafts with a 4 mm diameter and 0.3–0.4 mm wall thickness using the spraying phase inversion method, which are porous and have a layer-like morphology. The pore size, percentage and morphology of porosity can be controlled by adjusting the distance between spray guns and rotating mandrel, as well as rotational speed.[103]

The electrospinning technology is a versatile method for the formation of films and tubes with nano-/micro-meter fibers.[104] Electrospun fibers have many advantages over conventional fibers and nonwoven mats. The electrospinning technology has been applied to prepare fibrous grafts from PCU solutions.[105] Uniform nano- or micro-fibrous grafts with smooth fibers and controllable fiber diameters are easy to prepare. No beads, bundles or patches are found on the fiber surface (Fig. 5B). The morphology of fibers strongly depends on the process parameters, particularly solvent types and PCU concentration. At room temperature, the Young's modulus (E) of the electrospun grafts is found to be 0.9–1.9 MPa, which mimics the elastic characteristics of native arteries. Furthermore, the mechanical properties and morphology of PCU fibrous membranes do not show any change after degradation in phosphate buffer solution (PBS) for 3 months. The high biostability of PCU fibers is beneficial for vascular grafts. More importantly, PCU small-diameter vascular grafts promote faster luminal endothelialization, induce less chronic intimal proliferation, and produce a significantly thinner neointima than ePTFE grafts.[106] In addition, they can also lead to increased EC coverage in comparison with a PTFE-covered surface.[107]

The formation of a thrombus is mainly caused by platelet adhesion and the failure of rapid endothelialization, which is an enormous challenge for artificial vascular grafts. If artificial vascular grafts remain with a bare surface even after long-term implantation in the human body, the surface is not covered by an endothelium layer, which does not affect the clinical performance of large-diameter prostheses in aortic or iliac positions. However, this will result in the high failure rate of small- to medium-sized grafts.[108] Thus many efforts focus on the synthesis of novel biocompatible PUs, physical modification, and chemical surface modification of PUs to improve their hemocompatibility and enhance endothelialization. We will review the synthesis of biocompatible PUs here, whereas their surface modification will be introduced in Sections 3 and 4.

PUs are generally prepared from various diisocyanates, polyols and chain extenders or crosslinkers. This gives scientists many raw materials to choose from as well as many synthetic methods to synthesize biocompatible PUs for artificial vascular graft applications. A novel nanocomposite polymer, POSS–PCU, has been developed by covalently attaching a chemically robust polyhedral oligomeric silsesquioxane (POSS) nanocage to the PCU backbone with the aim to improve the poor in vivo biostability of PUs.[109] The beneficial effects of POSS nanoparticles (NPs) and PCUs, which include excellent antithrombogenicity and mechanical properties, allow POSS–PCU to be a suitable biomaterial for artificial vascular grafts. This POSS–PCU nanocomposite graft can resist hydrolytic and oxidative degradation both in vitro and in vivo.[109,110] Following subcutaneous implantation in an ovine model for 36 months, no sign of degradation or inflammation was observed. Moreover, with improved stability and hemocompatibility, POSS–PCU grafts implanted in the carotid artery of senescent sheep showed high long-term performance and displayed comparable functional properties to native arteries.[111] The patency rate of the POSS–PCU grafts was found to be 64% and they were free from intimal hyperplasia, aneurysm and calcification. These encouraging results indicate that POSS–PCU vascular grafts might be a promising option for clinical use.[112]

Considering peptide biofunctions, West et al.[113] synthesized YIGSR peptide and PEG-modified polyurethaneurea by the incorporation of the GGG**YIGSR**GGGK peptide sequence as a chain extender and PEG as a soft segment in the polymer backbone. They further incorporated both PEG and a diazeniumdiolate NO donor into the backbone of polyurethane to improve thromboresistance. The YIGSR modified PUs showed enhanced EC proliferation and decreased platelet adhesion compared with PU-PEG.[114] The laminin-derived cell adhesive peptide sequence, YIGSR enhances EC adhesion and migration; moreover, NO release is beneficial for EC proliferation. Recently, Masters et al.[115–117] modified PUs using hyaluronic acid (HA) and prepared grafts thereof. These PU-HA grafts reduce protein adsorption, platelet and bacterial adhesion, as well as fibroblast and macrophage proliferation while allowing the retention of both ECs and vascular-appropriate mechanical properties. More importantly, the HA density on bulk modified PUs remains unaltered after exposure to physiological conditions. Thus, they are able to fully retain the ability of EC adhesion and proliferation, which are beneficial for the formation of a morphologically healthy, confluent monolayer of ECs.

In addition, many studies involve the introduction of zwitterionic groups as side chains to modify PUs.[118] In our previous study, we used sulfoammonium zwitterionic polymers[119] and sulfoammonium zwitterionic PEG to modify PCU.[120] The PEG chain acts as a spacer to link the sulfoammonium zwitterion, and both of them can improve surface hydrophilicity and hemocompatibility. Wagner et al.[121] developed a series of biodegradable poly(ester urethane)urea (PEUU) elastomers with different amino contents (PEUU-NH$_2$ polymers) and then conjugated carboxylated phosphorylcholines to these PEUU-NH$_2$ polymers. They found that these materials significantly reduced platelet adhesion and inhibited rat VSMCs proliferation. The PEUU-NH$_2$

This journal is © The Royal Society of Chemistry 2015

Chem. Soc. Rev., 2015, 44, 5680–5742 | 5687

polymers offer great potential to address a variety of design objectives. Interestingly, in order to induce zwitterionic phosphorylcholine (PC) groups to aggregate at PUs surface, Fu et al.[122] designed and synthesized three monomers containing a fluorinated tail and/or PC groups, and then grafted them onto PUs via the end-capping method. The fluorocarbon chains drive the PC groups to arrange or assemble preferentially at the PU surface, and their synergistic effect contributes to improved hemocompatibility.

2.4 Poly(ε-caprolactone)

As mentioned above, PET, PTFE and PU are excellent biomaterials that have been used to prepare artificial vascular grafts. All of them are non-degradable polymers and can be implanted for long-term bioapplication. However, they were not initially designed for tissue engineering applications. Ideal biomaterials for vascular tissue engineering should have excellent biocompatibility and appropriate biodegradability to minimize inflammatory response, and they should also promote endothelialization. Therefore, compared with non-degradable materials, biodegradable materials as tissue engineering scaffolds have received particular attention because they can avoid reoperation and are of great importance to help improve the chances of successful implantation.[123,124] Especially, these biodegradable scaffolds are beneficial for EC seeding, adhesion and proliferation, endothelialization, tissue engineered vascular grafts, and blood vessel regeneration as well as its reconstruction.[125,126] Additionally, these biodegradable polymers can be easily processed to give various scaffolds with controllable pore size, multilayer structures or other complete structures. Therefore, a number of degradable scaffolds have been developed and used as vascular grafts.

PCL is a kind of semi-crystalline aliphatic polyester. PCL with various molecular weights and chemical structures are usually synthesized via the ring-opening polymerization (ROP) of ε-caprolactone (CL) with alcohols, amines or other initiators in the presence of an organic stannous compound as a catalyst.[127] PCL is well known for its low biodegradability, high biocompatibility and good drug permeability. Thus, it is very suitable for the design of long-term implantable devices and systems. PCL grafts show cell adhesion, growth and viability, as well as high mitochondrial activity for cells tested with L929 mouse fibroblasts.[128] Furthermore, it has been proven to have the potential utility as a suitable scaffold in vascular tissue engineering through the reactive oxygen species content analysis of ECs and SMCs.[129] Briefly, PCL has been widely demonstrated to be used as a suitable scaffold both in vivo and in vitro. However, the implantation of small-diameter vascular grafts of PCL can easily fail due to thrombosis and intimal hyperplasia. Thus, the rate of its long-term patency is not satisfactory.[130] Moreover, PCL generally has poor cell affinity due to its high hydrophobicity and lack of cell-binding signals. Thus, hydrophilicity improvement and the bioactive surface design of PCL grafts are significantly important for its application in tissue engineering.[131] Great effort has been focused on these points, which have been addressed. Apart from surface modification

that will be described in Section 3, we mainly review some other methods to improve the biofunctions of PCL grafts here.

Recently, PCL was covalently conjugated with heparin using 1-ethyl-3-(3-dimethylaminopropyl)-carbodiimide (EDC)–N-hydroxysuccinimide (NHS) chemistry, and subsequently electrospun into small-diameter tubular scaffolds and loaded with fibroblast growth factor-2 in aqueous solutions. The released heparin is effective in preventing the proliferation of VSMCs in culture; otherwise, their proliferation can cause graft occlusion and failure.[132] These heparin modified PCL vascular scaffolds could significantly improve cell morphology on the surface and they benefit from the growth factor.[133]

Composite scaffolds and multilayered scaffolds are fascinating directions to mimic natural vascular tissue and many studies have been performed to evaluate the biofunctions of PCL grafts in vitro and in vivo. To improve the tolerance to the physiological vascular environment, Yoo et al.[134] developed a type of graft composed of PCL and collagen, which possessed enough biomechanical properties to resist a high degree of pressurized flow over a long-term period. When the PCL/collagen grafts were implanted in New Zealand white rabbits, they were able to retain their structural integrity over 1 month. Furthermore, upon retrieval, the grafts continued to maintain their biomechanical strength, which was comparable to native arteries.[135] In addition, Bowlin et al.[136] fabricated a three-layered electrospun matrix comprised of PCL, elastin and collagen to mimic native arterial architecture. The compliance values of these three-layered grafts ranged from 0.8% to 2.8%/100 mm Hg and the uniaxial results demonstrated an average modulus range of 2.0–11.8 MPa. Both their modulus and compliance data displayed values within the range of native arteries. Through optimal chemical compositions, weight ratio of PCL and gelatin, peptides or other biopolymers, as well as surface modification methods, the inner layer can be fabricated so that ECs can preferentially attach and proliferate onto its surface, and then create a confluent, non-thrombogenic surface to prevent or significantly decrease intimal hyperplasia.[136–138] The middle layer can be tailored to have low modulus, and provide the distension required for proper compliance, which is biomimetically similar to native arteries. The outer layer is made from high elastic polymers to ensure enough mechanical properties of the graft so that it avoids overextending itself.[136] Usually, PUs with high elastic and mechanical properties can be electrospun to form the outer layer.[139,140]

Although the electrospinning technology has been widely used to fabricate small-diameter vascular grafts, these electrospun grafts often have relatively small pores. This shortcoming usually hinders tissue regeneration and remolding and limits the application of electrospun scaffolds in tissue engineering. In order to significantly increase the pore size in electrospun scaffolds and enhance cell migration, Kong et al.[141] prepared composite scaffolds consisting of PCL fibers and poly(ethylene oxide) (PEO) microparticles (MPs) by simultaneously using the electrospinning and electrospraying technologies. Larger pores were acquired by the removal of PEO MPs from the composites. They found that the average pore size was markedly increased to the range of 31.71 ± 8.07–37.63 ± 11.95 μm, which was about
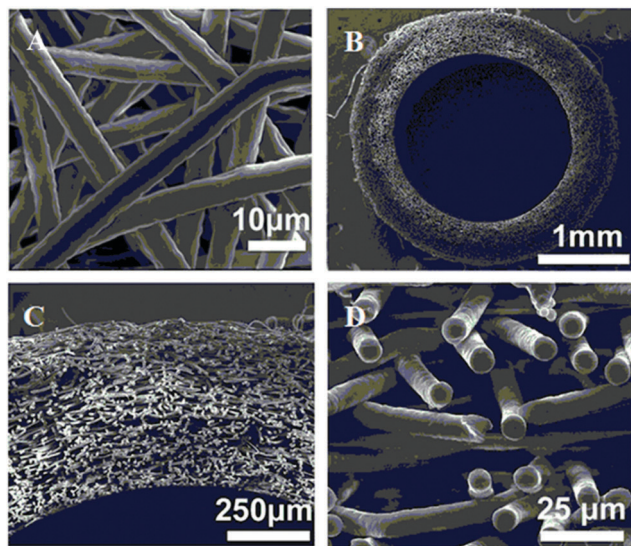
5688 | Chem. Soc. Rev., 2015, 44, 5680–5742

This journal is © The Royal Society of Chemistry 2015

Fig. 6 SEM images of electrospun PCL mats with thicker fibers (A) and cross-sections of the tubular thicker fiber grafts (B–D). Reproduced with permission from ref. 142. Copyright 2014, Elsevier.

2- to 3-fold larger than that of the corresponding regular electrospun PCL scaffolds, whereas the fiber diameters were not obviously affected by PEO MPs. As a result, the mechanical strength and burst pressure of these vascular grafts could reach the standard for vascular implantation.[141] Kong *et al.*[142] further prepared macroporous PCL scaffolds with thicker fibers (5–6 μm) and larger pores ($\sim$30 μm) (Fig. 6). The macroporous grafts markedly enhanced cell infiltration and ECM secretion. The *in vivo* implantation, by replacing rat abdominal aorta, results demonstrated that these grafts had satisfactory patency for up to 100 days and the endothelium coverage was complete at day 100 (Fig. 7). In addition, the regenerated smooth muscle layer was correctly organized with abundant ECM similar to those in native arteries,

and the regenerated arteries showed contractile response to adrenaline and acetylcholine-induced relaxation.

2.5 Biodegradable copolymers based on lactide, glycolide, trimethylene carbonate and other monomers

Although the properties of the above-mentioned PCL are attractive, its slow and un-adjustable degradability might limit its further application as tissue-engineered vascular grafts. Consequently, biodegradable polymers based on lactide (LA) and glycolide (GA), such as PLLA, PGA and PLGA, have been developed and used as biomaterials. The degradability of PGA is very rapid, which ultimately leads to implantation failure under physiological pressures. Although PLLA degrades slower than PGA, its stiffness still makes it less desirable as vascular grafts. Fortunately, the PLGA copolymer is a suitable biomaterial for vascular grafts because its degradability and stiffness can be adjusted by changing the weight ratio of LA and GA monomers in the copolymerization process. Venkatraman *et al.*[143] found that ECs could grow and proliferate well in PLGA (80/20) scaffolds with a suitable pore size (20–40 μm), whereas ECs grew relatively poor on PLLA scaffolds regardless of their pore features.

The electrospinning technology is widely used in the fabrication of fibrous grafts from PLGA and other biomaterials in order to improve their biocompatibility. Lee *et al.*[144] electrospun 2-methacryloyloxyethyl phosphorylcholine (MPC) copolymers with PLGA to acquire a type of biodegradable graft with good biocompatibility.

In addition to PLGA, numerous biodegradable homopolymers, random copolymers, diblock copolymers, multiblock copolymers and networks[145,146] have been prepared from trimethylene carbonate (TMC),[147,148] CL, *p*-dioxanone (PDO), morpholine-2,5-dione derivatives and other monomers. In addition, these monomers can also be copolymerized with LA and/or GA to obtain various copolymers, for example, poly(TMC)–PEO diblock copolymers,[149] poly(trimethylene carbonate-*co*-L-lactide),[150] poly(trimethylene
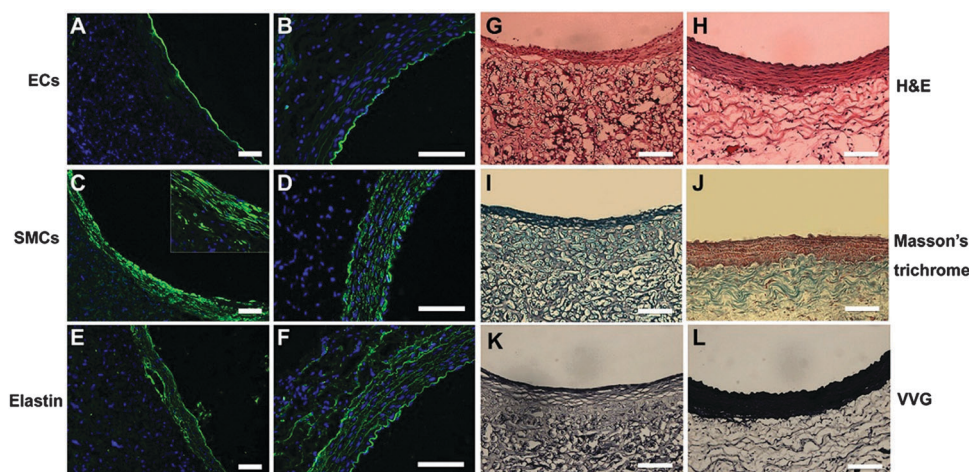

Fig. 7 Histological analysis and deposition of extracellular matrix in the regenerated grafts at day 100 in comparison with native aorta. Cross-sectional images of the regenerated grafts (A, C and E) and native artery (B, D and F), which were immunochemically stained to identify the endothelial cells, smooth muscle cells and elastin. H&E staining shows the structure of the explanted grafts (G) and native aorta (H). Masson's trichrome staining shows the presence of collagen (green) in the explanted grafts (I) and native aorta (J). Verhoeff's staining shows the presence of elastin (black) in the explanted grafts (K) and native aorta (L). Scale bar: 100 mm. Reproduced with permission from ref. 142. Copyright 2014, Elsevier.

This journal is © The Royal Society of Chemistry 2015

Chem. Soc. Rev., 2015, **44**, 5680–5742 | **5689**

carbonate-co-glycolide-co-dioxanone),[151] poly(para-dioxanone-co-L-lactide), poly[LA-co-(Glc-alt-Lys)],[152] poly(morpholine-2,5-dione)-block-polylactide,[153] poly(ω-pentadecalactone),[154] multiblock copolymers of poly(PDO) or PCL with PADOH (Diorez[a], Hyperlast)[155] and poly(rac-lactide)urethane.[156]

Biodegradable polyesters are often used for biomedical applications such as surgical sutures, tissue engineering scaffolds, functional NPs and carrier systems for the controlled release of drugs and genes.[157,158] However, upon degradation *in vivo*, they produce acidic degradation products that may cause low local pH, and consequently induce an inflammatory response upon implantation in the body. Recently, α-amino acids based poly(ester amide)s have attracted considerable attention because they have both ester and amide groups in their backbone chains, and they possess the good degradability of polyesters as well as high mechanical properties of polyamides.[159] Therefore poly(ester amide)s have become an important family of biodegradable synthetic polymers. Particularly, poly(ester amide)s containing α-amino acids are potential important tissue engineering scaffold biomaterials owing to their better cell–biomaterial surface interactions.[160] Moreover, the presence of the multifunctional α-amino acids provides the introduction of pendant bioactive groups or biomacromolecules and enhances the overall biofunctionality of poly(ester amide)s. The alternating copolymers of α-amino acids and α-hydroxy acids, which are called polydepsipeptides, are an interesting family of biodegradable poly(ester amide)s.[161,162]

In our previous studies, we have successfully prepared several linear, diblock, triblock and star-shaped poly(ester amide)s copolymers using the ROP of morpholine-2,5-dione derivatives with other monomers in the presence of various initiators and Sn(Oct)₂ as a catalyst.[163–171] Furthermore, we first used enzymes to catalyze the ROP of morpholine-2,5-dione derivatives to synthesize polydepsipeptides in order to avoid using the toxic Sn(Oct)₂ catalyst. Porcine pancreatic lipase type II crude, lipase type VII from *Candida rugosa* (CR) and lipase type XIII from Pseudomonas species (PS) showed high catalytic activity, while Novozym-435 could not catalyze the ROP of 3(S)-isopropyl-morpholine-2,5-dione or 6(S)-methyl-morpholine-2,5-dione.[172–174] Surprisingly, we observed the racemization of the L-lactic residue during the ROP of 3(S)-methyl-morpholine-2,5-dione (MMD) in the presence of enzymes. Recently, we further synthesized shape-memory polymers from poly(ester amide)s[175] and evaluated their biocompatibility.[176] The advantages of depsipeptide-based multiblock copolymers are that they have both shape-memory properties, and degradability; moreover, their degradation products containing α-amino acids may act as a buffer for hydroxy acids, thereby stabilizing the microenvironment pH value. Our results showed that these copolymers are promising candidates for soft, multifunctional implant materials, as well as gene and drug carriers.[177–180]

Other groups have also demonstrated poly(ester amide)s containing α-amino acids as tissue engineering scaffolds and delivery systems.[181,182] More recently, Mequanint *et al.*[183] used the electrospinning method to fabricate nanoscale three-dimensional scaffolds with average fiber diameters ranging from 130 to 294 nm and conjugated the transforming growth factor-b1 (TGF-b1) to the surface through pendant carboxylic acid groups. Their results showed that the aspartic acid containing poly(ester amide)s are good candidates for vascular biomaterials, while more detailed studies should further investigate the ability of conjugated TGF-b1 to initiate cell signaling activities on 3-D fibrous mats, including ECM production over extended culture periods. The EC viability, proliferation and adhesion on three surfaces, *i.e.* amino-functionalized, carboxylic acid functionalized and a neutral poly(ester amide)s films, were evaluated and all of them were noncytotoxic and noninflammatory *in vitro*.[184] Furthermore, the amino-functionalized positively charged film promoted the adhesion and proliferation of ECs to form a monolayer.[185]

2.6 Natural biodegradable polymers

In addition to synthetic biodegradable polymers, natural biodegradable polymers, such as collagen,[186] elastin,[187] gelatin,[188] silk fibroin,[189] chitin, chitosan[190] and cellulose,[191] have also been widely investigated for medical and pharmaceutical applications, especially for the preparation of artificial vascular grafts and tissue engineering scaffolds. Natural biodegradable polymers usually display good biocompatibility, biomechanical function, physical and chemical properties, and biological properties. More importantly, they can provide many motifs for cell attachment and proliferation. Therefore, various artificial vascular grafts and scaffolds for tissue engineered vascular grafts have been developed from natural biodegradable polymers using the following approaches: cell-populated protein hydrogels,[192] crosslinked protein scaffolds,[186,193,194] decellularized native tissues[195–197] and self-assembled vascular grafts.[198–201]

Compared with synthetic polymers for the construction of 3D scaffolds, natural biodegradable polymers, such as proteins or carbohydrates, could dominate in shaping cell behavior, especially biocompatibility.[202] One example is collagen hydrogels, which are widely investigated as scaffolds for vascular tissue engineering because of the abundance of collagen in the blood vessel wall. However, many results have demonstrated that collagen hydrogels exhibit relatively low stiffness and strength. In particular, their elastic modulus (1–100 Pa) is significantly lower than that of small-diameter vascular tissue (40–900 kPa). More recently, a collagen–PEG diacrylate interpenetrating polymer network (IPN) has been developed to address these limitations. This IPN displays improved stiffness, strength, physical stability and hemocompatibility, as well as retains the benefits of collagen hydrogels. In particular, cells can elongate and spread within collagen based IPN.[186] Elastin is derived from ECM as a potent pro-angiogenic factor that contributes to the visco-elastic property of arteries by combining with fibrillin 2. Elastin mainly dominates the elasticity of blood vessel walls, which directly decides the stretching and recoiling ability of blood vessels. Collagen and elastin tubular scaffolds have been prepared from their suspension solutions using the freeze-drying method. These scaffolds have high porosity and micron-scaled pores, but their mechanical properties are poor.[187,203] Gelatin is a natural biopolymer that is derived from collagen. A type of core–shell nanofibers with gelatin in the shell and poly(vinyl alcohol) in the core was prepared by coaxial

5690 | *Chem. Soc. Rev.*, 2015, **44**, 5680–5742

This journal is © The Royal Society of Chemistry 2015

electrospinning. These core–shell nanofibers can promote cellular viability and growth, as well as minimize platelet adhesion and activation, and possess appealing hemocompatibility for use in vascular applications.[188]

In addition to collagen, elastin and gelatin, silk fibroin (SF) is also a promising natural protein for the preparation of artificial vascular grafts because it possesses excellent biocompatibility, biodegradability and minimal immunogenicity. Electrospun SF and its blends with other biomaterials as small-diameter vascular grafts have been widely investigated.[189,204–210] Moreover, SF vascular grafts and heparin-loaded SF vascular grafts with high porosity and highly interconnected pores have been prepared by freeze-drying method. Heparin could be released in a sustained manner for approximately 7 days, thus inhibiting the proliferation of hSMCs within the scaffold *in vitro* while significantly promoting neovascularization *in vivo*. Therefore, these SF based scaffolds are attractive candidates for use as potential vascular grafts for implantation.[193,211]

Another type of natural polymers is natural carbohydrates, which have also been used as vascular graft materials. Among them, chitosan is attractive because of its low immunogenicity and inherent antimicrobial characteristics.[190,212,213] Chitosan vascular grafts and scaffolds have been prepared by the electrospinning and freeze-drying method.[202] In addition, bacterial cellulose obtained from bacteria is a kind of biocompatible polysaccharide.[214–217] Small-diameter vascular grafts with a supramolecular fiber network structure consisting of tubular hydrogels from bacterial cellulose were created using Gluconacetobacter strains and the matrix reservoir technology. These grafts provided a scaffold for cell ingrowth and seemed to support tissue engineering to form a three-layered structure organism, which was similar to those of native arteries with a single layer of endothelium with a basement membrane followed by a concentric layer of SMCs and an outer layer with adjacent tissue with ingrowing capillaries after 3 months in a sheep model. However, the overall patency rate was 50% at 12 weeks.[218] One of the challenges for using bacterial cellulose grafts is their densely packed network of cellulose nanofibrils. In order to address this problem, Davalos *et al.* developed a novel biofabrication method, *i.e.* irreversible electroporation, to incorporate porosity into bacterial cellulose scaffolds. This method can kill the bacteria in specific locations and cellulose deposition at these sites can be prevented.[219] Thus the porosity of bacterial cellulose scaffolds can be altered to facilitate cell ingrowth. In addition to bacterial cellulose, nanocrystalline cellulose has vast potential due to its remarkably high strength, which is stronger than steel and comparable to Kevlar. Nanocrystalline cellulose–fibrin nanocomposites provide potential new biomaterials for small-diameter vascular grafts.[220]

To mimic the structural complexity of the natural ECM and obtain negligible immunogenicity, various methods have been performed to fabricate artificial vascular grafts such as knitting or weaving technology, electrospinning technology,[221] electrospraying technology, consolidation technique,[65] extrusion-phase inversion technique,[111,222] thermally induced phase separation, gas foaming, liquid–liquid phase separation with freeze extraction technique,[223] layer-by-layer (LbL) technology

and three-dimensional (3D) printing technology.[224–227] Among these methods, electrospinning technology is now widely utilized to prepare nano- and micro-fibrous vascular grafts and scaffolds. Fiber diameter and pores can be easily controlled by the electrospinning parameters. The LbL technology is a great tool for the development of biocompatible surfaces of biomaterials. More recently, the 3D printing/bioprinting technology has appeared for biomaterial engineering. This technology can print a multitude of biocompatible materials, various types of cells and growth factors into a complex functional 3D format. A major advantage of this technology is its ability for simultaneously 3D printing various types of cells in defined spatial locations, which makes this technology applicable to regenerative medicine. The combination of the electrospinning and 3D printing technologies can be used to manufacture complex structures with defined microarchitectures and cell types in a confined area.[228] For example, artificial vascular grafts have been prepared from a blend of chitosan and PCL by electrospinning. Subsequently, the surface was coated with PCL strands using the 3D printing technology. This tubular vessel exhibits excellent mechanical properties for vascular reconstruction.[229] Thus, the combination of these technologies can be used to manufacture artificial vascular grafts with demanding properties, which include surface hemocompatibility, microarchitecture for cell ingrowth, complex macrostructures and mechanical properties.

2.7 Polymer blends for artificial vascular grafts

Although natural polymers display excellent biocompatibility and biodegradability, their mechanical properties (except for celluloses) are still insufficient for artificial vascular grafts. On the other hand, synthetic polymers usually have excellent mechanical properties and processability but lack biocompatibility and cell recognition sites. To overcome these problems, many research groups have blended natural polymers and synthetic ones to prepare desirable bio-composites for artificial vascular grafts.[230,231] Natural biopolymers, such as alginate, agarose, chitosan, peptide, gelatin, collagen, fibroin and elastin, are biocompatible and can be used to modify PUs.[232–234] For example, PU grafts were reported to be modified by the incorporation of superfine SF powder. Human umbilical vein endothelial cells (HUVECs) strongly attached, grew and proliferated rapidly on the surface of the modified grafts. The proliferation ability improved with the increased proportion of SF powder.[235,236] Recently, we fabricated a type of bilayered tubular scaffold, which was composed of elastic PU fibers as the outside-layer and hemocompatible gelatin–heparin fibers as the inner-layer using the electrospinning technology (Fig. 8).[26,104,237] The elastic PU layer improves the flexibility and decreases the rigid property of the gelatin layer. These bilayer tubular scaffolds have both appropriate stress and high elongation at break to maintain the elasticity under a periodically loaded stress field. They have desirable tensile properties for vascular grafts, which are generally accepted to be 1.0 MPa (stress at break) and 40.0% (elongation at break). Moreover, heparin release from the gelatin–heparin scaffolds is uniform from the 2nd to 9th day, which results in rare platelet adhesion in *in vitro* tests.[26]

Collagen and chitosan have also been used to improve the biocompatibility of PU grafts. Collagen–chitosan–PU blend grafts have excellent mechanical properties and biocompatibility;

This journal is © The Royal Society of Chemistry 2015

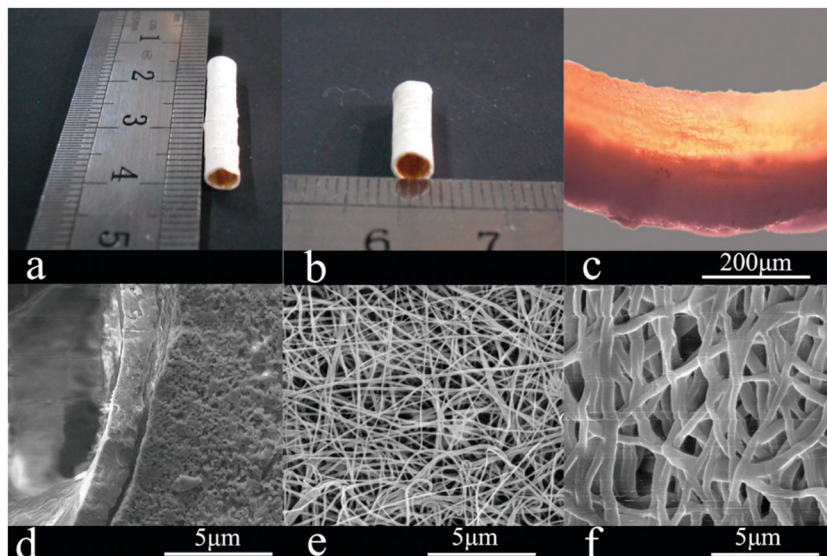*Chem. Soc. Rev.,* 2015, **44**, 5680–5742 | **5691**

Fig. 8 Macroscopic view and SEM images of the PU/gelatin–heparin tubular scaffolds. Images of the tubular scaffolds (a and b), images of the cross section of the tubular scaffolds (c and d), SEM image of gelatin–heparin (inner-layer of scaffold, heparin 1 wt%) (e), and SEM image of PU (outside-layer of scaffold) (f). Reproduced with permission from ref. 104. Copyright 2005, Springer.

furthermore, their aligned fibers could regulate cell morphology by inducing cell orientation.[238] To mimic the compliance and mechanical properties of native arteries, Wong *et al.*[239] fabricated aligned nanofibrous PU blend scaffolds with elastin, collagen or a mixture of both proteins. The elastin–PU blend scaffolds show the tensile stress and elongation at break of 7.86 MPa and 112.28%, respectively, which are similar to those of blood vessels. The aligned nanofibers of these scaffolds enable SMCs to proliferate in an environment with biomimetic structural organization to natural blood vessels. These blend vascular grafts benefit from elastin and collagen since elastin provides the necessary viscoelastic properties while collagen enhances the cellular interactions. Moreover, elastin-like polypeptides also show great promise as modifiers for candidate scaffolds for engineering contractile vascular tissues.[240,241]

Heparin is incorporated into electrospun PCL fiber scaffolds with the aim to prevent the proliferation of VSMCs in culture by the controlled release of heparin. Recently, Kong *et al.*[242] prepared PCL and chitosan grafts by the co-electrospinning technique. Heparin was immobilized on these grafts through ionic bonding between heparin and chitosan in the fibers. This provides a facile and useful technique for the development of heparinized vascular grafts.

Lelkes *et al.*[243] prepared a series of grafts from tertiary blends of PLGA, gelatin and elastin (PGE). All the PGE grafts supported the attachment and metabolization of ECs and cytoskeletal spreading as observed at 48 h post-seeding. Importantly, the EC monolayer generated on the PGE graft surface was non-thrombogenic and had biofunction. To improve the mechanical properties of grafts, Stamatialis *et al.* used the phase inversion method to prepare membranes from PLGA and PCL blends. These membranes exhibited good human adipose stem cell attachment and proliferation.[244]

Recently, our group electrospun SF and PLGA mixtures to form fibrous scaffolds with different SF/PLGA weight ratios (0/100, 30/70, 50/50, 70/30, 90/10) to mimic the morphology and ECM.[245] The introducing of SF improves the surface hydrophilicity of the grafts and enhances the viability, spreading and attachment of HUVECs on these SF/PLGA scaffolds in comparison with the pure PLGA scaffolds. To achieve rapid endothelialization and reduce the failure rate of implantation of small-diameter vascular grafts, we introduced gene complexes to PLGA grafts by electrospraying, which can promote the proliferation of ECs (Fig. 9).[246] This work has obtained some satisfactory results now and needs more effort in this aspect.

Pfeiffer *et al.* prepared three-layered vascular grafts from PCL, PLA and/or PEG. The outer layer and inner layer were spun from a polymer blend consisting of PCL–PLA or PCL–PLA–PEG, whereas the middle layer was spun from PCL solution. These small-diameter vascular grafts were pre-coated with fibronectin and seeded with ECs. ECs attached on the surface and appeared to have a cobblestone morphology with the high viability rate of 98%. Hence, they may be a promising improvement for small-diameter vascular grafts.[67]

It is well known that nitric oxide (NO) generated *in situ* can prevent platelet adhesion on artificial vascular grafts.[247–250] Thus, we blended PCU and a lipophilic Cu(II)-complex (Cu(II)–DTTCT) as a catalyst to enable its surface with the ability to generate NO in the presence of nitrite.[251] In order to improve the hemocompatibility and biocompatibility of the PCU surface, hydrophilic PEG modified PCU fibrous scaffolds were prepared from PEG and PCU solutions using the electrospinning technology.[13] The highly hydrophilic PEG can improve the hydrophilicity and anti-protein adsorption of scaffolds. The scaffold with 20 wt% PEG shows a lower possibility of thrombus formation and better cell attachment and proliferation than the control.[252] However, PEG can be dissolved out from blend scaffolds during culture; thus, the surface will change from hydrophilic to hydrophobic. In order to improve the modification stability of PEG in the blend scaffolds, we
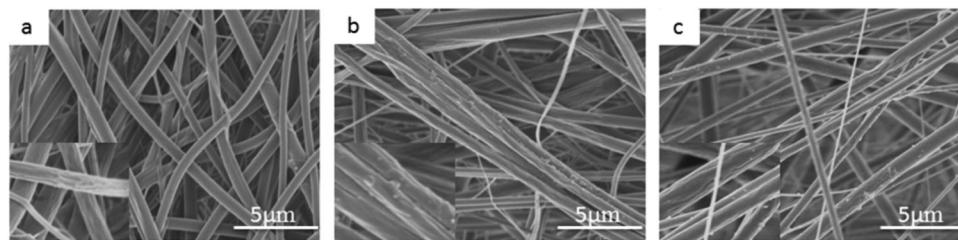
Fig. 9 SEM micrographs of (a) pure PLGA/SF, (b) composite scaffold of MPs–PLGA/SF, and (c) composite scaffold of MPs/pEGFP–ZNF580–PLGA/SF. Reproduced with permission from ref. 246. Copyright 2013 Trans Tech Publications Ltd.

electrospun a solution of PCU and poly(ethylene glycol)monoacrylate (PEGMA) to prepare hybrid nanofibers by *in situ* ultraviolet (UV) photopolymerization.[253] PEGMA was polymerized with a small amount of crosslinker to form a crosslinked polymer network in the PCU fibers. Thus, the fibers exhibited high hydrophilicity and good hemocompatibility even after a long period of immersion in PBS.[254,255]

In addition to PEG, zwitterionic PC polymers are well known hydrophilic and non-fouling materials and have been widely used to modify biomaterials by the blending and coating methods. Generally, PC-based random, block and graft copolymers are prepared from MPC, butyl methacrylate (BMA), 2-hydroxyethyl-methacrylate (HEMA), or 2-ethylhexyl methacrylate (EHMA) by radical polymerization, atom transfer radical polymerization (ATRP) or other living polymerization technologies.[256–258] The molecular architectures and chemical compositions of MPC copolymers affect the surface properties and bulk mechanical properties of modified materials. For example, the poly(MPC-*graft*-EHMA) graft copolymer layer shows high stability on the PU surface after immersion in an aqueous medium compared with the poly(MPC-*co*-EHMA) random copolymer and poly(MPC-*b*-EHMA) block copolymer, which is attributed to the intermiscibility of the hydrophobic poly(EHMA) segments in the domain of the soft segments of PU. Importantly, the modified surface exhibits high hydrophilic property and a dramatic suppression of protein adsorption. In addition, Nakabayashi *et al.*[259] blended the poly(MPC-*co*-EHMA) random copolymer with segmented PU, and then coated them on a polyester tube surface to make small-diameter vascular grafts (2 mm inner diameter and 2 cm long). These grafts were placed in rabbit carotid arteries for 8 weeks, and showed excellent antithrombogenic properties. However, it is to be noted that the vascular graft surface was prohibited from attaching both blood cells and ECs. Wagner *et al.*[260] fabricated fibrous vascular grafts (1.3 mm inner diameter) from the blend solution of biodegradable poly(ester urethane)urea (PEUU) and poly(MPC-*co*-methacryloyloxyethyl butylurethane) (PMBU) using the electrospinning technology. MPC based copolymers possess high hydrophilicity, hence they cannot be blended uniformly with the relatively hydrophobic PEUU. In order to blend well with PEUU, Wagner *et al.* designed and synthesized MPC copolymers having a urethane bond in each side chain. This fibrous surface markedly reduced platelet and SMC adhesion *in vitro*, which is most likely due to the presence of PC moieties on the surface. After implantation in

rat abdominal aorta for 8 weeks, the fibrous small-diameter vascular grafts showed high patency and reduced thrombogenicity; moreover, their surface allowed complete endothelialization and good anastomotic integration.[260]

Inorganic materials can also modify biomaterials for the application in small-diameter vascular grafts. Recently, Peng *et al.*[261] co-electrospun thermoplastic polyurethane (TPU)–graphene oxide (GO) blends with different contents of GO. The surface properties, tensile strength, Young's modulus and hydrophilicity of these grafts increased with the increase of GO content. The suture retention strength and burst pressure of the TPU–GO grafts (0.5 wt% GO) were found to meet the requirements of human blood vessels; furthermore, they showed reduced platelet adhesion and activation. Moreover, ECs were able to attach to the inner surface of the tubular grafts.

Numerous studies have demonstrated that drug eluting stents, PU scaffolds and artificial vascular grafts can effectively suppress local SMC proliferation.[262] Domb *et al.*[263] found that incorporating rapamycin into PU fibers did not significantly compromise the morphology and the mechanical properties of the ensuing fibers. These grafts showed high encapsulation efficiency and maintained bioactivity even after 77 days *in vitro* release. Thus, they can serve as effective drug reservoirs for the local inhibition of the proliferation of SMCs. These bilayered rapamycin-eluting grafts may be promising candidates for functional vascular grafts with the prospect of long-term safety and patency.

3. Surface modification for improving the hemocompatibility of artificial vascular grafts

Ideal artificial vascular grafts should have good surface properties such as excellent biocompatibility (especially hemocompatibility), anti-thromboticity and anti-infection. In particular, surface hemocompatibility is one of the most important properties for small-diameter artificial vascular grafts. Insufficient hemocompatibility impairs their functionality and safety through the activation of blood coagulation and immune systems. Thus, graft surfaces should be absolutely antithrombotic; otherwise, slow blood flow in the cavity of artificial vascular grafts is easy to cause mural thrombus, hemagglutination, thrombosis and occlusion. Therefore, it is highly desirable and critically important for us

to understand the fundamental mechanism that induces restenosis and thrombosis. When artificial vascular grafts are implanted into the human body, their surface is in direct contact with blood. Plasma proteins and blood cells, which are the main components of blood, will be adsorbed on the foreigner exposed to them within a few minutes. The unfavorable physical and chemical characteristics of the interface may cause a conformation change in adsorbed proteins, thus activating the coagulation cascade, which leads to the adhesion, activation and aggregation of blood platelets. Denatured fibrinogen and activated blood platelets grow to form a stable thrombus, which narrows the artificial vascular grafts and causes immune and inflammatory reactions.[264] As a result, the attachment and proliferation of vascular cells, such as ECs and SMCs, are disturbed and all these eventually lead to endothelial dysfunction.[265]

The hemocompatibility of biomaterials is mainly dependent on the physical and chemical characteristics of biomaterial surfaces; thus, surface modification is one of the most direct and effective strategies to minimize thrombogenicity and to improve the hemocompatibility of artificial vascular grafts.[266,267] One remarkable advantage of this method is that the intrinsic mechanical properties of biomaterials and grafts are not significantly changed after surface modification.

3.1 Surface modification of artificial vascular grafts by PEG

PEG has been widely used as a biocompatible material due to its high hydrophilicity. The hydrophilic PEG can bind water molecules strongly to form a surface hydration layer, which can effectively inhibit the adsorption of plasma proteins and most components of blood such as fibrinogen and lysozymes. Moreover, the flexible PEG chain segment can move easily and fast in water and its large exclusion volume may also suppress the adsorption of proteins, blood platelets and red cells; in particular, PEG can avoid protein conformation change to maintain their natural characteristics. Moreover, PEG has a tendency to autoxidize to non-toxic products. Nowadays, PEG has been certificated by the FDA as an additive for various biomaterials. As a bio-inert macromolecule, PEG is also non-immunogenic, which is fairly important for biomaterials. Due to these unique properties, PEG is often used to improve the hemocompatibility of biomaterials.[268,269]

Because PEG is soluble in aqueous media such as blood, it is necessary for it to be covalently grafted onto biomaterial surfaces. Lendlein *et al.* grafted monoamino PEG with different chain lengths (M_n = 1000 or 10 000 g mol^{-1}) and end groups (methoxy or hydroxyl) onto a poly(ether imide) surface by nucleophilic addition at pH = 11 and 70 °C for 17 h. The surface functionalization leads to a reduction in the adsorption of bovine serum album (BSA) but not fibrinogen.[270] Compared with grafting onto poly(ether imide), the grafting of PEG onto PU surface is more complex. Generally, PU surface was first treated with diisocyanates as coupling agents, using dibutyltin dilaurate (DBTDL) or Sn(Oct)$_2$ as a catalyst to introduce free isocyanate groups on the surface, and subsequently covalently grafting PEG *via* the reaction between the surface isocyanate groups and the hydroxyl groups of PEG.[271,272] Alternatively, in

many other approaches, the hydroxyl groups of PEG were functionalized firstly by an end-capping reaction with HMDI or IPDI.[273,274] For example, IPDI reacted with star shaped PEG to yield isocyanate-terminated reactive stars. Interestingly, the crosslinking and chain extension reactions of star shaped PEG were avoided by optimizing the reaction conditions. The isocyanate-terminated PEG was finally grafted onto the biomaterial surface *via* an allophanate reaction, and the reactive functional groups were introduced by this special PEG at the same time. Star-shaped PEG modified surfaces could prevent the non-specific adsorption of proteins and cells very efficiently. In addition, these functionalities on the surface can be used to incorporate ligands for biological targets, which endow surfaces with specific biological interactions.[275–278]

More recently, Gu *et al.* reported a PEO modified PU surface using the ozone activation method without the use of an organic stannous catalyst and highly toxic diisocyanates.[279] They successfully modified PU by PEO with various molecular weights, which ranged from 1000 to 300 000 g mol^{-1}. The modified surfaces exhibited high hydrophilicity (water contact angle less than 20°) and reduced platelet adhesion. Additionally, even the adhered platelets showed less shape deformation. Especially, no platelets were adhered on most areas of the surface of high molecular weight PEO (300 000 g mol^{-1}) modified PU.[279]

Liner PEG can be grafted directly onto a substrate surface, but the grafting density is limited due to high steric hindrance. A suitable method to increase the number of effective PEG chains involves the introduction of PEG in a brush-like structure on the surface of biomaterials.[280] In our previous studies, we employed UV initiated photopolymerization to graft PEGMA onto the PCU surface. By adjusting the reaction parameters, such as reaction temperature, PEGMA concentration, UV irradiation time and photoinitiator concentration, the grafting density of PEGMA could be controlled.[281] The grafted poly(PEGMA) chains on the surface had many PEG blocks as side chains, in which the end hydroxyl groups were introduced as functional groups for further modification. Anticoagulants, bioactive molecules or drugs could be immobilized onto the surface by means of coupling of these hydroxyl functional groups. PEGMAs with different molecular weights (400, 600, 800, 1000 g mol^{-1}) were used to investigate the influence of molecular weights on surface hydrophilicity and hemocompatibility. The ratio of hydrophilic PEG chains to hydrophobic polyacrylate chains can be controlled by the molecular weight of the macromonomer, PEGMA. The grafting density of PEGMA increased from 1.75 mg cm^{-2} for PEGMA M_w = 400 g mol^{-1} to 2.33 mg cm^{-2} for PEGMA M_w = 1000 g mol^{-1}, while the molar immobilization density, which is given by the ratio between the grafting density and M_w of macromonomer PEGMA, decreased from 4.38 μmol cm^{-2} to 2.33 μmol cm^{-2} with the increasing molecular weight of PEGMAs. This means that high molecular weight PEGMA has higher steric hindrance as well as lower ability for movement, which results in a decreased affinity for active free radicals and low molar immobilization density. The PEGMA modified surfaces exhibited excellent hydrophilic property and effectively resisted platelet adsorption compared with the unmodified surface.

Furthermore, PCU grafted PEGMA M_w = 800 g mol^{-1} minimized platelet adsorption and had the best hemocompatibility, which might be explained by the optimum balance between PEGMA immobilization density and PEG chain length.[254]

Surface-initiated atom transfer radical polymerization (SI-ATRP) method as living polymerization can easily control the length of grafting chains according to need or design. We employed SI-ATRP to graft controlled hydrophilic PEGMA chains onto the surface of electrospun PCU nanofibrous scaffolds, which had little change in fiber morphology.[282] It is worth mentioning that the mechanical properties of the modified scaffolds were similar to the scaffolds without modification, for example, the value of the elastic modulus was 2.83 ± 0.11 MPa, tensile strength was 2.34 ± 0.17 MPa, and the elongation at break was 110% ± 32%. The modified scaffolds showed significantly improved hydrophilicity, enhanced hemocompatibility and high tendency to induce cell adhesion. Moreover, ECs reached out pseudopodia along the fibrous direction and formed a continuous monolayer in vitro.[255]

Other approaches include the photografting of PEGMA (M_n = 570 g mol^{-1}) on cyclic olefin copolymers[283] and the development of hyper-branched surfaces of poly(PEGMA) (M_n = 360 g mol^{-1}).[284] In all these cases, the effectiveness of protein adsorption reduction has been significantly influenced by the chain length and surface density of PEG.[32,285,286]

Jiang et al.[287] constructed amphiphilic membrane surfaces based on PEO and polydimethylsiloxane (PDMS) segments and prepared a biomimetic topography PDMS surface for improving antifouling performances. The PEO segments are utilized to prevent biofoulant adsorption while the PDMS segments are used to drive away the adsorbed biofoulant. As a result, the amphiphilic surfaces exhibit good antifouling properties.[287] Additionally, hydrophobic PDMS segments in the PDMS-g-PEO copolymers can be used to anchor PEO onto a hydrophobic surface such as polystyrene or PDMS. The PEO segments are expected to extend outwards into the aqueous phase. The PDMS-g-PEO copolymers (having a PEO content from 58 to 80 wt%) can behave like molecular brushes, which are able to reduce the fibrinogen adsorption on the surface.[288]

In addition to PDMS-g-PEO copolymers, a type of triblock copolymer, namely, PEO–polybutadiene–PEO (PEO–PB–PEO), has been used to modify medical grade Pellethane, Tygon polyurethanes, PDMS and polycarbonate. A highly stable, protein-repellant PEO layer was formed on the surface by the adsorption and γ-irradiation of these PEO–PB–PEO triblock copolymers. During the self-assembly of the PEO–PB–PEO triblock polymers at the surface, the adsorption mechanism and kinetics depended on the triblock polymer concentration. When the concentration was slightly below the critical aggregation concentration, the most homogeneous coverage and highest grafting efficiency were achieved. In addition to the coating and self-assembly technology, the γ-irradiation process can induce covalent grafts onto material surfaces, and thus produce a stabilized PEO layer.[289,290]

Although PEG and PEO modified surfaces can improve hydrophilicity and anti-nonspecific protein adsorption, PEG and PEO could autoxidize rapidly, especially in the presence of oxygen and transition metal ions, which typically exist in biological media. Thus, these modified surfaces may face a problem, i.e. long-term poor protein repulsive property in vivo and in clinical applications.

3.2 Surface modification of artificial vascular grafts by zwitterionic polymers or groups

Zwitterionic polymers are well known as hydrophilic and non-fouling materials.[291–298] They have both cationic and anionic moieties on the same side chain while maintaining overall charge neutrality. The zwitterions usually mean zwitterionic betaines, which include phosphobetaine, sulfobetaine and carboxylbetaine. They are named according to the difference in the negatively charged groups, as shown in Fig. 10. Zwitterionic betaines generate a tightly bound, structured water layer around the zwitterionic head groups via electrostatic and hydrogen bond induced hydration in water, thus significantly reducing protein adsorption and platelet adhesion and effectively controlling coagulation cascade and immune inflammation. If biomaterial surfaces are modified by zwitterionic polymers, their surface hemocompatibility should be improved significantly.[296,299]

The zwitterionic PC group plays an important role in preventing blood coagulation on the surface of cell membranes. If PC groups are incorporated onto the surface of artificial vascular grafts, their surfaces become highly hemocompatible because of the biomembrane-like structures. PC groups on the surface can effectively reduce plasma protein adsorption, suppress platelet adhesion and activation, and improve the hemocompatibility of biomaterials when they are in contact with blood or cell suspensions.[297,300]

Many approaches have been developed to introduce PC groups onto biomaterial surfaces. Among them, most attempts apply PC containing monomers, in which MPC is widely used. MPC is a polymerizable methacrylate monomer. Its homopolymer, and random-type, block-type and graft-type copolymers have been immobilized on PU surface by coating,[301] blending,[302,303] grafting[304–307] or the formation of semi-interpenetrating polymer networks.[308–310] For example, PU has been modified
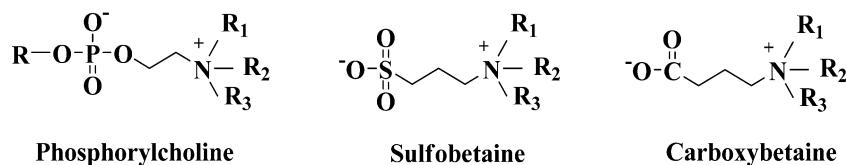

Fig. 10 The schematic structures of some zwitterions. R, R$_1$, R$_2$, R$_3$ = −CH$_3$, −CH$_2$CH$_3$, −CH$_2$CH$_2$OH, −(CH$_2$)$_n$OCOCCH$_3$=CH$_2$ or −(CH$_2$)$_n$NHCOCCH$_3$=CH$_2$, where n is 1, 2, 3, 4, 5 or 6.

by poly(2-methacryloyloxyethyl phosphorylcholine-*graft*-2-ethylhexyl methacrylate), which is composed of a poly(MPC) segment as the main chain and poly(2-ethylhexyl methacrylate) (poly(EHMA)) segments as the side chains. The domain of poly(EHMA) segments is intermiscible with the soft segments of PU; thus, this modified surface shows high stability in aqueous media. They can dramatically suppress protein adsorption from human plasma and effectively protect blood-contacting surfaces from thrombus formation, but they also decrease EC adhesion. Recently, we used MPC to modify the PCU surface by the Michael reaction,[31] UV-initiated and SI-ATRP polymerization[311] in order to improve surface hemocompatibility, as shown in Fig. 11.

The Michael reaction method to graft MPC onto the PCU surface involves three steps as shown in Fig. 11A. Firstly, HDI was coupled onto the PCU surface through an allophanate reaction. Then, tris(2-aminoethyl)amine (TAEA) was linked to the PCU surface through the coupling of the amino group of TAEA with the rest of the isocyanate groups of HDI to create primary amine groups on the surface. Here, owing to the fact that there are three primary amino groups in one TAEA molecule, TAEA introduced a high amino content on the PCU surface. Finally, MPC was grafted onto the PCU surface *via* the Michael reaction of MPC with amino functional groups.[31] The Michael reaction is a simple and effective method to introduce functional groups.[312] This modification method may not only be favorable for the polar head-group arrangement of PC on the PCU surface, but also greatly improves the grafting density of PC functional groups, where the P content of the modified PCU surface was 1.3%.

In our previous study, we synthesized an acrylate monomer that had a PC group (Fig. 12, PC monomer).[313] The intermediate product of (6-isocyanato *n*-hexyl)carbamoyloxyethylmethacrylate was firstly synthesized from HEMA and HDI in an equal molar ratio, and then reacted with L-α-glycerylphosphorylcholine. Since one HDI molecule has two equivalent reactive isocyanate groups, side reactions may result in isocyanato urethane methacrylate as
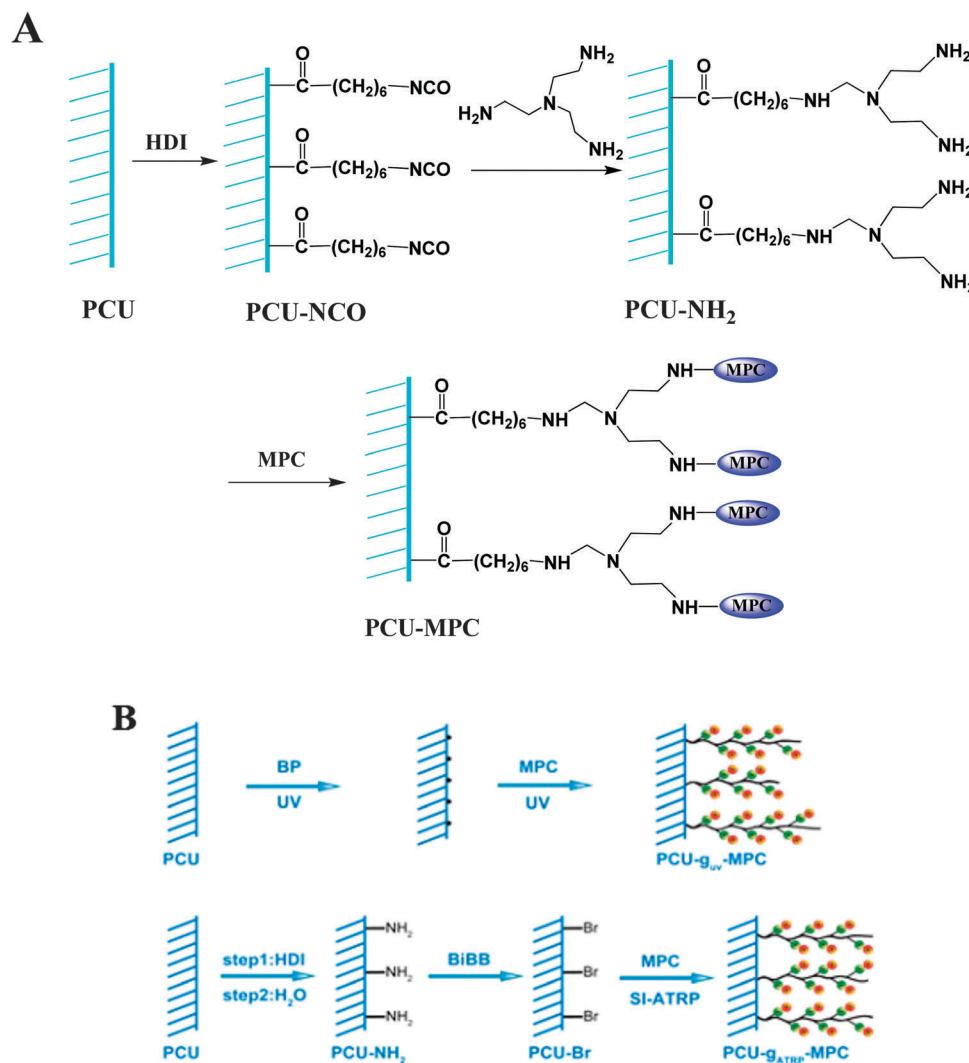

Fig. 11 Schematic diagram of grafting MPC onto the PCU surface *via* the Michael reaction (A), UV–initiated and SI-ATRP (B) polymerization. Reproduced with permission from ref. 31 and 311. Copyright 2013 Elsevier and Copyright 2011 Wiley-VCH, respectively.

5696 | *Chem. Soc. Rev.*, 2015, **44**, 5680–5742

This journal is © The Royal Society of Chemistry 2015

well as dimethacrylate diurethane. As a result, it is very difficult to completely purify the reaction mixture to obtain the goal monomer. This monomer was grafted onto the surface of PCU films by UV initiated polymerization in the presence of BP as a photoinitiator. The modified PCU film has a low water contact angle and high water uptake. Moreover, platelet adhesion was significantly decreased, which suppresses its activity and controls the coagulation cascade and immune responses.[314] Alternatively, L-α-glycerylphosphorylcholine was oxidized to obtain the aldehyde derivative phosphorylcholine glyceraldehyde (PCGA, in Fig. 12). Then, PC groups could be covalently linked onto the PCU surface via the reductive amination of PCGA.[315]

Furthermore, PC groups were covalently linked onto the PCU surface with a flexible chain as a spacer to improve their moving ability. 1,6-Hexanediamine reacted with the isocyanated PCU surface by coupling its amino group with the rest of the isocyanate groups on the polymer surface. Finally, PC groups were introduced onto the PCU surface via the reductive amination reaction between the aldehyde group of PCGA and the surface amino groups.[315] In another approach, the above hydrophobic spacer was replaced by a short hydrophilic PEG chain (Fig. 13).[316] Compared with other methods, the immobilization of PC groups onto the PCU surface using a flexible PEG chain as a spacer has apparently many advantages. For example, the flexible PEG segment enhances the mobility of the zwitterionic PC groups in water and endows them with self-assembling ability in an aqueous environment. Moreover, as mentioned above, the hydrophilic PEG chain also provides a large exclusion volume in an aqueous medium due to its unique coordination with surrounding water molecules, which forms a biocompatible layer to reduce the absorption of plasma albumen and red blood cells. The assembled PC groups form a specific biomimetic surface, which can resist the nonspecific adsorption of biomacromolecules via the bound hydration layer from the solvation

of the zwitterionic terminal groups, in addition to hydrogen bonding.[317] When 1,6-hexanediamine or amino-poly(ethylene glycol) (APEG) was used as a spacer to directly modify PCU, the grafting density of the PC groups was very low. Thus, we developed another method to graft PC on the surface of PCU films with a high grafting density but maintained the intrinsic mechanical properties of PCU (Fig. 14).[318] Firstly, PEGMA was grafted onto the PCU surface by UV initiated photopolymerization, thus providing a hydrophilic flexible PEG spacer and abundant reactive sites, i.e. −OH groups. Then IPDI acted as the coupling agent, i.e. one −NCO of IPDI was connected to the hydroxyl group of poly(PEGMA), while the other one hydrolyzed to form an amino group by reacting with water under mild conditions. Finally, the aldehyde groups of the PCGA molecules reacted with these amino groups to realize the grafting PC onto the flexible PEG spacer. The synergism of the PEG spacer and PC functional groups could improve the hydrophilicity and anti-platelet adhesion effect of the modified PCU film. The PCU–PEGMA–PC film may have potential applications in blood-contacting biomaterials and some relevant devices.

The above approaches grafted PC on the PCU surface, which improved its surface hydrophilicity significantly. Most areas of these modified PCU surfaces resisted blood platelet adhesion compared with the blank control; however, the graft density or PC concentration on the surface was low. Only the XPS method could prove the existence of the P element on the surface. Some areas of the surface may have not been covered with PC functional groups; thus, these areas still adhere some platelets, which finally results in coagulation. This low concentration of PC groups on some areas is mainly caused by low functional amino groups and incomplete functionalization, thus increasing the functional groups on the modified surface is still a big challenge.

In order to graft more functional PC groups, MPC can be polymerized to form poly(MPC) chains on the surface by
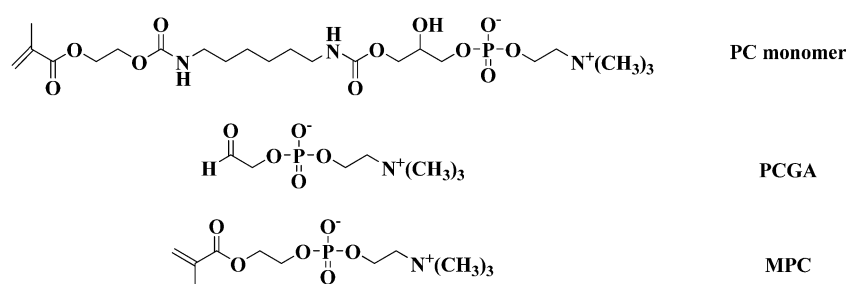

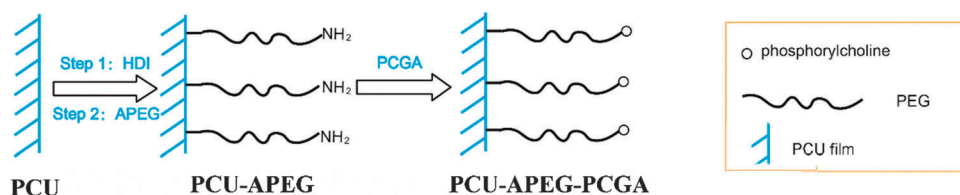Fig. 12 Chemical structures of the PC monomer, PCGA and MPC.

Fig. 13 Schematic diagram of phosphorylcholine glyceraldehyde modification on the PCU surface by a hydrophilic PEO spacer.
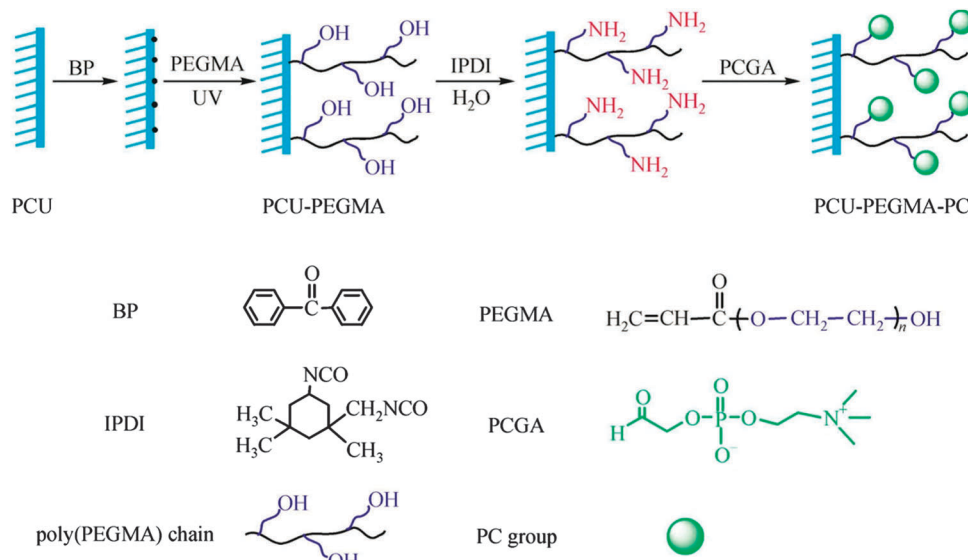
Fig. 14 Schematic illustration of grafting PEGMA and PCGA onto the PCU surface. Reproduced with permission from ref. 318. Copyright 2014 Springer.

photopolymerization[319,320] or SI-ATRP.[321,322] For example, MPC was grafted onto a PCU–PEG–Br surface *via* SI-ATRP. The required surface initiator for the biomimetic diblock copolymer brush of PEG-*b*-poly(MPC) was formed by the reaction between 2-bromoisobutyryl bromide (BIBB) and PEG on the PCU surface. Here, the grafted brush chains contained both soft PEG chains as a spacer and zwitterionic poly(MPC) chains as functional segments, as shown in Fig. 15.[322]

The hydrophilicity of the modified surfaces is in the following order: PCU < PCU-*g*-poly(PEGMA) < PCU–PEG–PCGA < PCU–PEG-*b*-poly(MPC). The structure and compositions of the grafted chains affected hydrophilic properties of the surfaces. The PCU-*g*-poly(PEGMA) surface showed a reduced number of adhered platelets 110 ± 21 number per mm^2 and PCU–PEG–PCGA surface demonstrated much lower platelet adhesion than the PCU-*g*-poly(PEGMA) surface. Significantly fewer platelets (10 ± 7 number per mm^2) adhered on PCU–PEG-*b*-poly(MPC), which was attributed to the synergistic effect of both blocks and the high content of PC groups on this modified surface. The number of adhered platelets on these modified surfaces is in the following order: PCU $\gg$ PCU-*g*-poly(PEGMA) > PCU–PEG–PCGA > PCU–PEG-*b*-poly(MPC), as shown in Fig. 16. This means that PC functional groups and PEG can improve anti-platelet adhesion; moreover, PC functional groups are more effective. In addition, the grafting of PC with a flexible

hydrophilic spacer is also a very effective method to prevent platelet adhesion.

Zwitterionic poly(3-dimethyl (methacryloyloxyethyl) ammonium propane sulfonate) (poly(DMAPS)) brushes have also been successfully grafted onto substrates for enhancing hemocompatibility by our group[298] and other groups.[323] Poly(DMAPS) brushes modified surfaces can decrease hemolysis, protein adsorption and platelet adhesion. Similar to the abovementioned PC modification results, the high coverage of grafted poly(DMAPS) can also improve surface hemocompatibility.

We have developed an approach by using poly(PEGMA-*g*-DMAPS) multicomb block copolymers to modify the PCU surface, in which the grafted PEG and sulfobetaine chains contribute synergistically to hemocompatibility, as shown in Fig. 17. These PCU–poly(PEGMA-*g*-DMAPS) surfaces were created by grafting DMAPS on a multifunctional macroinitiator PCU–poly(PEGMA–Br) surface, which was prepared by the reaction between BIBB and the hydroxyl groups of poly(PEGMA) on the PCU–poly-(PEGMA) surface. As expected, the PCU–poly(PEGMA–Br) surface had a significantly higher initiating activity, thus enabling a high grafting density of zwitterionic DMAPS chains. However, PCU–poly(PEGMA-*b*-DMAPS) surfaces modified by linear poly(PEGMA-*b*-DMAPS) block copolymers were prepared by grafting DMAPS on the remaining initiator species of the PCU–poly(PEGMA) surface, and they exhibited a contact angle of $30.5° \pm 2.6°$.
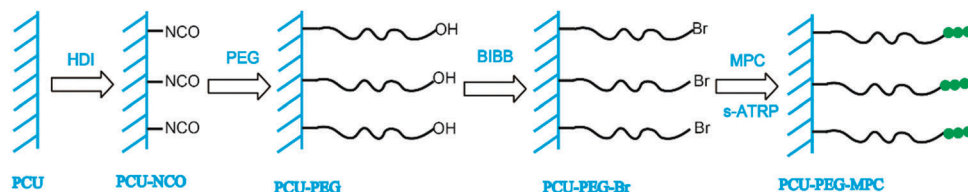

Fig. 15 The synergistic modification of the PCU surface with PEG and MPC. Reproduced with permission from ref. 322. Copyright 2012 Cambridge University Press.
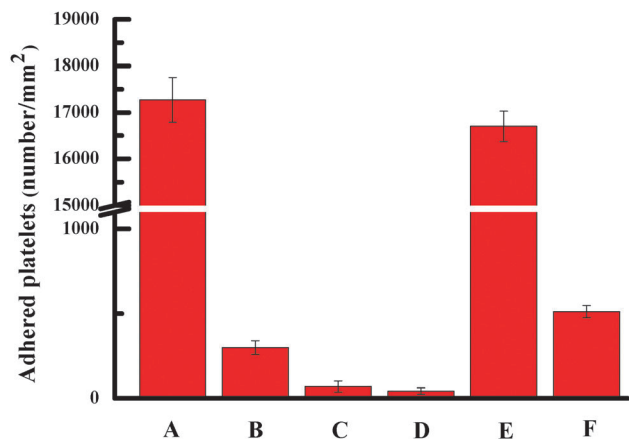
Fig. 16 Quantification of platelets adhering to the blank PCU (A), PCU-*g*-poly(PEGMA) (B), PCU–PEG–PCGA (C), PCU–PEG-*b*-poly(MPC) (D), PCU–PEG–Br (E), PCU–APEG (F) films.
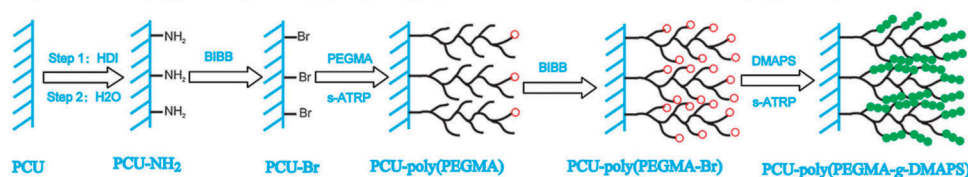
The PCU–poly(PEGMA-*g*-DMAPS) surface further showed high hydrophilicity with a low contact angle of $20.6° \pm 1.8°$ compared with the PCU–poly(PEGMA-*b*-DMAPS) surface. This might be attributed to the surface topology, which was more uniform for PCU–poly(PEGMA-*g*-DMAPS) compared with PCU–poly(PEGMA-*b*-DMAPS). Furthermore, the PCU–poly(PEGMA-*g*-DMAPS) surface showed very low platelet adsorption, which indicates that multicomb structure modified PCUs are preferred candidate materials for blood-contacting materials.[324]

In addition to surface modification by radical polymerization, we used a mild and friendly technique, *i.e.* a thiol–ene click reaction, to graft zwitterionic polynorbornene (poly(NSulfoZI)) onto the PCU surface.[325] Poly(NSulfoZI), which is a new emerging biomaterial,
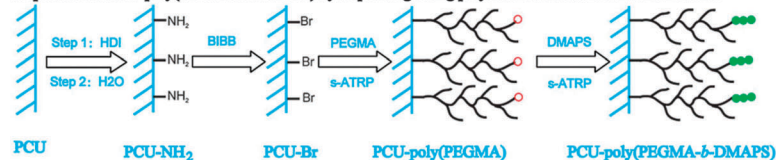
has many double bonds and zwitterions. Its zwitterionic moieties provide excellent hydrophilicity and non-fouling properties and the double bonds facilitate its modification. Free thiol groups were first introduced onto PCU surfaces by L-cysteine or β-mercaptoethanol, and then poly(NSulfoZI) was grafted by a photo-initiated thiol–ene click reaction. L-Cysteine was verified to be a proper thiol group donor with less toxicity in cell culture. In another way, thiol groups were first introduced onto poly(NSulfoZI) *via* a thiol–ene click reaction.[326] With HDI as the crosslinking agent, PCU was crosslinked with the thiolized poly(NSulfoZI). The poly(NSulfoZI) modified PCU showed good cytocompatibility and facilitated EC growth and proliferation.

More recently, Gao *et al.* found that the linked hydrophilic polymer chains such as PEG do not overlap at low grafting densities, but can rotate randomly without disturbance in the hydrate state and form a mushroom-like regime.[32] When the grafting density is high enough, PEG chains are in a crowed state and form a brush regime. Husson *et al.* also reported that poly(PEGMA) brush layers transformed from mushroom-like to brush regimes with an increase in grafting density.[327] This finding can explain why protein adsorption is reduced with the increase in grafting density. Generally, the grafting density of linear homopolymers and copolymers onto material surfaces depends on the concentration of active sites or initiators on the surfaces. One approach to increase the grafting density is to graft macromonomers with high molecular weights but unfortunately their reactivity is low. On the other hand, another approach is to introduce more initiators on surfaces as the abovementioned PCU–poly(PEGMA–Br). This method can graft more brushes onto surfaces by surface initiated polymerization.
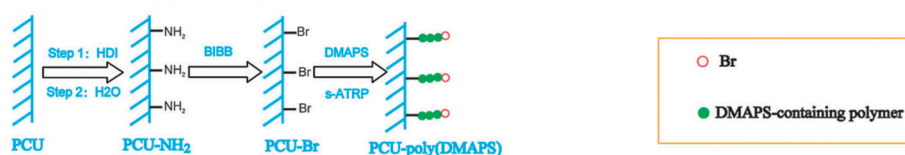

Fig. 17 Schematic of PEGMA and/or DMAPS grafting polymerization from PCU films *via* s-ATRP to prepare PCU–poly(PEGMA-*b*-DMAPS), PCU–poly(PEGMA-*g*-DMAPS), PCU–poly(DMAPS). Reproduced with permission from ref. 324. Copyright 2013 Wiley-VCH.

PTFE is a chemically and thermally stable material; thus, the surface modification of PTFE involves coating, high energy radiation, radiation-induced grafting process, and plasma treatment-induced grafting process.[328–332] For example, a doubly biomimetic random copolymer bearing cell antifouling PC groups and mussel adhesive protein catechol groups was adsorbed onto PTFE by the strongly adhesive catechol groups while at the same time forming a cell outer membrane mimetic antifouling surface.[333] These coated surfaces reduced protein adsorption and highly suppressed platelet adhesion from human serum. However, this modification needs a high catechol content (50%) in the copolymer to afford the effective adhesion on the hydrophobic PTFE surface. Furthermore, this research did not involve the stability of the modification layer *in vitro* and *in vivo*.

The PTFE surface was treated by high energy radiation in order to introduce active species, which was further used for the surface-initiated graft polymerization of acrylic acid (AAc). The grafting AAc onto the PTFE surface yielded a highly hydrophilic surface with significantly high water uptake when immersed in water. The carboxyl groups provided reactive sites for the immobilization of gelatin and other biomacromolecules so that the surface could adhere HUVECs and enhance their proliferation.[330] Another approach is covalently anchoring PC groups to the amine moieties of ammonia plasma-treated ePTFE arterial prostheses.[334] Interestingly, the PC grafting surfaces were homogeneous and stable to sterilization. They exhibited statistically lower thrombogenicity and lower neutrophil adhesion. Furthermore, they inhibited platelet activation, as well as showed good biocompatibility responses that were characterized by cell adhesion and proliferation.[334]

As another kind of zwitterionic material, polycarboxybetaines have also been used to modify biomaterial surfaces.[53,335,336] The modification methods are analogous with the abovementioned approaches for PEGMA, MPC and DMAPS. Interestingly, Jiang *et al.* first reported a non-fouling surface that contains a nanometer-scale homogenous mixture of balanced charge groups from counter-charged groups.[337] This surface is able to mimic zwitterionic polymer modified surfaces with the remarkable advantage of simple synthesis. More recently, the same group reported a biologically inspired stealth peptide sequence that is composed of alternating negatively charged glutamic acid (E) and positively charged lysine (K) residues. This alternating EK sequence mimics the surfaces of human proteins, which adapt to avoid nonspecific adsorption. This peptide sequence modified surface shows ultra-low fouling property because alternating charged groups are uniformly distributed at the molecular level to mimic zwitterionic groups. Its high resistance to nonspecific protein adsorption is comparable to what is achieved by PEG modified material surfaces. Moreover, this non-fouling functional peptide sequence can be extended with cyclic RGD to demonstrate specific cell targeting.[338,339] This method opens a new avenue to design and synthesize new non-fouling materials, and especially to modify biomaterial surfaces.

3.3 Surface modification of artificial vascular grafts by heparin

Heparin is a well-known anti-coagulation drug, which has the structure of a linear polysaccharide containing sulfonic,

carboxylic and sulfanilamide groups. The most common disaccharide unit of heparin is composed of 2-O-sulfated iduronic acid, and 6-O-sulfated and N-sulfated glucosamine residues. The anticoagulation function is based on its interaction with AT III, such as thrombin and factor Xa, which are serine protease inhibitors. The binding causes a conformational change in AT III, and accelerates the additional binding of serine proteases; thus, blood coagulation cascade can be prevented. Heparin has been successfully used to improve the hemocompatibility of biomaterials by coating,[340] covalent immobilizing,[341–343] and LbL technology.[344,345]

In our previous study, we covalently immobilized heparin and PC groups on the PU surface by the reaction between the amino groups of PU and the carboxyl groups of heparin as well as the aldehyde group of PCGA to improve surface biocompatibility and endow the surface with anticoagulant activity.[341] The immobilization amount of heparin can be tuned by controlling the grafting sites of PU, which has been first modified with PEI. The hydrophilicity and antithromboticity of the grafted surfaces were significantly improved with obviously decreased platelet adhesion.[341] We also used heparin and gelatin to prepare hemocompatible gelatin–heparin fibers as the inner layer and elastic PU fibers as the outer layer by sequentially using the electrospinning technology. Heparin retains its bioactivity after the electrospinning process. The controlled gradual release of heparin from these fibers is maintained over 14 days, which results in rare platelet adhesion *in vitro* and indicates a potential delivery system for the localized administration of heparin to the site of vascular grafts. These antithrombotic fibrous scaffolds have a high potential as artificial vascular grafts with appropriate mechanical properties.[26]

A number of covalent immobilizing heparin strategies have been investigated and evaluated.[271,346] Generally, for the immobilization of heparin onto biomaterial surfaces, amine or carboxylic acid groups should be first introduced to serve as the anchoring groups. For example, a biomaterial surface was pretreated using the plasma technology and UV-induced graft polymerization with AAc. Subsequently, heparin was covalently immobilized with the carboxylic acid groups of poly(AAc) *via* an esterification reaction using a 4-dimethylaminopyridine catalyst and dicyclohexylcarbodiimide (DCC) coupling agent.[347]

Another method involves the introduction of free amino groups onto material surfaces, such as the controlled aminolysis of a PDLLA film by 1,6-hexanediamine,[348] polydopamine-coated PLA and polyethylene membranes,[349,350] pulsed-plasma polymerized allylamine films on 316L stainless steel,[351] and surface prepared by the photopolymerization of *tert*-butyl-2-(acrylamide)ethyl-carbamate and deprotection of BOC groups.[352] Heparin modified surfaces are achieved by using a condensation reaction between the activated carboxylic acid groups of heparin by EDC–NHS and free amines on the surfaces.[189,353] In addition to aminated surfaces, a surface having hydroxyl groups such as poly(hydroxyethyl methacrylate) (PHEMA) was modified with low molecular weight heparin after activation by 1,1′-carbonyldiimidazole (CDI).[354] For the amplification of reaction sites of heparin, the "alkyne–azide" click chemistry technique was usually used in recent research.[197] The above methods for the preparation of heparin modified surfaces are based on covalent linkage formation between heparin and the

reactive groups of the substrates. However, they usually involve complicated multistep procedures and the heparin immobilization amount cannot be controlled precisely. Alternatively, Lee *et al.* reported a robust heparin coating method on the PU surface.[355] They prepared dopamine-conjugated heparin *via* the amidation reaction between the activated carboxylic acid groups of heparin and dopamine. 27% $\pm$ 8% of the carboxylic groups in heparin were conjugated with dopamine. The PU surface could be modified by immersion in an aqueous solution of dopamine-conjugated heparin. It is a simple and one-step procedure, and especially, neither plasma nor chemical pretreatment of the substrates is necessary. The heparinized surface by dopamine-covalent immobilization usually displays excellent hemocompatibility, and it is robust enough for long time immersion *in vitro*.

One heparin molecule has several carboxylic acid groups. These groups can react with amino groups and hydroxyl groups to yield multiple covalent linkages, which can robustly immobilize heparin on biomaterial surfaces. Multiple covalent linkages are able to prevent the immobilized heparin from being washed away when the surface is in contact with blood flow. However, the free movement of heparin molecules is hindered and restricted by the direct and unspecific immobilization. Therefore, the natural configuration of heparin might be affected and changed during and after immobilization. Thus, these immobilization methods may affect heparin activity after modification. One strategy to enhance the hemocompatibility of heparinized surfaces is to introduce a certain length hydrophilic spacer between heparin and the material surface. For example, heparin and PEG were sequentially immobilized onto a Ti surface *via* sequential immobilization using the carbodiimide covalent coupling method. This method can improve hemocompatibility and enhance EC adhesion and proliferation.[356]

Furthermore, the end point immobilization strategy has been proposed for surface modification of various materials by heparin. This strategy immobilizes each heparin molecule on the surface by a single covalent bond at the end of the heparin chain for the purpose of maintaining its natural configuration and bioactivity.[357] This process involves the partially controlled depolymerization of native heparin sodium with nitrous acid.[358] The terminal aldehyde of heparin is formed on the sugar unit of the cleavage site. Subsequently, heparin is covalently linked onto the material surface by a reductive amination reaction between the terminal aldehydes and the primary amines on the surface. End point immobilized surfaces have been proven to prevent activation of the coagulation cascade,[349,359] reduce platelet adhesion[353,360] and activation, as well as diminish complementary and inflammatory responses of blood to coated surfaces.[361]

Nowadays, the co-immobilization of heparin with other biomolecules onto biomaterial surfaces has been proposed as one of the most popular strategies to improve hemocompatibility and to prevent blood coagulation. For example, heparin-loaded mesoporous silica, catechol-modified chitosan and heparin were mixed together to form a heparin-releasing film, which was coated on a polydopamine-modified substrate. The long and narrow channels of mesoporous silica are beneficial for the sustained release of heparin. This heparin-releasing film shows low fibrinogen adsorption, platelet adhesion and hemolysis rate, which indicates good hemocompatibility.[362] Similarly, the co-immobilization of heparin with fibronectin can also improve the anticoagulant activity of heparin and obtain favorable hemocompatibility.[363] Fibronectin is an adhesion protein, which can promote EC attachment and spreading. Unfortunately, fibronectin can also cause platelet adhesion by the RGD peptide on itself and the integrin receptor on the platelet membrane. Interestingly, the co-immobilization of heparin and fibronectin may prevent platelet adhesion and blood coagulation. It is speculated that the reaction conditions, such as EDC and NHS, may enhance the anticoagulation activity of heparin and inhibit the platelet adhesion of fibronectin; however, the detailed mechanism is still unclear.

Heparin can also mediate cell adhesion and proliferation processes, which is unrelated to its anticoagulant activity. For ECs, heparinized PLLA/poly(L-lactide-*co*-ε-caprolactone) (PLLA/PLCL) scaffolds show good cellular attachment, spreading, proliferation and phenotypic maintenance *in vitro*. Furthermore, when subcutaneously implanted into New Zealand white rabbits, the heparinized scaffolds exhibited neovascularization.[364] Conversely, heparin could reduce SMC proliferation *in vitro* and *in vivo*, which may be determined by the overall level of sulfation and the disruption of exogenous or autocrine bFGF signaling. The heparin dose and release kinetics could sufficiently modulate the SMC phenotype, and significantly up-regulate SMC contractile markers such as smooth muscle α-actin (α-SMA).[365]

More recently, heparin and poly(L-lysine) (PLL) were mixed to develop a type of NPs *via* tight interactions between amine-rich PLL and negatively charged heparin.[366] These NPs were immobilized on a dopamine-coated surface to form a gradient surface of heparin.[367] The abundant amine groups of PLL are beneficial for the robust covalent immobilization of these NPs. It is noteworthy that the low heparin density (3.5 μg cm^{-2}) on the surface selectively prevented SMC proliferation but accelerated endothelialization.[367] Furthermore, a time-ordered heparin-releasing surface was developed by the immobilization of these NPs. In the early phase (1–7 days) after implantation, the surface released predominantly anticoagulant and anti-inflammatory substances and exhibited an antiproliferative effect against SMCs. After 7 days, EC proliferation was enhanced while SMC proliferation was selectively suppressed. Interestingly, the modified surface exhibited excellent properties *in vivo*, such as favorable hemocompatibility, anti-inflammatory effect, as well as inhibition of intimal hyperplasia.[340]

In order to immobilize heparin onto biomaterial surfaces, the LbL technology has also been utilized in recent research. Heparin is an anionic linear polysaccharide; thus, it can form a multilayer surface with cationic polymers or biomacromolecules by alternative immersion in their solutions.[368,369] Many cationic polymers or biomacromolecules have been used for this application such as PLL,[370,371] PEI,[372] poly(L-arginine),[373] collagen,[331] chitosan,[369,374] *N,N,N*-trimethyl chitosan,[375,376] kappa-Carrageenan,[377,378] and layered double-hydroxide.[379,380] Interestingly, heparin with other anionic polymers[381] or VEGFs[382] as the

This journal is © The Royal Society of Chemistry 2015

Chem. Soc. Rev., 2015, 44, 5680–5742 | 5701

polyanions has been employed to fabricate multilayers using LbL coating. Although LbL assembled multilayers have been successfully used in various areas of biomedical applications, they still suffer from a lack of stability, because this depends mainly on the electrostatic interaction between oppositely charged polymers.[381,383–385] In order to enhance the stability of LbL films, in the consideration of long-term applications in physiological media, chemical[386] and photo-crosslinking[387] methods have been employed to convert the interlayer forces from weak interactions to strong covalent bonds.

In addition, an interesting strategy has been explored by introducing catechol groups into branched PEI (bPEI) and anionic polymers. The catechol groups in multilayers can undergo rapid crosslinking through nonionic types of interactions (e.g., hydrogen bonding and π–π stacking) at biological pH conditions, thus enhancing stability. This catechol modification can serve as a general and efficient platform for various applications. The heparin/collagen multilayer-modified surface exhibits excellent hemocompatibility and promotes EC adhesion and proliferation.[388] Moreover, multilayer functionalized surfaces with the anti-CD133 antibody possess prolonged blood coagulation times, less platelet activation and aggregation, enhanced EC attachment and early rapid endothelialization *in vivo.*[331]

3.4 Surface modification of artificial vascular grafts by immobilization of gelatin and other bioactive macromolecules

Gelatin is a natural biomacromolecule, which consists of highly bioactive polypeptides that are derived from collagen in animal skin, bones and connective tissues. Generally, the triple helix structure of collagen is broken down into a single-stranded structure to form gelatin. Gelatin has many RGD integrin recognition sequences that are beneficial for cell attachment, migration, proliferation and differentiation. As a biological, excellently biocompatible, biodegradable and edible polymer, gelatin has attracted great interest in tissue engineering applications as well as in surface modification.

Gelatin is soluble in water above 40 °C, and the solution forms a gel when the temperature is cooled to room temperature. This sol–gel transition property limits its application in implantable materials and devices; thus, gelatin must be crosslinked to overcome this problem. Although many crosslinkers, such as glutaraldehyde, genipin, carbodiimide and epoxy compounds, can efficiently crosslink gelatin, cytotoxicity and chronic inflammation are usually caused by these chemical crosslinkers. Recently, microbial transglutaminase,[389–391] citric acid,[392] oxidized pectin[393–395] and alginate dialdehyde[396] have been used as nontoxic crosslinkers. In particular, gelatin can be crosslinked with alginate dialdehyde, oxidized pectin, gellan gum and K-carrageenan to form IPN materials by a combination of enzymatic and ionic crosslinking methods. An alternative approach involves methacrylated or acrylated gelatin by photopolymerization, which is controllable through the exposure time to UV light and irradiation intensity.[397–399] Methacrylated gelatin was synthesized by the reaction of methacrylic anhydride and the amine groups of gelatin. It has been proven to be able to deliver cells to generate vascular networks by *in situ* transdermal

photopolymerization. Interestingly, the proliferation, alignment and cord formation of ECs depend significantly on the micropattern structure. An optimal microstructure enables ECs to form a circular and stable cord structure. This is a preceding step to create tubulogenesis for engineered tissue constructs.[399]

In order to maximally utilize the excellent properties of gelatin in tissue engineering, gelatin has also been immobilized on biomaterial surfaces or modified with various materials.[400] For example, gelatin has been immobilized onto AAc-grafted PLCL biomimetic dual-layered scaffolds through EDC/NHS chemistry. These dual-layered scaffolds have one microfibrous layer and one nanofibrous layer. The gelatin modified microfibrous layer exhibited the proliferation and infiltration of SMCs owing to its large pores and coupled gelatin, while the nanofibrous layer accelerated proliferation of ECs.[401] Thus, these specially designed dual-layered scaffolds can alternatively mimic native blood vessels for use in vascular tissue engineering. Choong et al. used ATRP to graft glycidyl methacrylate onto the PCL surface to introduce epoxy side groups and subsequently covalently immobilize gelatin. The gelatin modified PCL surface showed significant improvement in EC attachment and growth and low expression of thrombogenic markers.[138] However, the non-specific reactivity of epoxide groups of poly(glycidyl methacrylate) towards surface proteins on ECs may also compromise normal cellular signaling activity and lead to the upregulation of inflammatory responses.[138] More recently, we grafted PEGMA on PCU nanofibrous scaffolds and then immobilized gelatin to obtain PCU-g-PEGMA-g-gelatin scaffolds. The scaffold surface changed from hydrophobic to hydrophilic and showed low platelet adhesion and excellent EC growth and proliferation.[402] Gelatin has also been modified by various compounds to change its hydrophilic and chemical properties. For example, gelatin reacted with phosphonobutyric acid in the presence of water-soluble carbodiimide, and the obtained phosphorylated gelatin had many phosphoric acid groups. This phosphorylated gelatin could enhance cell adhesion, as well as the binding affinity of gelatin to titanium surfaces.[403] Hydrophobically modified gelatin was achieved by the reaction of the amino groups of gelatin with hexanoyl chloride, decanoyl chloride and stearyl chloride. The hexanoyl chloride-treated gelatin possessed high wettability and significant cell adhesion compared with the others. Although the mechanism is not clear, the paper speculated that the hexanoyl residue can easily interpenetrate the surface of blood vessels and effectively enhance the bonding strength between the films and tissues.[404] Gelatin has also been electrospun to prepare gelatin nanofibrous scaffolds, but their mechanical properties are too poor, thus to improve their mechanical properties, gelatin was co-electrospun with synthetic polymers[405,406] and inorganic components.[407] The composite nanofibers exhibited enhanced biocompatibility over their counterparts that were composed solely of synthetic polymers owing to the biofunctions of gelatin. However, most of the gelatin exists in the bulk of the fibers, which reduces the availability of gelatin. The core–shell structured fiber with gelatin as a shell layer can maximally utilize the biological properties and biofunctions of gelatin as well as maintain the excellent mechanical properties of synthetic polymers.[408]

5702 | *Chem. Soc. Rev.*, 2015, **44**, 5680–5742

This journal is © The Royal Society of Chemistry 2015

The LbL technology can be used to immobilize gelatin and its derivatives onto biomaterial surfaces. Because gelatin is a negatively charged biopolymer, it was alternatively deposited with positively charged PEI onto an aminolyzed poly(propylene carbonate) surface. The outermost layer of the formed polyelectrolyte multilayer surface was covered by crosslinked gelatin. This surface showed high hydrophilicity, biocompatibility, and enhanced cell attachment and proliferation. On the other hand, when gelatin was treated with ethylenediamine and N'-(3-dimethylaminopropyl)-N'-ethylcarbodiimide hydrochloride, cationized gelatin was obtained. Positively charged cationized gelatin and negatively charged hyaluronic acid were alternatively coated on the surface of a PET artificial ligament graft by LbL self-assembly, and the modified surface efficiently enhanced cell adhesion, facilitated cell growth, as well as suppressed the expression of inflammation-related genes relative to the pure PET graft *in vitro*. The *in vivo* results proved that the surface inhibited inflammatory cell infiltration and promoted new tissue regenerated graft fibers.[409,410]

Serum albumin is a small and highly abundant plasma protein, which has highly specific functions, such as maintaining the colloid osmotic pressure in the blood and improving the hemocompatibility of materials. Many studies have demonstrated that albumin immobilization on material surfaces can mask the complement-activity sites and reduce thrombosis and hemolysis rate of biomaterials.[411–413] Although the pre-adsorbed protein surface inhibits thrombogenic protein adsorption and decreases platelet adhesion and activation, these functions will be lost by protein exchange when the surface is in contact with blood. Hence, the covalent immobilization of albumin is proposed as an effective method to overcome this limitation. Yin *et al.* successfully grafted poly(AAc) onto polypropylene non-woven fabric membranes with O_2 plasma treatment and the UV-irradiated technology, and subsequently grafted BSA onto the surface in the presence of EDC and NHS.[414] Zhu *et al.* immobilized BSA onto a porous polyethylene surface using strongly attached polydopamine as a spacer. The albumin immobilized surface exhibited excellent hemocompatibility because of albumin's biofunctions.[412] More recently, Yin *et al.* reported another approach to immobilize BSA onto polypropylene. They used SI-ATRP to create a surface with PEG and epoxy functional groups, followed by covalently immobilizing BSA by the ring-opening reaction of the epoxy groups.[413] The non-fouling ability as well as BSA conjugation sites were successfully controlled by adjusting the monomer ratio of PEGMA and glycidyl methacrylate. These modified surfaces showed low hemolysis rates, remarkably suppressed platelet adhesion and activation, as well as inhibited thrombosis formation. It is noteworthy that the excellent hemocompatibility is due to the hydrophilicity of the comb-like structures of the PEG chains and inertness of BSA. In conclusion, their high hydrophilicity and strong resistance of plasma protein adsorption provide an outstanding platform for the construction of hemocompatible surfaces.[415] Ji *et al.* successfully prepared multilayer films consisting of PEI and albumin on a biomedical surface *via* the electrostatic self-assembly technology. The multilayer coating exhibited excellently stability in Tris-HCl (pH 7.35) buffer solution for 21 days, and less than 10% albumin was

eluted by PBS in 45 days. This stable multilayer coating could resist platelet adhesion effectively.[416]

More recently, Chang *et al.* reported a protein-based conjugate with a biodegradable polyester for the first time. They used a tailor-made initiator to introduce a maleimide functional group into PCL *via* the ROP of ε-caprolactone with stannous octoate as a catalyst, and then covalently linked it to reduced BSA *via* the maleimide–sulfhydryl coupling reaction. The biodegradable amphiphilic BSA–PCL conjugate biohybrid displayed a well-defined structure, low cytotoxicity, excellent biocompatibility and self-assembly behavior.[417]

Although numerous surface modification approaches have been investigated with the purpose to create a surface to prevent clot formation, it appears that the ideal and complete anticoagulation of biomaterial surfaces is still difficult to be realized. An alternative approach is to design surfaces with natural fibrinolytic functions or clot dissolving ability. To prepare a biomaterial surface with these biofunctions, biomaterials are modified by the coating or immobilization of bioactive substances, such as tissue plasminogen activator (t-PA), urokinase and streptokinase.[418–422] For example, the streptokinase coenzyme was coupled onto the functionalized graft copolymer poly(vinyl chloride)-*g*-poly(ethylene glycol)methacrylate using the water soluble carbodiimide 1-ethyl-3-(3-dimethyl aminopropyl carbodiimide hydrochloride) and sulfo-*N*-hydroxysulfo succinimide.[420] Another example is the covalent immobilization of streptokinase on poly-glycerol dendrimer (generation 5) using 1-cyano-4-(dimethylamino)-pyridinium tetrafluoroborate.[423] PEG phospholipid conjugates bearing a maleimide group (Mal–PEG–lipid) and poly(vinyl alcohol) with thiol groups were used to immobilize urokinase.[419] The Mal–PEG–lipid anchored to cell membranes and further conjugated with thiolated urokinase and thrombomodulin by the reaction of thiol and maleimide. The bioactivity of the immobilized urokinase and thrombomodulin was maintained, and this modification prevented thrombus formation on the material's surface. Chen *et al.* prepared lysine modified poly(vinyl alcohol) in which the lysine residues have free ε-amino and carboxyl groups, because lysine with these functional groups has specific tethering affinity for t-PA. This surface can efficiently lyse the formed clot in *in vitro* plasma assays; moreover, the quantities of tethered t-PA on the surface and its release could easily be regulated by varying the blend ratio. An analogous chemical modification method was used to prepare a fibrinolytic PU surface by conjugating lysine to the distal terminus of surface-grafted PEG. The plasminogen adsorption and lysing fibrin ability were affected by the length of the PEG spacer. When the number average molecular weight of PEG was 300 g mol^{-1}, the lysine modified surface was more effective in lysing fibrin, which was formed on the surface, in advance for the purpose of analysis.[286] This new finding provides us with an interesting candidate and approach to develop vascular grafts and other blood contacting devices.[424]

We have reviewed the current and most promising surface modification strategies to develop improved hemocompatible surfaces for artificial vascular grafts, which include highly hydrophilic surfaces, heparin immobilized surfaces, and gelatin or other bioactive molecules modified surfaces. Although these approaches have been demonstrated to be efficient methods

individually, combining two or more of these approaches may be more beneficial for artificial vascular grafts. The modified vascular graft surfaces have been proven to have superior hemocompatibility *in vitro via* the immobilization of anticoagulants, bioactive molecules, PEG and zwitterionic polymers, but very few have achieved successful results *in vivo*. A potential reason for the failure of these modified surfaces involves the inadequate retention of surface chemistry and bioactivity once exposed to blood flow.[117] For example, the oxidation susceptibility of PEG may limit its long-term applications in biological environments because platelets can be adsorbed on some PEG modified surfaces during *in vivo* experiments.[317,425] Compared with PEG modified surfaces, surfaces modified by zwitterionic polymers or groups are relatively stable in biological environments, and show excellent anti-protein adsorption properties.[426] Moreover, heparin immobilized surfaces can also suppress platelet adhesion and protein adsorption, thus enabling biomaterial surfaces to possess superior hemocompatibility. Heparin can selectively accelerate endothelialization but prevent SMC proliferation at low heparin densities, while high densities are unsuitable for vascular cell proliferation and endothelium regeneration. Therefore, heparin density, bioactivity and the inherent short half-life of the immobilized heparin should be addressed in surface modification.

Surface modification strategies have successfully improved the hemocompatibility of artificial vascular grafts, but an ideal non-thrombogenic surface is still yet to be identified. The ideal graft surface should have superior hemocompatibility and regulate blood-graft responses spatiotemporally, enhance endothelialization, and accelerate to form an endothelial monolayer. The physical, biological and chemical properties of the surfaces need to be integrated and tuned for artificial vascular graft applications.

4. Surface modification for enhancing the endothelialization of artificial vascular grafts

In order to improve the hemocompatibility of artificial vascular grafts, one option is to functionalize their inner surface with the aim to minimize protein adsorption as well as to inhibit platelet adhesion and activation. For this purpose, hydrophilic surfaces have been created by various approaches such as linking hydrophilic polyethers or zwitterionic moieties onto the surface of the vascular graft. Examples for improving the hydrophilicity of artificial vascular grafts include surface grafting with PEGMA, PEG, MPC, DMAPS and monomers having carboxybetaines, as well as the immobilization of heparin, gelatin and other bioactive compounds. These surface modifications can enhance surface hemocompatibility, but at the same time highly hydrophilic surfaces hinder ECs from attaching onto and covering the graft. However, completely covering the inner surface of an artificial vascular graft with a biofunctional and confluent layer of ECs could mimic healthy blood vessel tunica intima and in this way potentially enable the long-term applicability of such implants. Otherwise, the lack of endothelialization in synthetic

grafts usually results in low patency rates in the long-term studies.[427] Hence, it is a tough challenge for researchers to specifically enhance adherence, migration and proliferation of ECs on hydrophilic and protein repellent surfaces.

It is generally assumed that rapid endothelialization and re-endothelialization of artificial vascular grafts *in situ* play a key role to prevent thrombus formation and avoid the restenosis of artificial grafts. Since cell adhesion onto an artificial scaffold is an important early stage in the generation of an EC layer on a material's surface, many strategies have been developed to enhance or endow surfaces with the ability to specially and selectively adhere ECs. Most of them involve immobilizing or fixing cell adhesive proteins and active peptides on the surface of artificial vascular grafts, which can promote EC adhesion and *in situ* rapid endothelialization on them.[428] Compared with proteins, active peptides have simple structures and high stability. Furthermore, active peptides can be coated, covalently grafted or immobilized onto material surfaces by either physical absorption or chemical reactions. In this section, we will review several active peptides and their applications in EC proliferation and endothelialization.

4.1 Surface modification by RGD peptide and RGD derived peptides

Usually, biological recognition between cell–surface receptors and their ligands is the key switch to mediate cell migration and adhesion in physiological environments. Integrins are the major cell–surface adhesion receptors to extracellular matrix proteins.[429] Integrins and their ligands that engage and activate integrin adhesion receptors on the cell surface play leading roles in cell spreading and proliferation.

The tripeptide sequence of Arg–Gly–Asp (RGD) was identified by Pierschbacher and Ruoslahti in 1984 as a minimal essential cell adhesion peptide sequence in fibronectin,[430] and now is known to serve as a recognition motif in multiple ligands that bind to numerous integrin species, especially integrins $\alpha_5\beta_1$ and $\alpha_v\beta_3$. In this view, the RGD tripeptide is by far the most often employed peptide sequence to modify synthetic biomaterial surfaces for simulating and promoting cell adhesion. Artificial vascular grafts, which are made from synthetic materials, usually exhibit perfect mechanical properties, biocompatibility and hemocompatibility. However, their surfaces, especially highly hydrophilically modified surfaces, often suffer from poor cell adhesion. Therefore, numerous approaches have been developed to promote EC adhesion and proliferation by modifying artificial vascular grafts with RGD. Fig. 18 summarizes the five usually used immobilization methods of the RGD peptide on material surfaces by different reactions. In most cases, RGD can be immobilized onto the surface of artificial vascular grafts through a stable amide bond, which is formed by the reaction of surface carboxylic acid groups and the free amino group at the N-terminus of the RGD peptide. In order to avoid side reactions between the carboxyl acid group of the RGD peptide and its own amine group, protected RGD peptides were usually used in some of the early immobilization studies.[431] However, in recent years, approaches involving carboxyl active esters have been developed
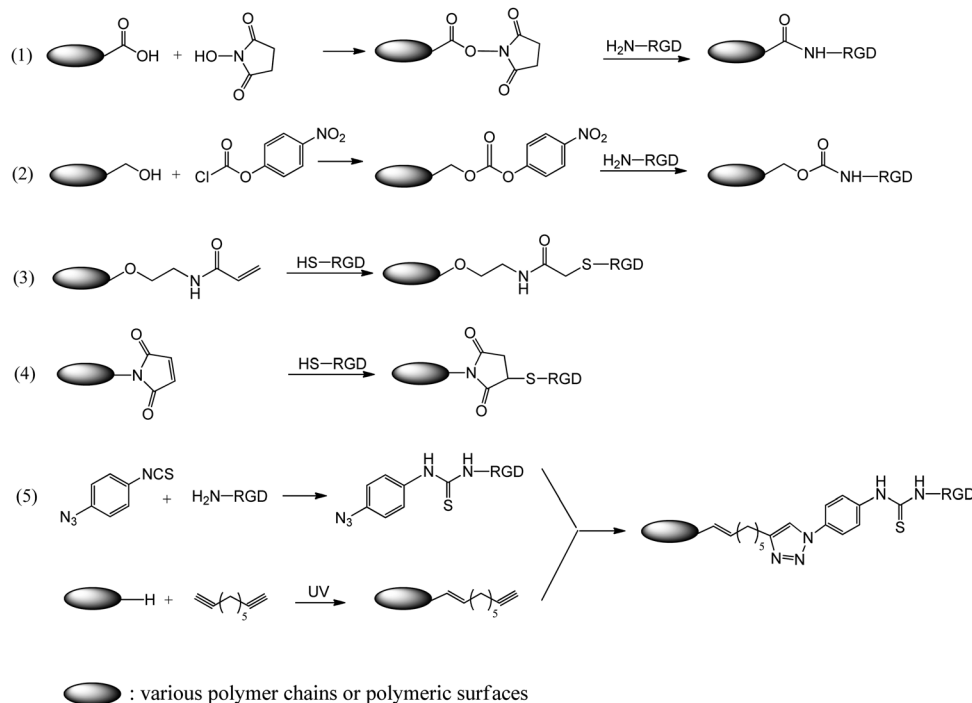
Fig. 18 Immobilization methods of the RGD peptide on biomaterial surfaces by different reactions: (1) activation of the carboxyl acid groups on the material's surface with NHS; (2) activation of the hydroxyl groups on the material's surface with p-nitrophenyl carbonate; (3) thiol-RGD peptide reacts with acrylic derivatives via the Michael addition reaction; (4) thiol-RGD peptide reacts with maleinimide via the Michael addition reaction; (5) immobilization of the RGD peptide via the azido–alkyne click reaction.

to link unprotected peptides to polymer chains and biomaterial surfaces. This technology makes the covalent immobilization of peptides easier and simpler than the protection and deprotection route. This is attributed to the activation of carboxyl acid groups with NHS, usually in the presence of EDC, DCC, CDI or water-soluble carbodiimide as a condensation agent.[432] Alternatively, if the material surface has hydroxyl groups, the pre-activation can be performed by tresyl chloride[433] and p-nitrophenyl carbonate.[434] Another approach involves using the Michael addition reaction: the RGD peptide is functionalized with thiol groups, such as by linking a cysteine to its end; thus, it could be immobilized via the Michael addition reaction onto acrylic ester or maleinimide functionalized surfaces.[435] Furthermore, click chemistry[436] and photo-induced reactions have also been employed to immobilize the RGD peptide to material surfaces.[437] In particular, the azido–alkyne click reaction offers a versatile and simple method to the specific immobilization of peptides on biomaterial surfaces by phenylazido-derivatized peptides.

As mentioned above, immobilizing the RGD peptide onto biomaterial surfaces generally requires the surface to have some reactive groups such as hydroxyl, amino or carboxyl groups. However, most biocompatible and biodegradable polymers of artificial vascular grafts do not have such functional groups on their surfaces to afford immobilization reactions with peptides. Therefore, some strategies have to be developed to solve or avoid this problem. One of the most popular approaches is the coating technology, by which some polymers containing peptide functional groups have been coated onto

substrate surfaces to realize surface modification with good initial cell adhesion. For example, Kong et al. modified electrospun tubular PCL grafts with Nap-FFRGD using the surface coating method. The Nap-FFRGD molecule contains both the RGD peptide and hydrophobic naphthalene group, which can self-assemble onto hydrophobic PCL surfaces to form an RGD coating layer.[438] The modified surface shows improved hydrophilicity and can enhance cell adhesion and spread in vitro.[438,439] In particular, the encouraging in vivo results have proven that this modified graft exhibits an excellent inhibition of platelet adhesion and can enhance cell infiltration, endothelium formation and high patency.

An alternative route, which involves a hydrophobic polymer with pendant RGD, has been used to produce RGD functionalized graft surfaces. Marchant's group synthesized a peptide fluorosurfactant polymer (PFSP), which was coated onto ePTFE vascular grafts to facilitate the adhesion and growth of ECs.[440] Firstly, a reactive glutaraldehyde-modified RGD peptide was synthesized by the Schiff base reaction of the terminal amine group of RGD with excess glutaraldehyde. Secondly, this peptide was attached to a poly(vinyl amine) backbone. Finally, perfluorocarbon chains were covalently linked onto this backbone by the reaction with N-(perfluoroundecanoyloxy)succinimide. These hydrophobic perfluorocarbon pendant branches enable them to be adsorbed onto the ePTFE surface[441] and they formed a stable layer in the test time (4 weeks). However, the hydrophilic peptide ligands migrated toward the surface during dip-coating and provided the modified surface with a stable attachment, growth and

This journal is © The Royal Society of Chemistry 2015

Chem. Soc. Rev., 2015, 44, 5680–5742 | 5705

function of ECs. This is a simple, quantitative and effective approach to physically modify ePTFE compared with other methods. The dip-coating method has also been used to modify the PU surface with a multiblock copolymer through strong hydrogen bonding. The multiblock copolymer has a "CBABC"-type structure with a central diurethane A block to form hydrogen bonds with the PU chains on the surface, which could improve the coating stability. The B block is a PEG spacer arm with a cleaving methanesulfonyl end group as the C block, on which the RGD peptide can be covalently immobilized *in situ* by the cleavage of the original mesyl end group. The PEO and RGD-modified surfaces are highly hydrophilic, exhibit good compatibility with HUVECs, and effectively promote HUVEC growth.[442] In addition, RGD has also been attached to PLL and subsequently coated on PLA surface to immobilize the RGD sequence.[443] However, coating methods have some drawbacks such as complicated preparation procedures, and only limited amounts of the peptides can be stably immobilized on substrate surfaces. Recently, researchers have developed a facile coating method based on polydopamine to immobilize peptides on implantable materials in order to improve coating stability.[444,445] RGD and other peptides have been successfully immobilized onto polydopamine-coated polystyrene,[446] PLGA,[447,448] PLCL,[449,450] as well as decellularized vein matrix.[445] In order to increase the immobilization efficiency of peptides, lysine with an ε-amine group or cysteine with a thiol group has been attached to the N-terminus of peptides.[445,446] Alternatively, copolymerization is another strategy to introduce functional peptide sequences onto biomaterial surfaces. Deng *et al.* synthesized a biodegradable triblock copolymer of PEG-*b*-PLA-*b*-PLL by the ROP of 3-benzyloxy-carbonyl-L-lysine *N*-carboxyanhydride with amino-terminated PEG–PLA–NH$_2$ as a macroinitiator. The pendant amino groups of the lysine residues were used to link RGD peptides.[451] Moreover, 3-[*N*^{ε}-(carbonyl-benzoxy)-L-lysine]-6-L-methyl-2,5-morpholinedione has also been used to introduce pendant amine groups by the ROP with LA and other morpholine-2,5-dione derivatives, following the deprotection of the protected groups.[162,452]

An additional strategy to modify surfaces involves introducing functional groups into polymer chains or onto biomaterial surfaces by chemical treatment, plasma treatment,[453] γ-irradiation graft polymerization,[454] or SI-ATRP,[455,456] and subsequently immobilizing peptides. For instance, Choi *et al.* chemically modified PU materials by a two-step reaction to enhance EC affinity. They grafted a PEG spacer containing an amine group onto electrospun PU matrix, followed by immobilizing the RGD peptide *via* amidation.[457] Causa *et al.* treated a PCL substrate with aminolysis by diamine solutions, and then the resultant primary amine groups on the PCL surface tethered **GRGD**Y peptides.[458]

Nowadays, RGD-modified biomaterials and surfaces have been investigated extensively. Many studies have demonstrated that RGD peptide modified surfaces show excellent cell adhesion and proliferation. Furthermore, the cell proliferation rate on RGD-modified surfaces mainly depends on the RGD peptide density. A high RGD density on the surface favors rapid proliferation of ECs. It should be noted that the retention of biological activity of peptides after surface immobilization may be affected by the

chemical covalent immobilization because of their short sequences. This means that the specific peptide sequences, retention bioactivity and surface density of peptides are critical for guiding these cellular responses. Thus, several Lys and glycine molecules are incorporated at the N-terminus of peptides, which could act as a spacer to endow the bioactive motifs with easier interaction with cells.[459] Moreover, a polymerizable peptide containing the RGD sequence, *i.e.* acrylamide-terminated peptide containing the biologically active sequence AAM–Gly–Gly–Arg–Gly–Asp–Ser (AAM–GG**RGD**S), has been used to modify biomaterial surfaces *via* surface initiated free radical polymerization.[460] This approach provides us with a method to control the RGD density on modified surfaces. However, the synthesis of polymerizable acrylamide-terminated or acrylate-terminated peptides often involves solid phase synthesis with acryloyl chloride.[461,462] These synthetic methods have serious limitations on the large scale and in the application of high molecular weight PEG. Alternatively, a simple synthetic route was reported through the conjugation of the **GRGD**S peptide to acrylate–PEG–NHS or activated PEGMA by free **GRGD**S peptides or **GRGD**S trifluoroacetate salt in the presence of CDI.[463]

More interestingly, a facile immobilization method of the RGD peptide on electrospun PU meshes was performed in the presence of tyrosinase and P**RGD**GGGGGY peptide in 0.01 M PBS at 37 °C for 1 h.[464] The amount of immobilized peptide varied from 0.045 to 0.120 nmol per mg-mesh when the peptide concentration was increased from 0.1 to 2.0 mg mL^{-1}. Tyrosinase catalyzed the oxidation of phenol molecules into *o*-quinones in the presence of oxygen and conjugated peptides on various polymer surfaces;[465,466] however, the conjugation mechanism of *o*-quinone groups is still unclear.[467]

Ding *et al.* found that the immobilizing site affected the bioactivity of the c(–**RGD**fK) modified amphiphilic triblock copolymer PCLA–PEG–PCLA.[45] When c(–**RGD**fK) was immobilized to the hydrophobic blocks (PCLA) by the end-capping reaction with succinic anhydride, followed by coupling with c(–**RGD**fK) in the presence of EDC and NHS, the PEG corona shielded the peptide on the hydrophobic block, thus decreasing its biofunction. On the other hand, this peptide was immobilized onto the hydrophilic PEG block by photografting a bifunctional linker (4-(*p*-azidophenyl)-*N*-succinimidyl butanoate) and then by the reaction with the free ε-amino group of Lys in the cyclic peptide. This immobilized c(–**RGD**fK) onto PEG block could stretch out of the PEG corona; thus, the modified surface enhanced cell adhesion much more significantly than peptides in hydrophobic blocks. This effect is also due to the spacer function of PEG because a sufficient spacer plays an important role in ligand–receptor binding.[468,469] It is to be noted that PEG in the modified polymers acts as a hydrophilic block as well as a spacer. More recently, Ding *et al.* further successfully prepared nanopatterns of RGD on a non-fouling PEG hydrogel with five RGD nanospacings, from 37 to 124 nm, to study cell adhesion and differentiation.[470] They used the transfer lithography strategy to provide the surface with a strong and persistent non-fouling background against cell adhesion,[471] so that the adhesion results could exhibit the effect of RGD-nanopatterns only, but not the background's adhesion. They found that the cell density and spreading area decreased with the increase of nanospacing, which is consistent with previous studies

5706 | *Chem. Soc. Rev.*, 2015, **44**, 5680–5742

This journal is © The Royal Society of Chemistry 2015

about cell adhesion.[472,473] Since integrin has a size of about 12 nm, each RGD ligand on the nanopatterns can eventually bond to a single integrin. The nanospacing of the RGD ligand determines the integrin nanospacing in the cell membrane. Furthermore, the effect of the RGD nanospacing on cell shape parameters was evaluated quantitatively. As shown in Fig. 19, the cell circularity increased with the increasing RGD nanospacing, but the average aspect ratio of the cells did not change significantly. This finding of the nanospacing effects is stimulating for new biomaterial surface design with the appropriate spatial arrangement of ECM-mimetic ligands.

It is to be noted that numerous studies have demonstrated that linear RGD and cyclic RGD peptides can enhance EC adhesion, growth and proliferation.[445,474] The linear RGD, **GRGD**SP, **GRGD**NP and **RGD**SPASSKP sequences are selective for $\alpha_5\beta_1$, while cyclic RGD peptides, which include GPen**GRGD**SPCA and cyclo(**RGD**f(NMe)V), bind preferentially to $\alpha_v\beta_3$.[475] Compared with linear RGD, cyclic RGD peptides are usually stable *in vivo* in the presence of enzymes.[428]

Apart from the enhancement of EC adhesion and growth, RGD functionalized vascular grafts usually lead to platelet deposition and adhesion, because the RGD peptide has the ability of recognizing $\alpha_{IIb}\beta_3$ integrin and mediating platelet adhesion.[476] Although platelets are absorbed on the surface, they are still not activated, so neither thrombosis nor coagulation is formed, although some studies have observed thrombosis or coagulation formation. The possible explanation for this is that the modified surfaces are not completely covered by peptides. If only a few enzyme molecules become activated, they will initiate coagulation since the coagulation process is an amplification cascade event. In addition, RGD motifs can selectively target and bind integrin GPIIb–IIIa on the activated platelets.

Generally, vascular graft surfaces should be designed or modified to facilitate the promotion of EC attachment, proliferation, and *in vivo* rapid endothelialization, whereas minimizing platelet adhesion. To accomplish this goal, the ligands on the vascular graft surface should predominantly interact with EC adhesion receptors such as $\alpha_v\beta_3$ and $\alpha_5\beta_1$ but not platelet-adhesion receptors such as $\alpha_{IIb}\beta_3$. Unfortunately, RGD and cRGD modified surfaces usually adhere platelets significantly; furthermore, a high proportion of the adherent platelets exhibit spread morphology.[477] This is because RGD and cRGD predominantly
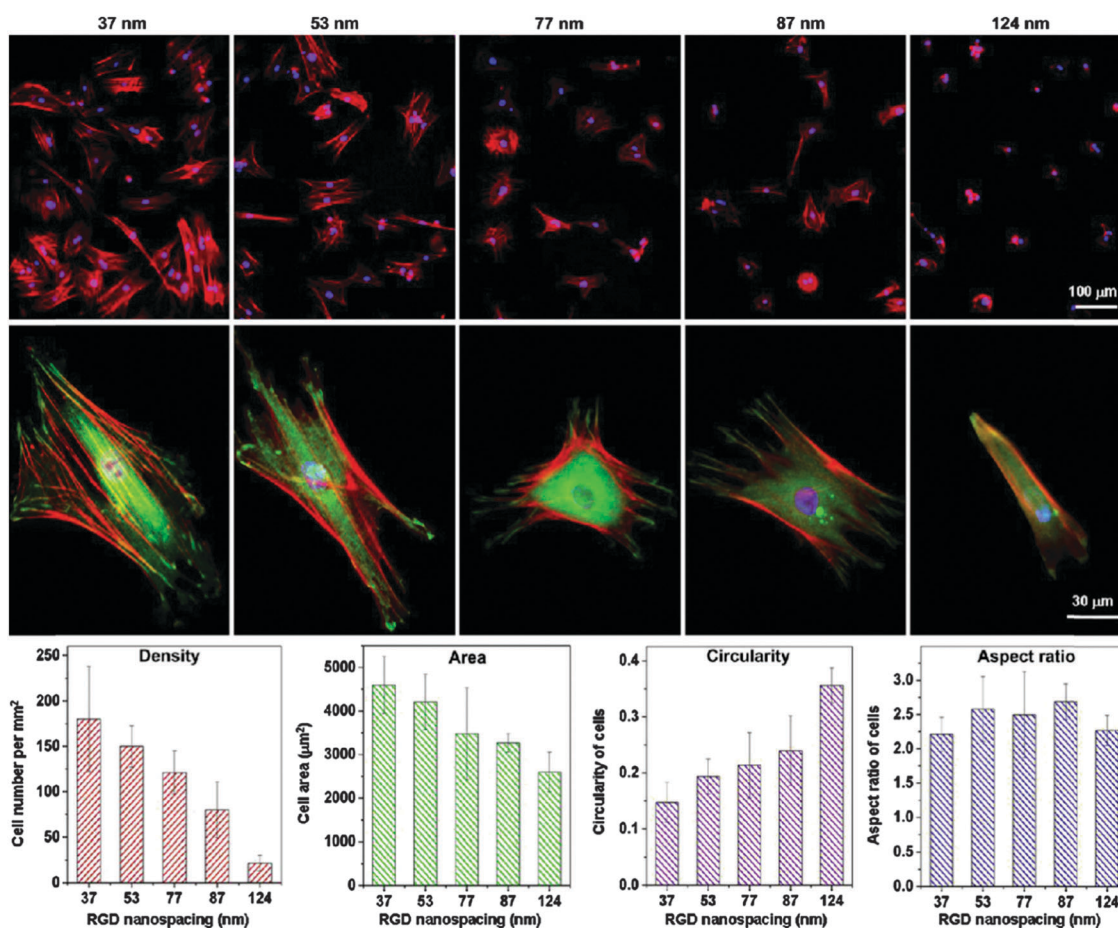

Fig. 19 Cell adhesion on nanopatterned surfaces with various nanospacings. The top and middle rows show low-magnification and high-magnification fluorescent micrographs of MSCs cultured on nanopatterns for 24 h, respectively. Cells were stained to visualize F-actins (red), vinculins (green) and nuclei (blue). MSCs on the surfaces of the small RGD nanospacings got high densities and exhibited more spreading morphology, more mature skeleton and stronger focal adhesion. The bottom graphs are statistical results of the cell adhesion: the *p* values from Student *t*-tests are listed in supplementary Tables S2–S5 in ref. 470. Reproduced with permission from ref. 470. Copyright 2013, Elsevier.

interact with the integrin β-subunit while various integrins possess the same β-subunit.[478] This means that they may be insufficient to selectively adhere ECs over platelet adhesion. In contrast, another peptide, cRRE, exhibits significantly lower affinity for $\alpha_{IIb}\beta_3$ than the RGD peptide but similar affinity for $\alpha_5\beta_1$. In addition to extensive interactions with the β_1-subunit through the Arg–Arg–Glu sequence, cRRE has a Trp residue that can interact with the Trp residue on the α_5-subunit.[479] As a result, cRRE is more suitable for selectively promoting integrin binding in ECs than RGD and cRGD peptides.

In addition to anti-platelet adhesion and EC-selective adhesion as important goals in the modification of artificial vascular grafts, the balanced control of the adhesion and proliferation of ECs and SMCs is another critically important factor during vascular regeneration. The competitive growth of SMCs or other cells can interfere with the formation of an endothelial monolayer, thus leading to low patency of artificial vascular grafts *in vivo*.[480] As is well known, RGD and its derivative peptides can enhance the adhesion of many types of cells; thus, novel peptides should be screened and found to have selective binding biofunctions to the special integrins in ECs.

4.2 Surface modification by CAG peptide

Kato *et al.* screened the EC- or SMC-selective tripeptides from the specifically enriched tripeptides in collagen type IV, but not in types I, II, III and V by the peptide array-based interaction assay of solid-bound peptides and anchorage-dependent cells.[481,482] They found 12 novel EC-selective tripeptides (cell-selective rate >1.0, in Table 1) and SMC-selective tripeptides (cell-selective rate <−1.0). Among these EC-selective tripeptides, the Cys–Ala–Gly (CAG) tripeptide possesses the best EC-selective function according to the cell-selectivity adhesion assay. The CAG peptide has high affinity for ECs, but its affinity for SMCs is far lower than RGD. To further evaluate the EC-selective performance of CAG peptide modified materials, PCL was blended with the CAG peptide to fabricate a fine-fiber sheet with the peptide concentration <1.0 nmol mm^{-2} using the electrospinning technique.[481] The results showed that CAG significantly enhanced EC adhesion on this modified PCL sheet *in vitro* under serum-free conditions, with a nearly twofold rate compared to SMCs. Moreover, ECs were found to spread widely and cover an apparently large area of the CAG modified sheet, while SMCs appeared shrunken and rounded. It is clear that CAG can enhance EC adhesion and at the same time inhibit SMC adhesion.

In 2012, Narita *et al.* prepared a small-diameter vascular graft (0.7 mm in diameter and 7 mm in length) from PCL and the CAG peptide. The degree of endothelialization of the inner surface of the grafts was significantly higher for the CAG modified graft group than the control group. After 6 weeks implantation, the degree of endothelialization was up to 97.4% ± 4.6% for the CAG modified graft group *versus* 76.7% ± 5.4% for the control group, while no significant difference in patency rate was observed *in vivo*.[483]

In the view of the CAG peptide's high specificity for EC adhesion, we functionalized the PCU surface by covalently

Table 1 List of cell-selective tripeptides. Reproduced with permission from ref. 481. Copyright 2012, Wiley Periodicals, Inc.[a]

Cell selectivity	Number	Sequence	r_{RATIO} (—) EC	SMC	Cell-selective rate (—) ((r_{RATIO} of ECs) − (r_{RATIO} of SMCs))
EC	1	CAG	2.85	1.18	1.67
	2	CNG	2.68	1.05	1.63
	3	CSG	2.43	0.88	1.55
	4	GYL	2.57	1.24	1.32
	5	CNY	2.25	0.94	1.31
	6	PCG	2.56	1.37	1.19
	7	CDG	2.31	1.16	1.15
	8	AVA	2.19	1.05	1.15
	9	FLM	2.03	0.90	1.14
	10	GPY	2.38	1.28	1.10
	11	GCP	3.07	2.01	1.06
	12	QAL	1.97	0.94	1.03
SMC	1	DGY	1.35	3.04	−1.69
	2	SLW	1.01	2.47	−1.46
	3	EGF	1.10	2.45	−1.35
	4	HSQ	1.06	2.34	−1.28
	5	EAP	0.98	2.22	−1.24
	6	CNI	0.96	2.15	−1.20
	7	GFG	2.47	3.59	−1.12
	8	RND	1.13	2.18	−1.05
	9	PFI	1.01	2.03	−1.02
	10	SYW	1.28	2.29	−1.01
		RGD	3.20	2.29	0.91

[a] Note: the relative ratio of cell adhesion (r_{RATIO}) of individual cells was obtained by comparison to the negative control. Cell selective rates were expressed as the difference between the r_{RATIO} of ECs minus the r_{RATIO} of SMCs.

linking the CAG peptide *via* photo-initiated thiol–ene click chemistry.[484] Firstly, we grafted hydrophilic PEGMA and the active monomer pentafluorophenyl methacrylate onto the PCU surface to form diblock copolymer or brush copolymer modified surfaces *via* SI-ATRP. After postpolymerization modification with allyl amine, the formed pendant allyl groups on the surfaces were functionalized with the cysteine terminated short peptide sequence CAG *via* photo-initiated thiol–ene click chemistry. These peptide modified surfaces exhibited selective and rapid growth of ECs in the co-culture of ECs and HASMCs. Furthermore, they reduced platelet adhesion and activation in contact with platelet-rich plasma for 2 h. Therefore, CAG functionalized surfaces may be an effective anti-thrombogenic platform for vascular tissue engineering application.

To the best of our knowledge, there are only three publications about the EC-selectivity of the CAG peptide since this peptide was first identified to have this special function *in vitro* in recent years. Its biofunctions still need more investigations to be proven *in vitro* and *in vivo*.

4.3 Surface modification by REDV peptide

The tetrapeptide, Arg–Glu–Asp–Val (REDV), is a fibronectin-derived peptide that can specifically bind to the $\alpha_4\beta_1$ integrin, which is abundant on ECs, whereas scarce on SMCs. Owing to its special ability to selectively adsorb and proliferate ECs rather than SMCs,[47,476,485] REDV has gained much attention in the surface modification of biomaterials, especially for the

enhancement of rapid endothelialization because of its specific affinity with ECs.

Seeto et al. investigated the dynamic adhesion of endothelial progenitor cells (EPCs) to REDV peptide-grafted hydrogels. They conjugated REDV to acryloyl–PEG–succinimidyl valerate and then grafted it onto poly(ethylene glycol) diacrylate hydrogels.[486] REDV is able to capture endothelial colony forming cells (ECFCs, one type of EPCs) under flow since it can specifically interact with the surface receptor on ECFCs. Furthermore, REDV-grafted hydrogels reduce the ECFC rolling velocity to a significantly greater extent. This demonstrates that the ECFC rolling velocity depends on the particular grafted PEG–REDV peptide and indicates that $\alpha_4\beta_1$ integrin bound by REDV maybe play an important role in ECFC rolling.

Ji et al. successfully immobilized the REDV peptide onto the PET surface by dip-coating in a reactive copolymer solution, followed by the covalent conjugation of the REDV peptide.[47] They synthesized several binary copolymers via the conventional radical polymerization of BMA and p-nitrophenyloxycarbonyl poly(ethylene glycol)methacrylate (MEONP with $n1$, $n6$ and $n10$ indicate the repeating unit number of the PEG block), whereas terpolymers were prepared from PEGMA, BMA and MEONP by the same method. PET films were coated with the reactive copolymers and then reacted with the REDV peptide in PBS (pH 7.4) at 4 °C for 24 h. Through this method, PEG chains and REDV peptides were introduced onto the PET surface with different structures. They gave a schematic of the modified surfaces to clearly understand the mechanism of nonspecific resistance and specific adhesion, which is due to PEG and the REDV peptide, respectively (Fig. 20). It is well known that the density and length of PEG play an important role for the nonspecific resistance of PEG modified surfaces. When PET surfaces were modified by binary copolymers with a short PEG spacer ($n < 10$) and end tethered REDV peptides, the surfaces exhibited slight selectivity for ECs over SMCs. However, the modified surfaces by the terpolymers with free PEG chains and end tethered REDV peptides, especially for $n = 6$, showed significant HASMC adhesion resistance, but promoted HUVEC attachment, proliferation and growth. The short PEG chains ($n = 6$) in the terpolymers are more suitable for forming EC selective surfaces in co-cultures of HUVECs and HASMCs than long chains because long PEG chains possess a strong repulsion effect, which inhibits the attachment of all types of cells including HUVECs and HASMCs. Thus, REDV peptides on modified surfaces can effectively exhibit high selectivity for HUVECs, but only when the surfaces have a suitable structure, as well as the PEG chains have optimal length.

Ji et al. and Yuan et al. further fabricated several antifouling polymers with EC selectivity by covalently immobilizing REDV peptides onto zwitterionic polycarboxybetaine copolymers,[53] phosphorylcholine copolymers,[487] polysaccharide multilayer surfaces and polysaccharide hydrogels.[488,489] Synergic effects of antifouling hydrophilic zwitterionic carboxybetaine, phosphorylcholine, or polysaccharide and bioactive peptide REDV have been demonstrated by these modification methods. In particular, zwitterionic carboxybetaine not only offers a functionalizable binding site for the REDV peptide but also helps to realize selectivity because of its resistance to SMCs. In addition, the surface modification by REDV–phosphorylcholine copolymers was performed via the reaction of poly[2-methacryloyloxyethyl phosphorylcholine-co-n-stearyl methacrylate-co-p-nitrophenyloxy-carbonyl poly(ethylene glycol)methacrylate] and REDV similar to the above-mentioned PEG and REDV method. The modified surfaces exhibit superior hemocompatibility and antifouling properties. More importantly, they are able to enhance the competitive growth of ECs, and inhibit the adhesion, proliferation, and migration of SMCs. The in vivo results have successfully demonstrated that the competitive ability of ECs over SMCs plays a very important role in the development of a pure confluent layer of ECs and the attainment of a better anti-restenosis effect.[480]

More recently, Yuan et al. investigated cell migration, adhesion and proliferation with in vitro as well as in vivo tissue responses and blood vessel formation on REDV, RGD and YIGSR peptide modified alginate scaffolds.[489] REDV exhibited the best ability to enhance EC proliferation and promote angiogenesis in vivo. Furthermore, the REDV-modified alginate scaffold showed selective adhesion to HUVECs and enhanced the completive growth between ECs and other cell types. The blood vessel density in the cambium fibrous tissue of the REDV-modified alginate scaffold was about 1.5 times higher than that of other scaffolds.

In addition to the above-mentioned modification methods for the introduction of REDV onto biomaterial surfaces, dopamine was electropolymerized with REDV to construct bioactive
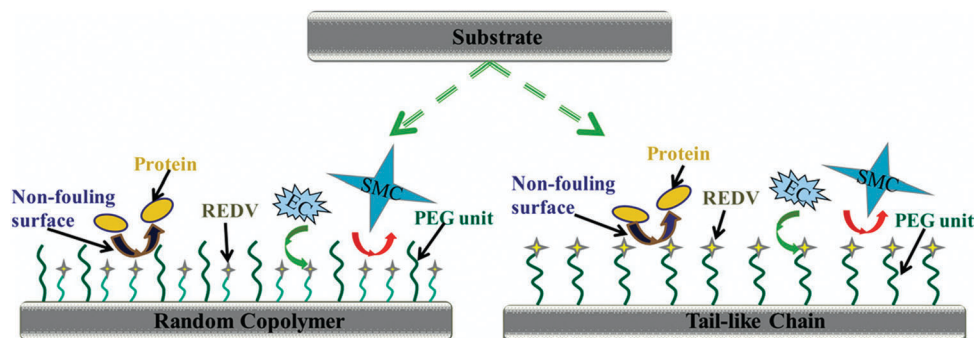

Fig. 20 Schematic illustration of different surfaces coated with the REDV peptide. Reproduced with permission from ref. 47. Copyright 2011, Elsevier.

functionalized surfaces *via* a one-pot strategy using precisely controlled electrochemical parameters. This one-pot modification method is an easy and rapid way to create a bioactive molecule modified surface on complicated conductive biomaterials and devices.[490,491]

4.4 Surface modification by YIGSR peptide

Tyr–Lle–Gly–Ser–Arg (YIGSR) is a segment of the basement membrane matrix glycoprotein laminin. YIGSR is crucial for binding to integrin $\alpha_4\beta_1$ on the cell membrane. YIGSR peptide mediates the attachment and migration of cells including ECs, fibroblasts and SMCs.[492] Furthermore, the YIGSR peptide can interact with the 67 kDa laminin binding protein (67LR), which is highly expressed on the membrane surface of ECs.[493]

Hubbell *et al.* grafted the YIGSR peptide onto PET and PTFE surfaces by the reaction of the N-terminal amine of the peptide with surface hydroxyl moieties using tresyl chloride chemistry. In order to increase the grafting density, the surfaces were first hydroxylated to yield high hydroxyl containing surfaces and then conjugated with the peptide. The YIGSR-grafted surface supported cell adhesion and spreading, even when only albumin was present, while the control groups (PET and PTFE surfaces) did not support adhesion.[494] By incorporating the GGG**YIGSR**GGGK peptide sequence into a polymer backbone, Jun and West synthesized a bioactive polyurethaneurea, which may improve the endothelialization of vascular grafts.[495] In addition, YIGSR was used to modify hydrogels,[496] PLLA nanofibers, PLGA films and nanofibers,[497,498] poly(3-hydroxybutyrate-*co*-3-hydroxyhexanonate),[499] poly(ethylene-*co*-vinyl alcohol),[500] nanostructured polyurethane–poly(lactic-*co*-glycolic acid) scaffolds,[501] polystyrene carboxylated nanoparticles,[502] as well as decellularized blood vessels.[445]

Recently, Gao *et al.* successfully fabricated a complementary gradient surface of PHEMA brushes and YIGSR peptides using a dynamically controlled reaction process.[492] Based on this complementary gradient, the selective directional migration of one type of cells over another type has been investigated and evaluated. ECs exhibited a significant preferential orientation and enhanced directional migration behavior on the gradient surface toward the region of lower PHEMA density and higher YIGSR density, while SMCs did not show either preferred directional migration or enhanced mobility on the gradient surface as shown in Fig. 21.[492] This important finding indicates that the specific interaction between ECs and material surfaces plays a decisive role in the selective guidance of EC migration over SMCs. YIGSR can selectively enhance and induce EC migration along peptide modified surfaces, such as the inner surface of vascular grafts, and thus guide ECs to form an endothelial layer.

4.5 Surface modification by other active peptides

In addition to the abovementioned peptide sequences for surface modification, many other active peptides with cellular recognition have also been investigated. The Ser–Val–Val–Tyr–Gly–Leu–Arg (SVVYGLR) sequence is an integrin-binding site which is adjacent to the RGD sequence in osteopontin.[503] The SVVYGLR sequence can be recognized by the $\alpha_4\beta_1$, $\alpha_4\beta_7$, $\alpha_9\beta_1$ and $\alpha_v\beta_3$ integrins.[504,505]
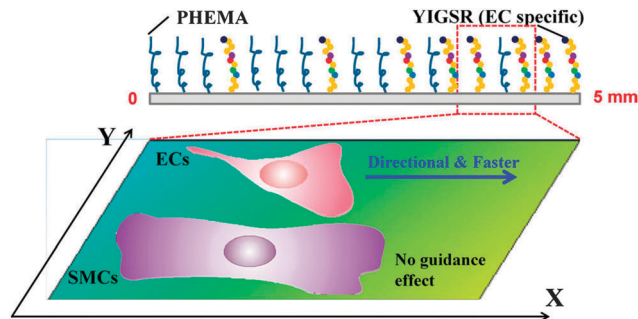

Fig. 21 Schematic illustration to show the structure of the complementary density gradient of PHEMA and YIGSR and its influence on the mobility of ECs and SMCs. The direction of increased YIGSR density and decreased PHEMA density is defined as the "+X" direction. Reproduced with permission from ref. 492. Copyright 2014, American Chemical Society.

The SVVYGLR peptide can be adhered to ECs sufficiently and also potentiate migratory activity, while it does not influence EC proliferation ability.[506]

Lei *et al.* used the cell adhesive RGD peptide, EC specific REDV and YIGSR, or angiogenic SVVYGLR sequence to functionalize the PET surface. They covalently immobilized each peptide individually or two kinds of peptides combinatorially onto the PET surface.[507] When the surface was modified by the combination of RGD with SVVYGLR or YIGSR peptide, the peptide functionalized surfaces can significantly induce EC adhesion, spreading and migration, which takes advantages of the synergy effects of both peptides. This modification method is beneficial for promoting the endothelialization of vascular grafts.

As discussed in this section, various peptides have been immobilized onto biomaterial surfaces to promote the endothelialization of artificial vascular grafts. However, it should be noted that different peptide sequences show different effects on EC adhesion, spreading and migration on biomaterial surfaces. RGD as a cell adhesion peptide can enhance the adhesion and proliferation of various types of cells, while YIGSR and SVVYGLR peptides seem to improve cell spreading and migration effectively.[507] The different biofunctions of various peptide sequences are associated with integrins, which are a family of heterodimeric transmembrane adhesion receptors.[429] RGD consists of hydrophilic amino acid residues and could be recognized by many integrins. Moreover, different peptides mediate different cell signaling pathways, which consequently results in different levels of cell spreading and migration. For example, the RGD and REDV peptides have been proven to induce inhibition of cell spreading and migration,[507] while the YIGSR peptide can enhance the adhesion and spreading of ECs.[508] In addition, the SVVYGLR peptide has an important ability to promote EC migration.[506]

For the endothelialization of artificial vascular grafts, it should be comprehensively considered to balance various factors, which include peptide sequences and appropriate peptide density, with the aim to obtain optimal or suitable adhesion, spreading and migration of ECs. For example, cell attachment and spreading are mainly related to both the peptide density and peptide distribution on biomaterial surfaces for a certain peptide. A certain level of RGD density can

enhance cell migration on biomaterial surfaces because it is beneficial for the formation of a focal contact, but a too high level leads to reduced cell migration, resulting in an overall biphasic relation of ligand density and cell migration.[428] Therefore, in order to optimize EC specific responses and promote the endothelialization of artificial vascular grafts, it is necessary to consider peptide sequences and their density as well as distribution on surfaces to take advantage of them. Furthermore, with the development of the 3D bioprinting technique,[509] artificial vascular scaffolds with hierarchical structures can be produced to mimic the physiological assembly of blood vessels with surface lining ECs and underlying SMCs. The 3D bioprinting technique can precisely control the concentration and distribution of cells, peptides, growth factors and other bioactive molecules in scaffolds. Through the understanding of peptide biofunctions and the development of the 3D bioprinting technique, ECs and SMCs will be selectively or preferentially cultured in different layers of scaffolds and consequently novel artificial vascular grafts may be developed.

5. Gene delivery for enhancing the endothelialization of artificial vascular grafts

Surface modifications with PEG, zwitterionic polymers, heparin, gelatin, targeting peptides and other bioactive macromolecules have been demonstrated to significantly have positive effects on hemocompatibility, EC attachment and spreading, which are beneficial for artificial vascular grafts. However, rapid endothelialization on artificial vascular grafts is a complex process that mainly involves EC adhesion, migration, proliferation and differentiation, which are regulated by numerous signals.[510] ECM proteins act as nonsoluble cues to modulate cell fate through cell signaling cascades. Numerous growth factors, in particular, VEGFs and bFGF, are implicated in the regulation of EC activities and new blood vessel formation either by direct binding to cellular transmembrane receptors or to ECM proteins. Moreover, the interactions between ECs and SMCs in the blood vessel wall may also control the growth and function of blood vessels, while *in vitro* these interactions can affect the gene and protein expression of angiogenic factors.

Gene engineering is an alternative and favorable strategy to enhance endothelialization because a new endothelial layer on vascular graft surfaces can be rapidly created *via* transfected ECs. The success of gene transfer into cells plays an important role for the transfection efficiency of ECs. However, owing to the intrinsic resistance to foreign genes, the transfection efficiency of ECs is relatively low in direct intravascular gene transfer. Hence, the transfer of genes into ECs usually needs highly efficient gene carriers. To increase the transfection efficiency of ECs, the selection of reasonable gene carriers, efficient cell growth factors and specific genes for EC growth and proliferation are significantly important. Although viral gene carriers are more efficient than non-viral gene carriers for gene delivery, they may bring serious risks to patients.[511] On the other hand, non-viral gene carriers are inherently safer than

viral gene carriers.[512,513] Furthermore, non-viral gene carriers have many advantages, such as simple preparation, possible versatile modifications to enable them with targeting function, as well as less immunogenicity. Nowadays, non-viral gene carriers, such as liposomes, PEI, oligoethylenimine modified polymers, cationic dendrimers and cationic polysaccharides, have been widely used in gene delivery because of their safety and practical application.[514–526]

Gene complexes that are prepared from non-viral gene carriers, cell growth factors and genes, have been commonly used to enhance the endothelialization of artificial vascular grafts. Another promising method for the selective and efficient transfer of genes into specific cells, such as ECs, involves multifunctional gene carriers or systems with targeting functions.[527] Excellent active targeting ligands and peptides endow gene carriers with specific cell targeting ability and high transfection efficiency. In this section, we will review several non-viral gene carriers and their applications in EC proliferation and endothelialization.

5.1 Non-viral gene carriers in gene delivery for the endothelialization of artificial vascular grafts

5.1.1 Liposomes as gene carriers. Liposomes have been developed as non-viral gene carriers for the transfection of ECs. They are composed of three parts, *i.e.* a cationic headgroup, hydrophobic chains and a connector linking these two parts. The cationic headgroup can bind with negatively charged DNA *via* electrostatic interactions, which play an important role in the transfection efficiency of liposome–DNA complexes, while hydrophobic chains affect the crimping capacity of liposomes. In addition, the connecting linker determines the stability and biodegradability of liposomes. Simultaneously, this linker can also provide reaction sites for targeting and diagnostic reagents. Nowadays, *N*-[1-(2,3-dioleyloxy)propyl]-*N*,*N*,*N*-trimethyl-ammonium chloride (DOTMA),[528] 1,2-dioleoyl-3-trimethylammoniumpropane (DOTAP),[529] dioctadecylamido-glycylspermine (DOGS)[530] and 2,3-dioleyloxy-*N*-[2(sperminecarboxamido)ethyl]-*N*,*N*-dimethyl-1-propanaminium trifluoroacetate (DOSPA)[531] are commercially available lipid reagents.

In 1997, Nabel *et al.* first investigated whether liposome-mediated gene transfer into HUVECs is feasible. They evaluated the transfection efficiency of β-galactosidase or the placental alkaline phosphatase gene into HUVECs by cationic liposomes and compared them with the particle-mediated gene transfer by biolistics, calcium phosphate and DEAE-dextran.[532] The results of this study demonstrated that gene expression was detectable in a high percentage (20.28% ± 1.38%) of HUVECs after transfection by liposomes while biolistics-mediated transfection was less efficient (3.96% ± 0.37%), and the transfection efficiency of calcium phosphate and DEAE-dextran were the lowest with the values of 2.09% ± 0.33% and 0.88% ± 0.21%, respectively.

In addition to HUVECs, the transfection of corneal ECs by liposome-mediated carriers has also been extensively described in early reports.[533,534] Dannowski *et al.* used Lipofectamine™ as a carrier to transfect plasmids coding for the acidic fibroblast

This journal is © The Royal Society of Chemistry 2015

Chem. Soc. Rev., 2015, **44**, 5680–5742 | **5711**

growth factor (aFGF) and enhanced green fluorescent protein (eGFP) into human corneal ECs, and then compared it with other commercial transfection reagents: DMRIE-C™, DAC-30, Effectene™ and FuGene™6. The transfection efficiency and toxicity of these gene carriers as well as the corresponding proliferation of human corneal ECs were investigated. The results showed that Lipofectamine™ transfected corneal ECs more successfully than the other carriers, transfection efficiency (17% ± 2.02%) was the highest and toxicity was low. Unexpectedly, only the DAC-30–FGF complexes resulted in an evident proliferation of corneal ECs, while the other carriers did not result in any proliferation.[533]

It should be noted that the low transfection efficiency limits liposome application in the gene therapy although liposomes are safe gene delivery carriers for ECs. Therefore, many modification methods have been investigated to improve the transfection efficiency of liposome-mediated complexes such as structural modification *via* manipulation of the cationic headgroup, hydrophobic chains and connecting linker.[534–536] Moreover, physical methods can also contribute to promote the transfection efficiency in ECs.

Negishi *et al.* developed a type of peptide-modified bubble liposomes (BLs) as pcDNA3-Luc plasmid carriers to improve the transfection efficiency of HUVECs by ultrasound (US).[537] The liposomes were prepared by a reverse-phase evaporation method using dipalmitoylphosphatidylcholine (DPPC), 1,2-distearoyl-phosphatidylethanolamine-methoxy-poly(ethylene glycol) (DSPE-PEG2000-OMe) and 1,2-distearoyl-*sn-glycero*-3-phosphatidyl-ethanolamine-poly(ethylene glycol)-maleimide (DSPE-PEG2000-Mal). The EC-targeted peptide, Cys-AG73, was grafted onto these liposomes by the reaction of the cysteine in the Cys-AG73 peptide and the maleimide in the liposomes. Then AG73 peptide-modified BLs (AG73-BL) were prepared by filling perfluoropropane gas into the cavity of the corresponding liposomes. As shown in Fig. 22, AG73-BL can specifically bind to tumor angiogenic HUVECs *via* the recognition of the AG73 peptide to the syndecan of tumor HUVECs. When these AG73-BL attached with HUVECs and were exposed to

ultrasound, the bubble was destroyed immediately. This forms an instantaneous jet stream in the cavity of AG73-BL, which results in a large ejection of extracellular plasmid or other nucleic acids into the cytosol. Subsequently, the capability for plasmid to enter into cells is enhanced. Their results confirmed this interesting strategy. The transfection efficiency was significantly improved when AG73-BL attached to HUVECs was exposed to ultrasound compared with BL-modified with no peptide or inactive peptides. Moreover, cell viability was higher than 80% after transfection by AG73-BL.[537]

Lajunen *et al.* used microfluidic technology to control the size of liposomes with the aim to prepare small-sized liposomes for increased penetrability into cells.[538] As is known to all, the size of gene carriers is an important factor for entrance into cells, especially retinal pigment epithelium, because the capillaries below the retinal pigment epithelium are densely fenestrated with small pores. The diameter of these pores is only 75–85 nm. This means that the size of the delivery carriers used in eye drops must be smaller than 85 nm to reach the posterior segment of eyes. Hence, they used microfluidizer methods to prepare small sized liposomes (<85 nm, as the test group) and large sized liposomes (≥100 nm, as the control group), and the effect of liposome sizes on their *in vivo* distribution in rat eyes after topical administration was investigated. The results exhibited that liposomes with diameters less than 80 nm could permeate the retinal pigment epithelium, while liposomes with diameters of 100 nm or more were distributed to the choroidal endothelium. The great significance of their research on the transfection of ECs is the microfluidic technology that controls the size of gene carriers, which may be used in the optimization of other gene carriers to achieve high transfection efficiency.[538]

The above results have demonstrated that liposomes act as a safe gene carrier for the transfection of ECs, while their transfection efficiency should be improved for applications in gene therapy. Thus, new technologies and other non-viral gene carriers needed to be explored for improving the transfection efficiency of ECs.
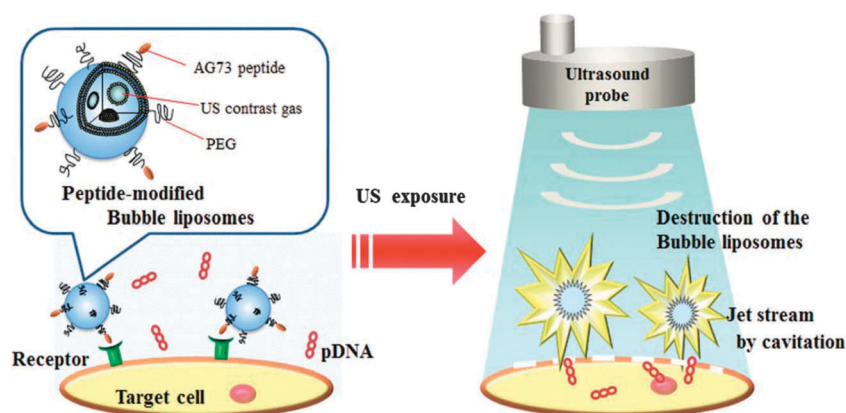

Fig. 22 Scheme of gene transfection with AG73-BLs exposed to US. If AG73 peptide-modified BL, which can attach to the cell membrane of HUVECs, is used for gene delivery in combination with US exposure, after binding the AG73-BL onto the cell membrane of the HUVECs and exposing it to US, it may be possible for efficient cavitation to be induced on the target cell membrane, which leads to efficient gene delivery into the target cell. Reproduced with permission from ref. 537. Copyright 2013 Wiley Periodicals, Inc.

5712 | *Chem. Soc. Rev.*, 2015, 44, 5680–5742

This journal is © The Royal Society of Chemistry 2015

5.1.2 Polyethyleneimines as gene carriers. Because of its high charge density capacity, PEI is one of the most efficient and widely used non-viral carriers in gene delivery systems both *in vitro* and *in vivo*.[539,540] The abundance of amine groups endows PEI with easy protonation ability at pH 6–8 in biological conditions. PEI is usually divided into bPEI and linear PEI (lPEI) according to its chain architectures and they are prepared by different synthetic methods. bPEI can be synthesized by the polymerization of aziridine under acid catalysis,[541] while lPEI is usually prepared by the ROP of 2-ethyl-2-oxazoline, followed by acid hydrolysis using an excess of hydrochloric acid.[542] The preparation of lPEI is tanglesome because of the low reaction temperature required and repeated purification processes.

Since PEI shows relatively high transfection efficiency and acceptable cytotoxicity, PEI-mediated gene carriers have achieved great success in gene therapy. PEI has become a strong alternative candidate as an effective non-viral gene carrier. It has been approved that the transfection efficiency of PEI is mainly connected with its molecular weight and chemical structure. High molecular weight PEI shows high transfection efficiency but it is often accompanied with significant cytotoxicity.[543] Therefore, reducing its cytotoxicity is requisite for gene delivery. PEGylation is one of the most frequently used methods for modifying high molecular weight PEI and other gene carriers.[544,545] PEGylated PEI can create a hydrophilic exterior that improves the biocompatibility of polycationic gene carriers. Zhang *et al.*[546] prepared a series of PEG 5 kDa conjugated PEI 25 kDa (PEG–PEI) copolymers with different PEG grafting densities and investigated their cytotoxicity and transfection efficiency to ECs as pEGFP–VEGF165 gene carriers. Their results proved that PEG–PEI copolymers showed low cytotoxicity compared with PEI 25 kDa, and the transfection efficiency was influenced by the number of PEG side chains in PEG–PEI, as well as the molar ratio of PEI nitrogen to DNA phosphate (N/P ratio) in the PEG–PEI–DNA complexes. When the mass ratio of PEG and PEI was 1/9 and N/P was at 30, the transfection efficiency reached a maximum value, which was much higher than that of PEI 25 kDa. In addition, the results also demonstrated the increased expression of the VEGF protein and accelerated EC proliferation after transfection. Their research indicated that PEGylated high molecular weight PEI can be used as effective gene carriers for the delivery of the pEGFP–VEGF165 gene and further promote endothelialization. In addition to PEGylation modification of PEI, partial acetylation has also been used to shield the amino groups and reduce PEI intrinsic cytotoxicity and genotoxicity. Calarco and coworkers prepared bPEI 25 kDa nanoparticles (PEI-NPs) and partially acetylated bPEI 25 kDa modified PLGA nanoparticles (AcPEI-NPs) by using the emulsion–solvent-evaporation method.[547] The biocompatibility and genotoxicity of these two kinds of NPs were investigated by using ECs as model cells. The produced reactive oxygen species (ROS) in endocytosis was determined to evaluate the genotoxicity of the NPs using the DCFH-DA assay. The equivalent cellular viability of PEI-NPs and AcPEI-NPs exhibited that their biocompatibility was basically consistent, while their genotoxicity and transfection efficiency were significantly different. The AcPEI-NPs did not increase ROS-production at 50–300 μg mL^{-1} nanoparticle concentration.

However, an ROS increase in a dose-dependent manner could be clearly found in the PEI-NPs group. Based on the mechanisms of the genotoxic effect,[548] the production of ROS probably damaged plasmid DNA, which would cause serious genotoxicity. Calarco group's and other groups' studies[549] demonstrated that the partial acetylation of PEI and other cationic polymers could reduce the toxicity of gene carriers, which provides us with an alternative method to prepare low toxic gene delivery carriers for the transfection of ECs.

Compared with bPEI, lPEI consists of two primary amine groups and abundant secondary amines, which act as both proton donors and acceptors. This chemical structure endows lPEI with lower toxicity than bPEI carriers with a similar molecular weight.[550] However, unfortunately, lPEI cannot efficiently buffer at a low pH in secondary lysosomes, which limits the escape of gene complexes from lysosomes. The number of publications about modified lPEI is far less than that of modified bPEI; furthermore, very few studies involve chemically modified lPEI and its application in the field of transfection and proliferation of ECs lines. One example of modified lPEI is the glucose-grafted lPEI (lPEI-Glc$_4$) for the transfection of HUVECs.[551] After incubation for 4 h in 150 mM sodium chloride solution, the transfection efficacy of lPEI-Glc$_4$–luciferase gene complexes was significantly higher than that of optimal formulated lPEI–luciferase complexes. In addition, the cytotoxicity of the lPEI-Glc$_4$–luciferase complexes was significantly lower than that of the lPEI gene complexes. The lower cytotoxicity of lPEI-Glc$_4$–luciferase complexes benefits from the glycosyl residues grafted on their particle surface, which has less positive charges compared with lPEI–luciferase DNA complexes.[551]

In addition to the glycosyl residue modification of lPEI, cholesterol,[552] biodegradable PLGA[553] and hydrophilic poly-(*N*-propylethylenimine)[554] have also been used to modify lPEI. Compared with original lPEI polymers, these modified lPEI can promote transfection efficiency as well.

5.1.3 Polycations based on PEI copolymers. Compared with high molecular weight PEI, low molecular weight PEI possesses weak ability for compressing plasmid DNA because of its low cation density while its cytotoxicity is acceptable.[555] Therefore, crosslinking low molecular weight PEI *via* inert polymers or crosslinking reagents has become one of the most promising strategies for enhancing the cationic charge of this low molecular weight PEI, and further for promoting its ability to condense DNA. Forrest *et al.* synthesized a degradable PEI derivative by combining PEI 800 Da with a diacrylate crosslinker. The structure, size, and DNA-binding capability of this PEI derivative were similar to commercially available PEI 25 kDa, while this carrier exhibited higher gene expression and nontoxicity to human breast carcinoma cells.[556] In addition to the diacrylate crosslinker, low molecular weight PEI can also be crosslinked by dithiobis(succinimidylpropionate),[557] dimethyl-3,3′-dithiobispropionimidate·2HCl and PCL[558] crosslinking reagents. The modified PEIs also show high gene expression and acceptable cytotoxicity.

More recently, we have developed a strategy *via* the combination of chemical modification and the self-assembling method to improve the transfection efficiency of low molecular

weight PEI.[61,559] We synthesized a series of amphiphilic block copolymers containing a biodegradable hydrophobic segment of depsipeptide based copolymers, P(LA-co-MMD), and short PEI chains, and explored them as gene carriers for pEGFP-ZNF580 gene delivery into ECs *in vitro*. The core of a single nanoparticle is formed from several P(LA-co-MMD) segments, whereas hydrophilic short PEI chains are preferentially located on the surface of the NPs (Fig. 23). These NPs with the high zeta potential of 28.0–36.2 mV could condense pDNA and protect them against deoxyribonuclease I. The transfection efficiency of the NPs–pEGFP-ZNF580 complexes is approximately similar to that of Lipofectamine™ 2000. These results indicate that these NPs might have potential as a carrier for pEGFP-ZNF580, which could support the endothelialization of cardiovascular implants.[559]

Furthermore, we prepared a type of diblock copolymer of methoxy-poly(ethylene glycol)-*block*-poly(3(S)-methyl-2,5-morpholinedione-*co*-glycolide) *via* the ROP of 3(S)-methyl-2,5-morpholinedione and glycolide in the presence of methoxy-poly(ethylene glycol) as an initiator, and then grafted PEI to form amphiphilic triblock copolymers of methoxy-poly(ethylene glycol)-*block*-poly(3(S)-methyl-2,5-morpholinedione-*co*-glycolide)-*graft*-polyethyleneimine (mPEG-*b*-P(MMD-*co*-GA)-*g*-PEI). MPs were prepared by self-assembling mPEG-*b*-P(MMD-*co*-GA)-*g*-PEI triblock copolymers. The biodegradable P(MMD-*co*-GA) segments of the amphiphilic triblock copolymers preferentially formed the hydrophobic core while PEG as well as short PEI chains served as the hydrophilic shell (Fig. 24). The short PEI chains and PEG chains were linked on the surface of the MPs. The hydrophilic PEG is responsible for the stabilization and low cytotoxicity of the MPs and PEI provides the MPs with positive charges for gene delivery. This special structure endows the MPs with hydrophilic and positive charge characteristics. The MPs could efficiently deliver the pEGFP-ZNF580 gene into EA·hy926 ECs, and the transfection efficiency of MPs/pEGFP-ZNF580 complexes was as high as the Lipofectamine™ 2000 reagent for EA·hy926 ECs. The proliferation and migration of EA·hy926 ECs were improved greatly by the expression of the pEGFP-ZNF580 gene after 60 hours.[61] Based on this study, we further synthesized a series of amphiphilic biodegradable copolymers with different biodegradable hydrophilic blocks, PEG and low molecular weight PEI chains

such as methoxy-poly(ethylene glycol)-*block*-poly(3(S)-methyl-morpholine-2,5-dione)-*graft*-poly(ethyleneimine) (mPEG-*b*-PMMD-*g*-PEI), methoxy-poly(ethylene glycol)-*block*-poly(3(S)-methyl-morpholine-2,5-dione-*co*-lactide)-*graft*-poly(ethyleneimine) (mPEG-*b*-P(MMD-*co*-LA)-*g*-PEI) and methoxy-poly(ethylene glycol)-*block*-poly(3(S)-methyl-morpholine-2,5-dione-*co*-lactide-*co*-glycolide)-*graft*-poly-(ethyleneimine) (mPEG-*b*-P(MMD-*co*-LA-*co*-GA)-*g*-PEI). The biodegradable hydrophilic blocks of polydepsipeptides and poly(ester amide)s provide the gene carriers with a controllable degradation rate. We prepared the corresponding complexes from these self-assembled MPs with the pEGFP-ZNF580 gene. The low cytotoxicity and high transfection efficiency of these biodegradable gene carriers benefit from the surface PEG and PEI chains. They could be a type of biodegradable non-viral gene carrier for the pEGFP-ZNF580 gene to enhance rapid endothelialization.[60]

The above strategies involve the synthesis and self-assembly of triblock copolymers. The chemical structures and compositions of triblock copolymers can affect the formation and properties of MPs, especially the ratio between PEI and PEG, but it is difficult to control. Thus, we used another method to prepare complex micelles as gene carriers with the aim to improve the cationic charges of low molecular weight PEI.[560] As shown in Fig. 25, two kinds of block copolymers, *i.e.* methoxy-poly(ethylene glycol)-*b*-poly(lactide-*co*-glycolide) (mPEG-*b*-PLGA) and poly(ethyleneimine)-*b*-poly(lactide-*co*-glycolide) (PEI-*b*-PLGA-*b*-PEI), were prepared and then the complex micelles were formed in aqueous solution.[560] After the addition of the pEGFP-ZNF580 gene into the complex micelle suspensions, pEGFP-ZNF580 plasmid-loaded micelles were obtained. The MTT assay demonstrated that the cytotoxicity of these complex micelles can be regulated well by controlling the mass ratio of PEI and PEG, which can be very easily realized by varying the relative amount of PEI- and PEG-containing polymers. The transfection efficiency of these pEGFP-ZNF580 plasmid-loaded micelles is under study in our laboratory.

5.1.4 Cationic dendrimers as gene carriers. Poly(amido amine) (PAMAM) dendrimers are a class of hyperbranched polymers with an ethylene diamine or ammonia core and amido amine branching structures.[561–563] The synthesis of PAMAM dendrimers is performed by Michael addition and amidation, repetitively. Take ethylene diamine for example (Fig. 26A), one ethylene diamine molecule as a nucleophilic
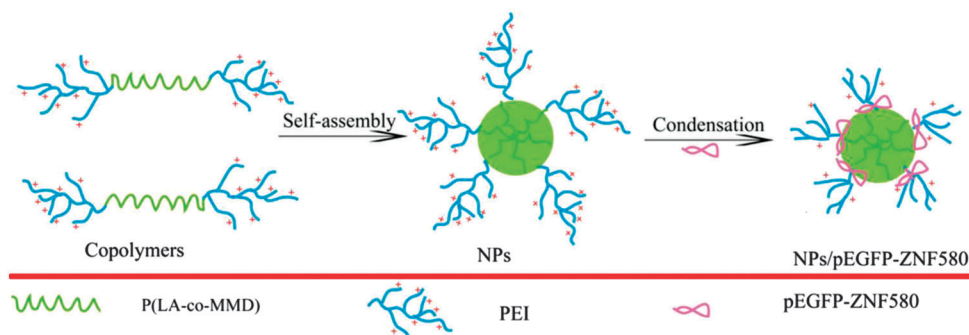

Fig. 23 Formation of NPs from PEI–P(LA-*co*-MMD) block copolymers and process of delivery of pEGFP-ZNF580 into EA·hy926. Reproduced with permission from ref. 559. Copyright 2015 Wiley Periodicals, Inc.
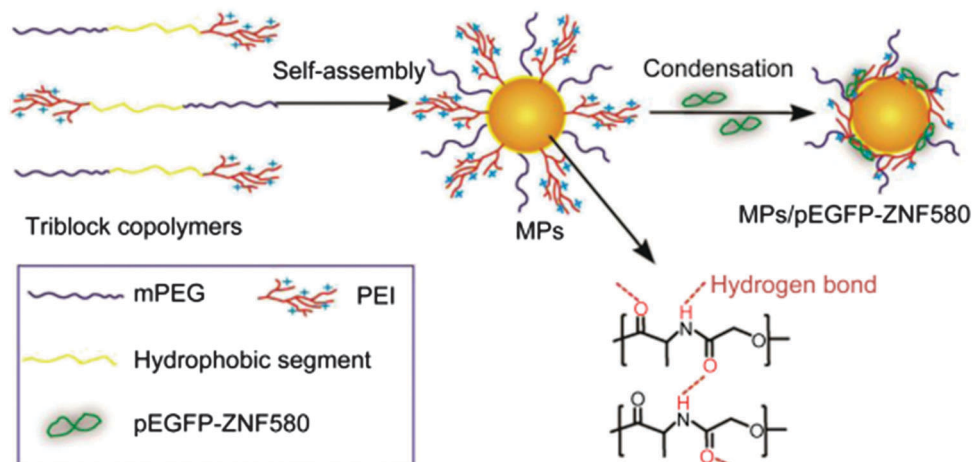
Fig. 24 MPs were prepared by the self-assembly of amphiphilic triblock copolymers, and MPs–pEGFP-ZNF580 complexes by condensation with pEGFP-ZNF580. The self-assembly process was illustrated by the example of the mPEG-*b*-PMMD-*g*-PEI1 triblock copolymer, the PMMD hydrophobic segments act as the core and PEI and mPEG form the cationic shell and hydrophilic corona. The P(MMD-*co*-LA) or poly(MMD-*co*-LA-*co*-GA) segments act as the hydrophobic core for other MPs. Reproduced with permission from ref. 61. Copyright 2014 Elsevier.
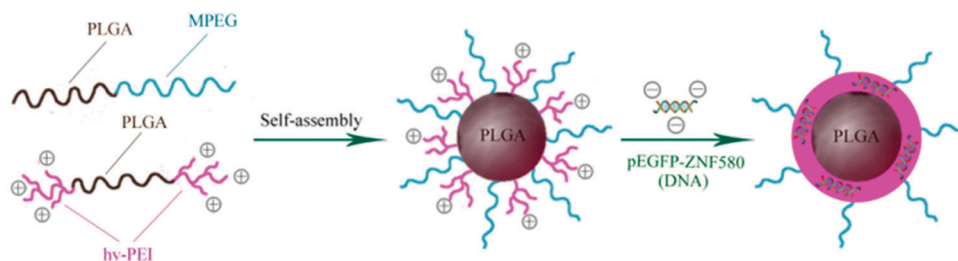

Fig. 25 Self-assembly of complex micelles and pEGFP-ZNF580-loaded micelles. Reproduced with permission from ref. 560. Copyright 2014 Wiley-VCH Verlag GmbH & Co. KGaA, Weinheim.

core reacts with 4 methyl acrylate molecules by Michael addition, following by amidation of the resulting ester with ethylene diamine. When similar alternating Michael addition–amidation reactions are further continued, one additional PAMAM is generated; moreover, the dendrimer diameter increases about 1 nm, and the number of functional amino groups doubles.[564] Owing to the unique size, perfect structure, and active surface properties of these dendrimers, PAMAM has become one of the most widely studied cationic dendrimer polymers for gene therapy.[565] Fig. 26A illustrates PAMAM dendrimers with a depiction of shell generation.[566]

Hudde *et al.*[567] activated a PAMAM dendrimer by heating in water, and this activated dendrimer was used to transfect rabbit and human cornea ECs *in vitro*. They investigated the transfection efficiency of this activated dendrimer and compared it with that of the non-activated dendrimer. After optimizing the ECs and the ratio of TNF receptor fusion plasmid DNA (TNFR-Ig)/dendrimer, the transfection efficiency of the activated PAMAM dendrimer can be increased more than 50-fold. More importantly, a bioassay indicated that the cornea ECs transfected by TNFR-Ig plasmid were able to inhibit the cytotoxicity, which results from the TNF receptor. Their results showed that the activated PAMAM dendrimer is a promising non-viral carrier

for experimental research, which may be potentially used in *in vivo* corneal storage before transplantation.

Owing to its proper size and low cytotoxicity, fourth generation PAMAM has been mostly used in gene delivery compared with the dendrimers with other generations.[568] Nam *et al.* synthesized two kinds of amino acid modified PAMAM dendrimers, namely, an arginine modified dendrimer (PAM-R) and lysine modified dendrimer (PAM-K).[569] They conjugated the hydroxyl-terminated PAMAM dendrimer with Fmoc-ʟ-Arg(pbf)-OH or Fmoc-Lys-(Fmoc)-OH through esterification, and then deprotected the protected groups to obtain PAM-R and PAM-K, respectively. They used ^{1}H NMR spectroscopy to evaluate the degradation patterns of PAM-R and PAM-K in D$_2$O. The results showed that both PAM-R and PAM-K were easily degraded under physiological conditions (pH = 7.4, 37 °C), while they hardly degraded under endosomal conditions. These amino acid-modified dendrimers had excellent buffering capacity between pH 5.1 and 7.0, which means that PAM-R and PAM-K with a large endosome buffering effect could escape from endosomes quickly. Unexpectedly, the transfection efficiency of PAM-K was not satisfied for gene delivery. In contrast, PAM-R displayed significant improvement in transfection efficiency and lower cytotoxicity. Their findings demonstrated that the arginine-grafted PAMAM dendrimer could be a
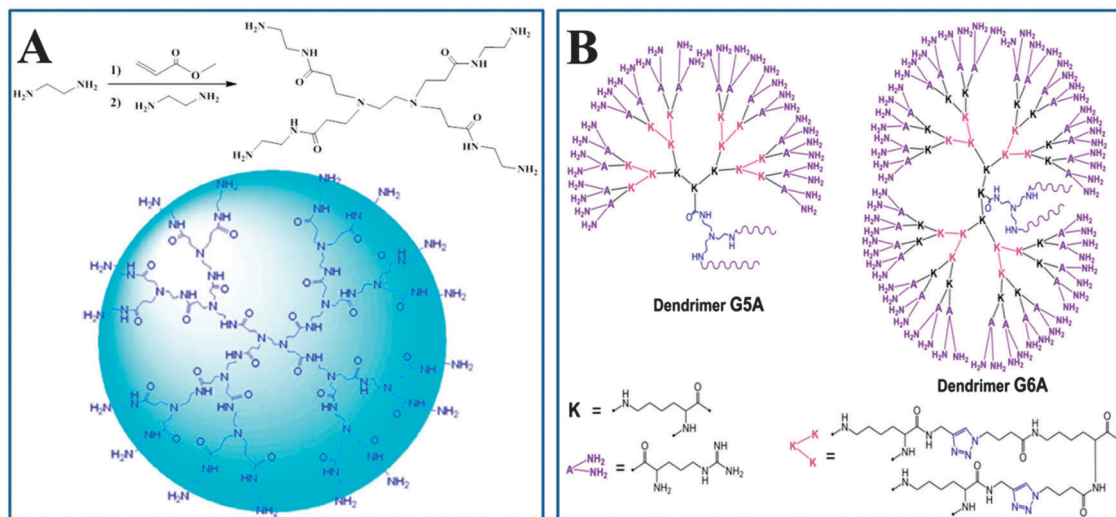
This journal is © The Royal Society of Chemistry 2015

Chem. Soc. Rev., 2015, **44**, 5680–5742 | **5715**

Fig. 26 (A) Synthetic route of PAMAM dendrimers and schematic illustration of the structures of the (PAMAM) dendrimer (G = 2). Reproduced with permission from ref. 566. Copyright 2010 Elsevier. (B) Structures of peptide dendrimers. Reproduced with permission from ref. 572. Copyright 2012 Elsevier.

potential candidate as an efficient and safe gene delivery carrier for ECs gene therapy. Recently, single-, dual- and triple-amino acid functionalized PAMAM (G5) dendrimers with Arg, Phe and His were reported for gene delivery.[570] These three amino acids show synergistic effects, *i.e.*, Arg in the conjugates is essential for complex formation, Phe facilitates the cellular uptake process through the balance of hydrophobic and hydrophilic properties on the dendrimer surface, and His improves pH-buffering capacity and reduces the cytotoxicity of cationic dendrimers.

In addition to PAMAM dendrimers and amino acid modified PAMAM dendrimers, peptide dendritic polymers are a new-generation of cationic carriers that have been developed recently (Fig. 26B).[549,571,572] These dendritic polymers are usually synthesized from amino acids, especially from L-amino acids. Recently, Gu *et al.* synthesized dual-functionalized low generation peptide dendrons (PDs) by the condensation reaction of H-Lys-OMe·HCl and Boc-Lys(Boc)-OH with EDC, 1-hydroxybenzotriazole hydrate, and N,N'-diisopropylethylamine in CH$_2$Cl$_2$ under a nitrogen atmosphere.[573] After the removal of the N-*tert*-butoxycarbonyl groups, all peripheral groups of the PDs were functionalized with Boc-Arg(Pbf)-OH. Then, the core of the arginine-functionalized PDs was modified with lipoic acid derivatives. The dual-functionalized PDs self-assembled onto oil-soluble CdSe/ZnS inorganic NPs *via* coordination interactions to generate multifunctional supramolecular hybrid dendrimers. These peptide dendrimers exhibited a well-defined nanostructure, arginine-rich peptide corona, and fluorescent signaling properties. More importantly, they offered both considerable gene transfection efficiency and real-time bioimaging capabilities *in vivo*. Thus, they may have promising biomedicine applications.[573]

Wimmer *et al.* also synthesized a low-generation cationic dendrimer with a lipophilic peptide as the core. They prepared the complexes from these polycationic polymers and oligonucleotides and used them to transfect human retinal pigment epithelium cells. The transfection efficiency was indirectly measured according

to the decreased production of hVEGF in the medium. Compared with the cytofectin GSV™ transfection agent, this polycationic polymer carrier showed high transfection efficiency, which indicates its potential application in EC transfection and endothelialization of artificial blood vessel materials.[574]

5.1.5 Cationic polysaccharides as gene carriers. Owing to the excellent biocompatibility and biodegradability of polysaccharides, cyclodextrin, chitosan and dextran have been used in the field of gene delivery.[575–577] However, due to their weak ability of compressing DNA and low transfection efficiency, these polysaccharides cannot meet the requirements for application in gene therapy. Thus, scientists have developed many strategies to overcome these shortcomings, *e.g.*, conjugating or incorporating polysaccharides with cationic polymers such as oligoamines, PEI or amino acids.[578] These polysaccharide derivatives or polysaccharides complexes exhibit high transfection efficiency and biocompatibility compared with that of the original polysaccharides or cationic polymers.[579–582]

Domb *et al.* synthesized a novel class of cationic polysaccharides based on spermine–dextran conjugates and evaluated the transfection efficiency of these gene carriers by using pCMV-GFP as a model plasmid. The spermine–dextran conjugates were prepared by the reductive amination of spermine with oxidized polyaldehydes. Their results showed that the mole ratio of spermine/aldehyde, pH and temperature of the medium had a significant effect on the efficiency of the spermine–dextran carriers. When the spermine/aldehyde mole ratio was 1.25, the four amino groups of spermine were conjugated to a short chain dextran (5–10 kDa) at pH 11 at room temperature, and the transfection efficiency was about 50% in HEK293 and NIH3T3 cells.[583] However, the strong hydrophilicity of these spermine–dextran conjugates might inhibit the transfection efficiency in a high serum concentration. Hence, they further modified these conjugates with oleic acid to obtain a novel cationic polymer, *i.e.*, dextran–spermine. The results showed that the dextran–spermine/pGeneGrip plasmid complexes were effective to

transfect the HCT-116, HeLa, NIH 3T3 and CHO cell lines, especially CHO cells, and the transfection efficiency compared well with PEI and liposome polyplexes *in vivo*.[584] Based on these results, it can be concluded that cationic polysaccharides serve as a good carrier to deliver and transfect low differentiation cells such as HCT-116, HeLa, NIH 3T3, CHO and HEK-293 cells. However, for the highly differentiated cell lines, the transfection efficiency of cationic polysaccharide carriers is still very low.[577] Therefore, it is still a challenge for researchers to improve the transfection activity of cationic polysaccharide carriers.

Peng *et al.* synthesized a β-cyclodextrin-linked PEI (CD-PEI) polymer, and then prepared CD-PEI–VEGF165 gene complexes. They investigated the *in vitro* expression of the VEGF gene in the transfection of epidermal stem cells (ESCs) and *in vivo* topical application in wound treatment. Gelatin scaffold incorporated β-tricalcium phosphate (β-TCP) was utilized as the substrate for the culture and transfection of ESCs. The 3D transfection system was formed by incorporating CD-PEI–VEGF165 gene complexes with a gelatin–β-TCP scaffold. Compared with the conventional 2D transfection system of just culture ESCs in common medium, the 3D transfection system could prolong VEGF expression significantly. At the N/P ratio of 5, CD-PEI exhibited a relatively higher transfection efficiency than that by the commercial non-viral carrier, Lipofectamine™ 2000. Moreover, the CD-PEI–VEGF165 gene complexes showed no obvious cytotoxicity to ESCs when the N/P ratio was up to 20. The transfected ESCs by the CD-PEI–VEGF165 gene complexes combined with gelatin–β-TCP scaffolds

were pasted over the wound skin of mice for topical application *in vivo* (Fig. 27). The results showed that the application of transfected ESCs *in vivo* could promote dermal collagen synthesis, skin re-epithelization and hair follicle regeneration. This promising strategy of incorporating CD-PEI–VEGF165 gene complexes with a 3D transfection system can increase the transfection efficiency of ESCs and may be potentially applied in wound healing.[582]

5.1.6 PEG or zwitterionic polymers modified cationic polymers. It is well known that the modification of PEI cationic polymers by PEG can decrease systemic toxicity, as mentioned in Sections 5.1.2 and 5.1.3. In addition to low toxicity, the introduction of PEG into cationic polymers is also favorable for high colloidal stability, long circulation time of complexes, and reduction of nonspecific uptake by the reticuloendothelial system (RES).[585] Zhong *et al.* grafted various quantities of PEI 1800 Da on PEO chains to obtain a series of PEO-*g*-PEI copolymers such as PEO (13 kDa)-*g*-10PEI, PEO (24 kDa)-*g*-10PEI, and PEO (13 kDa)-*g*-22PEI, where 10 and 22 are the number of 1800 Da PEI per PEO chain. These PEO-*g*-PEI copolymers were evaluated *in vitro* as non-viral gene carriers. With the increase of PEO molecular weight and decrease of PEI graft density, the reduced cytotoxicity of the PEO-*g*-PEI polyplexes was demonstrated by MTT assays in 293T cells. The transfection activity of PEO (13 kDa)-*g*-10PEI was the best in these three copolymers, which was 3- and 4-fold higher than that of PEI 25 kDa complexes under serum-free and 10% serum conditions, respectively (Fig. 28). The higher transfection efficiency of the
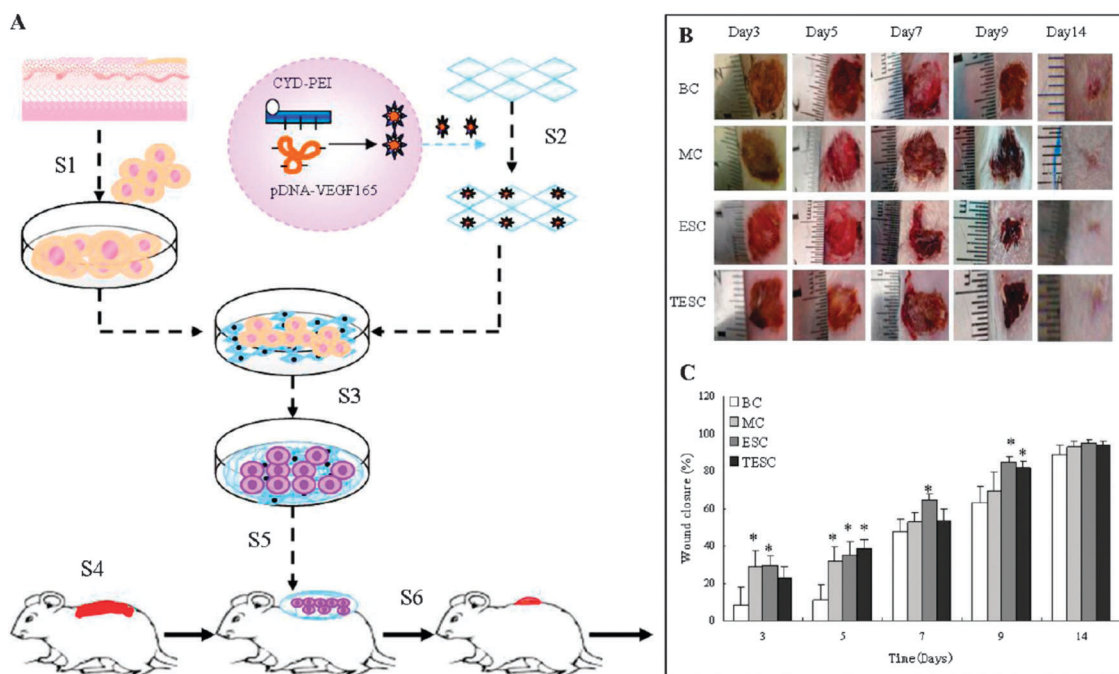

Fig. 27 (A) Flowchart of the animal study procedure. S1: isolation and culture of ESCs. S2: construction of the CYD-PEI/pDNA polyplexes and gelatin−β-TCP matrix based 3D transfection system. S3: culture and transfection of the ESCs in the gene-activated matrix. S4: establishment of rat full-thickness skin wound. S5: application of the recombinant ESCs with the 3D matrix to the wound site. S6: wound treatment by the recombinant ESCs. (B) Wound sites appearance on days 3–14 postwounding. (C) Wound closure rates on days 3–14 postwounding (*$p < 0.05$, *versus* blank control group). BC, MC, ESC, and TESC represent the blank control, matrix control, ESCs topical treatment, and TESCs topical treatment, respectively. Reproduced with permission from ref. 582. Copyright 2013 American Chemical Society.

PEO (13 kDa)-*g*-10PEI polyplexes may be due to their superior colloidal stability. PEO with 13 kDa molecular weight and 10 PEI chains give them median polyplex sizes (126–131 nm) and positive zeta potentials (+18.8 to +20.2 mV) at N/P ratios between 10/1 and 30/1. Thus, these stable PEO (13 kDa)-*g*-10PEI polyplexes can effectively deliver DNA into the cell nuclei, resulting in high levels of gene expression.[586]

Ko *et al.* mixed PEI 2.7 kDa with oligodeoxynucleotides (ODN) to prepare PEI–ODN complexes, and then encapsulated them into PEGylated liposomes. The combination of PEI–ODN complexes with PEG-stabilized liposomes (PSL) is expected to enhance *in vivo* stability with prolonged circulation time. It has been proven that the PSL entrapping PEI–ODN complexes were very stable even in the presence of serum. Upon intravenous administration, the DNA in PSL showed high passive accumulation due to long half-life in circulation as compared with the naked PEI–ODN complexes, and the transgene expression in PSL increased about 3.2-fold compared with the DNA that was not condensed by PEI. Their research indicated that the encapsulation of PEI–ODN complexes within a long-circulating PEGylated liposome provided a promising DNA delivery system for *in vivo* application.[587]

Zwitterionic polymers, such as poly(DMAPS) and poly(MPC), have been used for surface modification in order to resist the nonspecific adsorption of proteins and cells as discussed in Section 3.2. In addition to this, zwitterionic polymers can also shield redundant positively charged complexes in the physiological environment for the reduction of the toxicity of cationic polymers. It is well known that serious aggregation of cationic polymers on the surface of cell membranes would induce significant cytotoxicity both *in vitro* and *in vivo*. Therefore, effective shielding of positively charged complexes is very important and necessary in gene delivery. Chen *et al.* designed and synthesized a novel zwitterionic copolypeptide, *i.e.* PEI–poly(L-lysine)–poly(L-glutamic acid) (PELG), by the ROP of Lys(Z)-NCA and BLG-NCA in the presence of PEI 1.8 kDa as a macroinitiator, followed by the deprotection of benzyloxycarbonyl and benzyl protection groups in trifluoroacetic acid and hydrobromic acid, respectively.[588] PELG was used to shield PEI

25 kDa/DNA and to form ternary complexes in the physiological environment. At acidic pH, such as tumor extracellular environment (about pH = 6.5), the zeta potential of PELG zwitterionic copolypeptide changed from negative to positive, which means that complexes with positive charges can be restored easily. Complexes encapsulated in tumors are beneficial to the electrostatic interaction between positive complexes and negative tumor cells, which leads to high cell uptake efficiency and transgene expression. *In vitro* transfection and an uptake efficiency assay demonstrated the superiority of the PELG copolypeptide and the *in vivo* anti-tumor therapy experiment also proved that the tumor growth rate decreased significantly after introducing PELG into PEI 25 kDa/DNA complexes.[588]

The advantages of PEG and zwitterionic polymers for prolonging circulation time and shielding positively charged polyplexes can also be used in ECs gene therapy, which may improve EC expression and endothelialization in revascularization applications. However, this still needs more *in vitro* and *in vivo* experiments to be proven.

5.1.7 Other gene carriers. In addition to the aforementioned non-viral gene carriers, other gene carriers, such as PLL,[589,590] cationic peptides, poly(dimethylamino ethylmethacrylate),[492,591] hyperbranched poly(dimethylamino ethylmethacrylate),[592,593] poly(carboxy betaine methacrylate ethyl ester) (PCBMAEE), poly(carboxy betaine methacrylate ethyl ester)–poly(carboxy betaine methacrylate) (PCBMAEE–PCBMA),[594] have also been investigated for potential application in gene delivery systems. The DNA binding capability of PLL depends on its molecular weight. High molecular weight PLL can improve transfection efficiency but its cytotoxicity is high. Therefore, PLL has been modified by PEG[595] or other NPs[596] in gene therapy applications. Compared with liposomes, PEI and dendrimers, PLL shows relatively low transgene expression activity, which limits its application in gene therapy.

Jiang *et al.* developed a type of charge shifting cationic polymer to reduce the cytotoxicity of cationic gene carriers.[597,598] They synthesized PCBMAEE polymers, whose anions were hidden by ester bonds, and thus they could condense DNA in the cationic state. These gene carriers enhanced DNA release after passive
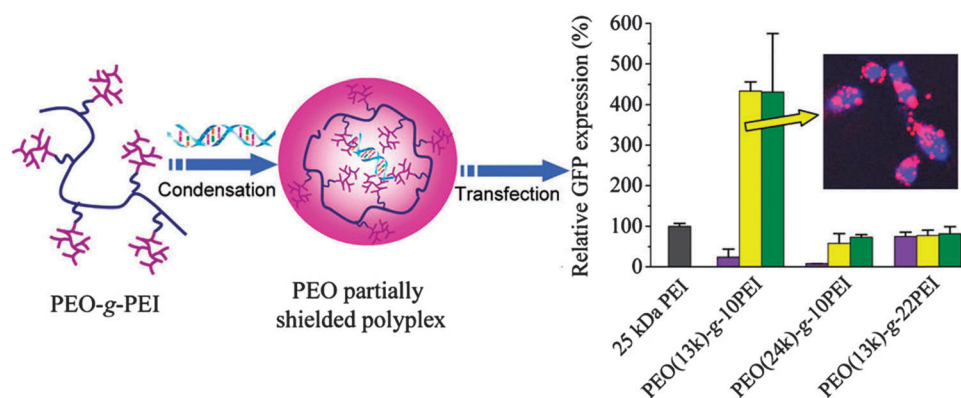

Fig. 28 PEO modified PEI copolymers effectively deliver DNA into the cell nuclei with high transfection efficiency. Schematic from ref. 586. Copyright 2012 American Chemical Society.

hydrolysis (or with the help of intracellular esterases) into the zwitterionic state and minimized the cytotoxicity caused by the accumulation of the positively charged polymers in host cells. The hydrolysis rate of the ester bonds in PCBMAEE-based polymers can be readily tuned by changing the alkyl chain length, head group size, hydrolytic groups, or leaving groups, which may solve the drawbacks of these carries for gene release. PCBMAEE carriers showed high gene transfection efficiency in serum-free media, but they lack a fouling resistant shell, which may reduce the endocytosis of DNA complexes due to serum protein adsorption.

Therefore, Chen *et al.*[594] developed diblock copolymers based on the hydrophobic PCBMAEE segment and nonfouling zwitterionic PCBMA segment (Fig. 29). Importantly, due to the nonfouling characteristic of the zwitterionic PCBMA segment, these carriers can reduce the interference from serum proteins, without impeding endocytosis. The complexes formed by PCBMAEE–PCBMA with luciferase or the pEGFP gene exhibited significantly higher transfection efficiency of pDNA than that by PEI 25 kDa or Lipofectamine™ 2000 in HUVECs. Furthermore, these complexes also showed significant advantages in transfection rate, dosage effectiveness and preservation of transfecting activity in serum containing growth media. These results demonstrated that this polymeric gene carrier, which consisted of a convertible hydrophobic polyzwitterionic precursor and polyzwitterionic nonfouling segment, is a promising candidate for high and stable gene transfection in complex growth media.

Cell-penetrating peptides (CPPs) have been developed and used in gene delivery because they exhibit excellent membrane activity, low cytotoxicity, high uptake by a variety of cell types, dose-dependent efficiency, and no restriction with respect to the size or type of cargo.[599,600] CPPs have been proven to be potent for promoting transfection efficiency by overcoming the first barrier to successful gene delivery.[601–605] However, CPPs, such as oligoarginine, TAT and penetratin, are often too short (10–25 peptide residues) and lack adequate cationic charge to efficiently condense and deliver genes by themselves; thus, CPPs often serve as membrane active ligands to improve delivery efficiency by incorporating or conjugating to delivery carriers.[606] Zhang *et al.* designed and synthesized a peptide of TAT-PKKKRKV as a carrier for VEGF165 plasmid to facilitate *in vivo* angiogenesis.[601,607] This peptide exhibited low cytotoxicity and efficient transfection ability with serum, which might be beneficial for clinical applications. More importantly, they found that the application of TAT-PKKKRKV/VEGF165 complexes in hindlimb ischemia rats obviously promoted the expression of the VEGF protein and further enhanced effective angiogenesis. Their results demonstrated that TAT-PKKKRKV is an efficient gene carrier with low toxicity both *in vitro* and *in vivo*, which has great potential for clinical gene therapy.[601,607]

5.2 Cell growth factors and target genes for the endothelialization of artificial vascular grafts

5.2.1 Fibroblast growth factors (FGFs). FGFs are a type of polypeptide growth factor that exists widely in many tissues of the body. FGFs mainly include two classes, namely, acid FGF (aFGF) and basic FGF (bFGF or FGF-2). FGFs can promote
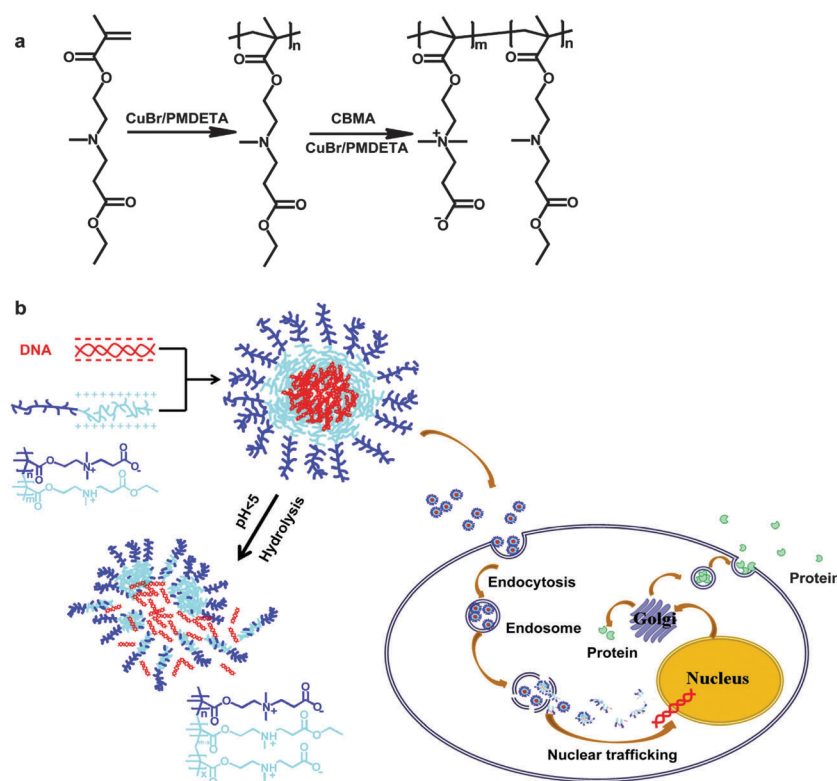

Fig. 29 (a) Synthesis of PCBMAEE–PCBMA diblock copolymers *via* ATRP; (b) polyplex formation and process of gene delivery mediated by PCBMAEE–PCBMA. Reproduced with permission from ref. 594. Copyright 2014 Elsevier.

fibroblast mitosis, EC migration and SMC proliferation; thus, FGFs act as a potent stimulator of vasculogenesis.[608,609]

Thompson et al. investigated the influence of fibrin and FGF on wound healing in a rabbit model.[610] After a same-thickness wound was made on the dorsum of each test rabbit, four groups were divided by the treatments of the wounds: control, FGF, fibrin and FGF/fibrin scaffold groups. Two weeks later, mechanical testing was used to evaluate the healing response. The tensile strength of the new tissue in the FGF/fibrin treatment group was significantly higher than that of the fibrin treatment group. Histomorphometric analysis indicated that the percentage of new epithelium generated by FGF and FGF/fibrin treatments was higher than that of other treatments.[610]

Although FGF is important for cell migration, proliferation and vasculogenesis, its short half-life, lack of long-term stability, and slow tissue penetration limit its application in tissue engineering. In particular, bFGF has been well known to be highly unstable under normal culture conditions.[611] Therefore, many strategies have been investigated for the delivery and controlled release of FGF. In recent years, the application of microspheres and microbeads for the local release of growth factors has been developing rapidly.[612,613] Generally, microspheres with FGF can be implanted to increase local tissue regeneration. Importantly, they can enhance local vascularization when microspheres are simultaneously implanted with encapsulated cells.[614,615] More recently, Brey et al. prepared the multilayered alginate microbeads with core and shell structures.[616] The inner core was generated by using low viscosity sodium alginate (20–200 mPa s, high mannuronic acid content) and $CaCl_2$ as a crosslinker, while the outer layer was prepared from sodium alginate (high glucuronic acid content) with two different doses of FGF-1 supplemented with heparin. The in vitro release results showed that the FGF-1 loaded microbeads had an initial burst release, followed by the long-term release of FGF-1 over 30 days. Furthermore, these multilayered alginate microbeads were surgically implanted into rats to evaluate the increased neovascularization in vivo. The rats implanted with the microbeads were fed for 4 days, 1 week and 6 weeks, and then were sacrificed to harvest the samples. The in vivo experiment results demonstrated that the alginate microbeads were still visibly intact inside the omentum pouch at all harvest times. Moreover, FGF-1 loaded alginate microbeads implanted for 6 weeks provided a relatively high vascular density compared with the microbeads implanted for 4 days and 1 week. Their results demonstrated that the sustained delivery of FGF-1 from multilayered alginate microbeads could stimulate local neovascularization.[616]

Recently, microspheres containing FGF have been prepared for the controlled release and delivery of growth factors.[613] Kok et al. prepared gelatin microspheres containing FGF-2 using a coacervation technique and incorporated them in the middle of two electrospun nanofibrous layers for controlled growth factor delivery.[617] The bottom layer was formed from PCL/PLLA nanofibers with high mechanical strength, whereas the upper layer was made from PCL/gelatin nanofibers with excellent cell adhesion. Preliminary cell culture studies demonstrated that FGF-2 was actively loaded into the microspheres and could enhance cell attachment and proliferation. Importantly, this sandwich system exhibited the hydrophilic and bioactive nature of the upper layer and promoted cell attachment to the surface, which is attributed to gelatin and the controlled release of FGF-2 from the microspheres.[617]

In addition to the sandwich system, multilayer materials have also been prepared for FGF controlled release. Hong et al.[618] used the LbL assembly technology to prepare a chitosan/starch/FGF-2/starch nano-assembly surface coating by the sequential adsorption of positively-charged chitosan, starch, FGF-2 aqueous solutions, and negatively charged starch through electrostatic interactions. Interestingly, they found that the release rate of FGF-2 could be controlled by heat-treatment, because high temperature induced starch gelatinization and rearrangement of internal film structures. The same group further prepared another multilayer nanofilm from PLL, FGF-2 and starch using the LbL technology.[619] PLL provided enhanced geometric compatibility and cell adherence, whereas starch increased film stability. FGF-2 release was sustained for over 10 days. In the presence of released FGF-2, human induced pluripotent stem cells maintained their undifferentiated morphology and expression levels of pluripotency marker proteins and AP activity. Considering the many choices of various biomaterials for the LbL technology, this multilayer approach is expected to be a great tool for the development of therapeutic surface coatings with controllable release of the growth factor, FGF.

In addition, Brewster et al. engineered a thrombin-resistant mutant of FGF-1 through a lysine (K) for arginine (R) base substitution at residue 136 (termed R136K), which is the primary thrombin induced cleavage site.[620] Compared with FGF-1, R136K exhibits superior chemotactic activity on ECs in a thrombin-rich environment while retaining FGF-1's mitogenic activity on ECs.[621] They further ligated R136K with a collagen binding domain (termed R136K-CBD) in order to direct this growth factor to the sites of exposed vascular collagen or bioengineered scaffolds. Interestingly, R136K-CBD exhibits the advantages of both R136K and CBD, such as the angiogenic, chemotactic, and mitogenic activities of R136K, as well as the selective binding activity of CBD, without diminishing R136K's thrombin resistance. These advantages enable R136K-CBD with selectivity and high affinity binding to exposed collagen in the ECM after endothelial injury or to bioengineered collagen matrices. These beneficial characteristics are useful in promoting the vascular regeneration of injured arteries or endothelialization of collagen-based bioengineering scaffolds with good control of growth factor delivery. This collagen binding domain ligated R136K can intelligently promote the endothelial regeneration of selected matrices.[620] In addition to FGF-1 and R136K, FGF-2 has been fused with a recombinant human collagen-binding domain to obtain rhCBD-FGF-2. rhCBD-FGF-2 with collagen matrices, which could improve tissue repair and regeneration by controlling cellular adhesion, proliferation and differentiation.[622]

All of the aforementioned results demonstrate that FGF is a potent angiogenic factor for improving the endothelialization of vascular prosthesis.[623–625] Several studies were conducted in ePTFE grafts or decellularized porcine arterial grafts coated with fibrin, heparin, FGF and other growth factors.[626,627] FGF-2

5720 | Chem. Soc. Rev., 2015, 44, 5680–5742

This journal is © The Royal Society of Chemistry 2015

coating on the heparin bound decellularized grafts significantly increased EC proliferation and the seeded cells were stable under perfusion conditions. However, unfortunately, the decellularized vascular graft with PDLA and FGF coating showed massive stimulation of giant cells and eosinophils, which resulted in complete graft encapsulation. It has to be noted that different studies may obtain opposite results, which might be caused by the materials, coating methods, FGF concentrations, controlled release rate of FGF, as well as the animal models.

Furthermore, owing to its wide distribution and the lack of signal peptides, FGF can elicit diverse biological effects (include promoting proliferation, survival, migration, motility, adhesion, apoptosis and physiopathology) on numerous cell types such as ECs, SMCs, fibroblasts and keratinocytes.[628] Because of these complicated physiological actions, further studies should be performed both *in vitro* and *in vivo* to evaluate the biofunctions and safety of FGF in the application of artificial vascular grafts.

5.2.2 Vascular endothelial growth factors (VEGFs) and VEGF genes. As specific heparin-binding growth factors in vascular ECs, VEGFs are important signaling proteins that are involved in both vasculogenesis and angiogenesis processes by mediating the migration and mitosis of ECs and methane mono-oxygenase and $\alpha_v\beta_3$ activities.[629] The biological function of VEGFs is mediated by its specific membrane receptor-vascular endothelial growth factor receptors (VEGFR). VEGFR1 (Flt1), VEGFR2 (KDR) and VEGFR3 (Flt4) are three kinds of VEGFRs that have already been discovered in vascular ECs. Among them, VEGFR2 is the first molecule known to be expressed on mesodermal cells, which enhances the proliferation of EPCs.[630,631] The key functions of VEGFs and their receptors for the early embryogenesis of ECs were initially investigated and established with gene-targeting experiments in mice. After knocking out the genes for VEGFR-2 or VEGFR-1, the differentiation of EPCs and vasculogenesis were obstructed, respectively, leading to the death of embryos between 8 and 10 days.[632] These results indicated that the VEGFs and VEGF genes are essential for EC embryo formation and vasculogenesis in the EC embryo. VEGFs can induce enhancement of the endothelial functions that mediate the inhibition of vascular smooth muscle cell proliferation, suppression of thrombosis, and anti-inflammatory effects. Nowadays, the VEGFs and VEGF genes are usually used to enhance the proliferation of ECs in *in vitro* and *in vivo* studies.[633,634]

Generally, the administration of VEGFs for the treatment of coronary artery diseases is by injection, which includes intracoronary injection,[635] intramyocardial injection,[636] intravenous injection[637] and intra atrial injection.[638] Banai *et al.* treated dogs with 45 μg VEGF daily by the intracoronary injection method. After 28 days, enhanced collateral blood flow to the canine ischemic myocardium can be observed, which means that VEGF plays an important role in myocardial collateral formation.[635] Subsequently, Hendel *et al.* investigated the effect of the recombinant VEGF protein on the human vascular endothelial growth. Their research results indicated that the intracoronary and intravenous recombinant VEGF165 protein is safe and tolerable for patients.[639] However, these clinical trials were performed in a small number of patients and few had placebo controls. Henry *et al.* carried out a double-blind and placebo-controlled trial in 178 patients with coronary artery diseases to evaluate the safety and efficacy of the VEGF165 protein, and an interesting dose–response relationship was observed. VEGF was very safe and tolerable in the low-dose group by intracoronary and intravenous administration, while significant side effects occurred in the high-dose group.[640]

Because of its short biological half-life, VEGFs are rapidly degraded in serum less than 1 h after injection.[641] Therefore, control release of VEGFs to maintain the long presence of growth factors at target sites is very important for enhancing vessel formation. Recently, coacervates,[642] gels,[643,644] micro-gels,[645] biomimetic microspheres[646,647] and core–shell fibrous membranes[58] have been used to control the release of VEGFs in the bloodstream.

Kim *et al.* developed a combined strategy by using outgrowth endothelial cells (OECs) and angiogenic proteins for the treatment of vascular disease.[643] They used RGD-conjugated alginate to prepare an injectable multifunctional micro-sized gel system (microgel) *via* electrospraying. OECs, VEGF and HGF were encapsulated in these microgels. Their results demonstrated that the RGD–alginate microgels exhibited a sustained release of the encapsulated growth factors. Owing to the absence of an early burst release, the injectable microgel system showed no toxicity to the targeted sites. Furthermore, the increased angiogenesis in the *in vivo* mice model was also observed by treatment with RGD-microgel containing OECs and growth factors. This injectable multifunctional microgel system can be used for the well-controlled release of growth factors and potentially applied in the treatment of vascular diseases.[643] In addition, Poldervaart and coworkers used gelatin microparticles (GMPs) for the controlled release of VEGF to prolong its activity.[648] Compared with VEGF incorporated with matrigel, the complexes of VEGF/GMPs showed a slow VEGF release in PBS/0.5% BSA. Moreover, VEGF maintained its biological activity well by VEGF/GMPs, which was proven by migration assays using the 24-well Transwell system. *In vivo* experiment results showed that the controlled release of VEGF led to a significant increase in vessel formation from the quantification of the stained vessels.[648]

In addition to gels and MPs, an interesting fiber system has also been developed using the electrospinning technology for the sustained release or staged release of VEGF and other fragile water soluble bioactive agents.[647,649] Yuan *et al.* fabricated core–shell electrospun fibrous membranes with a double-layer structure for the dual-delivery of VEGF and platelet-derived growth factor-bb (PDGF) to regulate the proliferation of vascular ECs and VSMCs. PDGF can stimulate the proliferation of SMCs, which plays a significant role in vascular maturity and stability.[58] The inner layer of the coaxial electrospun membrane was composed of chitosan hydrogel and poly(ethylene glycol)-*b*-poly(L-lactide-*co*-caprolactone) (PELCL) loaded with VEGF, while the outer layer consisted of methoxy poly(ethylene glycol)-*b*-poly(L-lactide-*co*-glycolide) (PELGA) and PELCL loaded with PDGF. Fig. 30 shows the SEM micrographs of the double-layered electrospun membranes. The *in vitro* release demonstrated that VEGF had a higher release percentage

This journal is © The Royal Society of Chemistry 2015

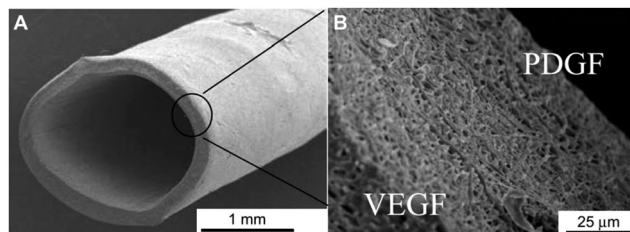*Chem. Soc. Rev.*, 2015, **44**, 5680–5742 | 5721

Fig. 30 SEM micrographs of the small-diameter vascular graft with a 2.2 mm diameter. (A) Gross appearance; (B) cross section of the fibrous membrane with inner–outer double layers loading VEGF and PDGF, respectively. Reproduced with permission from ref. 58. Copyright 2013 Elsevier.

(about 66%) in the initial 6 days, which reached 96.5% ± 7.4% on day 28. Contrarily, only 38.4% ± 13.9% of PDGF was released in the initial 6 days, which reached 90.1% ± 14.4% on day 28. As shown from the proliferation results of vascular ECs and SMCs, the dual-release of VEGF and PDGF could accelerate vascular ECs proliferation in the first 6 days and generate rapid proliferation of vascular SMCs after day 6. After four weeks, the *in vivo* replacement of the rabbit carotid artery demonstrated that vascular ECs and SMCs developed on the lumen and exterior of the artificial vascular grafts, respectively, and no thrombus or burst appeared. These results confirmed that the release of VEGF can be controlled well by fibrous membranes. Moreover, the release profiles of both growth factors can be modulated by adjusting the compositions of electrospun fibers to meet variable requirements.

In addition, Yuan *et al.*[650] further prepared a multilayered vascular graft (1.5 mm diameter) with sufficient mechanical properties as well as dual-delivery of VEGF and PDGF. They electrospun PELCL and gelatin to obtain the inner layer using the dual-source and dual-power electrospinning technology,[651] and then prepared the middle layer from PLGA and gelatin. Finally, PCL and gelatin fibers were applied to form the outer layer to enhance mechanical properties and delay PDGF release (Fig. 31). This multilayered scaffold showed spatio-temporal dual-delivery of VEGF and PDGF from its inner and middle layers, which is beneficial for new blood vessel formation and maturation. More importantly, this specially designed vascular graft with dual-loading VEGF and PDGF could keep long-term patency in the replaced rabbit left common carotid artery *in vivo* for 8 weeks. The animal test results demonstrated that this multilayered scaffold is better than the grafts that load only one kind of growth factor or without loading any growth factor. The superior properties and *in vivo* successful results benefit from the spatio-temporal release of VEGF and PDGF, which is specially controlled by the inner PELCL and middle PLGA layers, respectively; moreover, the outer PCL layer contributed to the mechanical stability.

In addition, MP and NP loaded VEGF have been successfully prepared using double emulsion solvent evaporation method or other methods.[652–654] VEGF can be delivered, locally controlled and have sustained release by these particles for several weeks *in vitro*. Importantly, heparin/chitosan nanospheres with VEGF highly facilitate neovascularization and ECM production and accelerate vascularization in mouse subcutaneous implantation models *in vivo*.[655]

In addition to the application of VEGF in vascular tissue engineering, plasmids encoding VEGF (pVEGF) are also widely
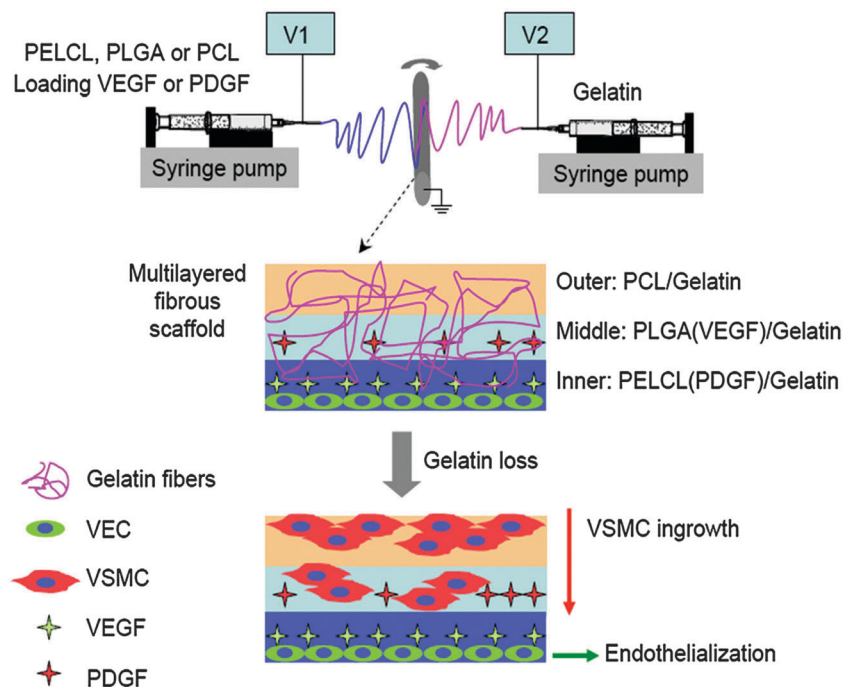

Fig. 31 Schematic representation of the preparation of the multilayered electrospun membranes and the cell growth tendency. Reproduced with permission from ref. 650. Copyright 2013 Elsevier.

used for angiogenesis. In the early studies, many trials used injection of naked plasmid DNA in ischemia tissue to promote angiogenesis. Takeshita *et al.* transfected pVEGF or plasmid encoded β-galactosidase (control) into the ischemia limb of mice, which was evaluated by microangiography.[656] The development of collaterals in the ischemic limb was observed after four weeks treatment. The morphological results showed that the collateral arteries developed more extensively in the VEGF-treated group than that of the control group. The microvascular reactivity test was performed by the administration of papaverine to collateral vessels. The evident vasodilator effect of papaverine was found in relatively large vessels in both groups, while at the microvascular level (diameter < 100 μm) papaverine induced significant vasodilation only in the VEGF-treated groups and almost no vasodilation was found in the controls. The above results demonstrated that gene transfer of VEGF produced significantly more extensive and collateral networks at the microvascular level.[656]

Compared with the injection of naked plasmid DNA, the sustained delivery of pVEGF over a specific period provides a powerful alternative to produce angiogenic growth factors in transfect cells, which is generally advantageous for long-term effects in peripheral artery diseases and clinical ischemic heart trials. The delivery and release of pVEGF are considered preferentially by electrospun membranes,[657] non-viral gene carriers and viral gene carriers,[656,658,659] which have been extensively studied in the endothelialization of artificial vascular grafts.

More recently, Li *et al.* developed a new strategy involving the combination of pDNA condensation and the electrospraying technology.[657] They used the reverse microemulsion method to prepare calcium phosphate (CP) NPs that encapsulated pVEGF and plasmids encoding bFGF (pbFGF), and then electrosprayed these NPs with the biodegradable PELA polymer and hydrophilic PEG to form CP-pDNA/PELA MPs. Therefore, each MP has several plasmid NPs. PEG with M_w of 2, 4 and 6 kDa, which was blended into the MPs, creates many microscopic holes in the MPs after its dissolution in buffer solution or physiological condition. This effect can modulate the pDNA release because PEG with high molecular weight induces the formation of large channels and cavities in the MPs, which is beneficial for the medium exchange and pDNA release. The gradual release of pDNA from these MPs (4 weeks) led to an incremental expression of VEGF and bFGF to stimulate cell growth *in vitro*. Furthermore, they studied the *in vivo* performance of these MPs by subcutaneous infusion. The results demonstrated that the MPs with both pVEGF and pbFGF plasmids induced the rapid proliferation of ECs and created considerably high densities of vascular prosthesis compared with the MPs only containing individual plasmid NPs.[657]

In addition to MPs, non-viral gene carriers[660] and viral gene carriers[661,662] have also been widely used to deliver VEGF genes with high transfection efficiency. Considering the toxicity and potential risk of viral gene carriers, non-viral gene carriers are the preferred choice for the transfection of VEGF genes. Kim *et al.* synthesized a reducible disulfide poly(amido ethylenediamine) (SS-PAED) polymer and used it as a non-viral gene carrier for VEGF gene delivery *in vivo* and *in vitro*.[658] The *in vitro* transfection efficiency of SS-PAED with a weight ratio of 12 : 1 (polymer/DNA) showed 16-fold higher expression of luciferase than that of the optimized bPEI control group. Furthermore, the *in vivo* delivery of the VEGF gene by SS-PAED was investigated in a rabbit myocardial infarct model and compared with the injection of the SS-PAED/RTP-Luc control. The results demonstrated up to a 4-fold increase in VEGF protein expression by SS-PAED gene delivery than that by direct intravenous injection.[658]

Park *et al.* combined pVEGF with an arginine-grafted cationic dendrimer, PAM-RG4, to treat diabetic skin wounds. RT-PCR and ELISA were used to measure the VEGF expression level in the wound tissue. After subcutaneous injection of PAM-RG4–pVEGF165 complexes, the VEGF expression was first detected on the fourth day, and the expression level gradually increased with the extension of time. Histological staining demonstrated that the skin wounds in the diabetic mice were generally healed and displayed a well-ordered dermal structure after day 6.[663]

Recently, a lipopolysaccharide-amine nanopolymersome (LNP) carrier has been developed by Huang and coworkers. They synthesized a water soluble, degradable, amphiphilic and amphoteric brush copolymer from PEI 1.8k, cholesteryl (Cho) and oxidized sodium alginate (OA), where OA serves as the backbone and Cho-grafted PEI 1.8k (PEI-Cho) acts as the side chains. This brush copolymer can self-assemble into empty LNPs with a particle size of 110 nm and zeta potential of +39 mV, which can efficiently deliver pEGFP with higher than 95% transfection efficiency in MSCs in serum-free or serum transfection.[664] Furthermore, LNPs can completely condense pVEGF and form pVEGF–LNP complexes (N/P = 60) with the shape of an empty football.[665] The morphology, diameter and zeta potential of these complexes are nearly the same as that of pEGFP loaded LNPs. Interestingly, the pVEGF–LNP complexes showed low toxicity to MSCs because cholesteryl and OA in the copolymer can decrease cytotoxicity by reducing the positive charge density and decrease the immediate toxicity from aggregation by facilitating endocytosis.[666,667] They can induce MSCs to express a high level of VEGF *in vitro* and produce significant angiogenesis *in vivo*. The high expression is attributed to the synergism of its three components, *i.e.* cholesteryl, OA and PEI. Moreover, the formation of nanopolymersomes is beneficial to high expression since this nanostructure helps them break through the key barriers in transfection. More importantly, the expression of VEGF can conveniently be controlled by adjusting the pVEGF dose or N/P ratio. It should be noted that the level of VEGF synthesized by cells at 5 ng per 10^6 cells per day is sufficient to establish normal homogeneous capillary like vessels, because a too high level (> 70 ng per 10^6 cells per day) will cause abnormal angiogenesis.[668]

Although PEI has been used to deliver VEGF genes for many years,[669] the efficiency and cytotoxicity of PEI-mediated gene transfection increase simultaneously with the increase of both N/P ratio and PEI molecular weight. It is still a challenge for researchers to develop more efficient strategies to increase

This journal is © The Royal Society of Chemistry 2015

Chem. Soc. Rev., 2015, **44**, 5680–5742 | 5723

the transfection efficiency and decrease cytotoxicity of gene carriers. Recently, a novel technology, namely, microbubble inertial cavitation, has been demonstrated as a promising noninvasive method to enhance gene transfection efficiency both *in vitro* and *in vivo*.[537] By employing ultrasound-induced microbubble inertial cavitation, optimized bPEI-mediated VEGF transfection efficiency can be achieved even at relatively low N/P ratios with the appropriate ultrasound parameters.[670] Alternatively, β-cyclodextrin-linked polyethylenimines were synthesized by conjugating PEI600 with β-cyclodextrin *via* a polycondensation reaction, which showed no apparent cytotoxicity to ESCs with the N/P ratio of 20.[582] Compared with the external administration of VEGF, the controlled release of VEGFs and VEGF gene delivery systems by non-viral or other active carriers may be potential methods for promoting the endothelialization of vascular prosthesis in clinic trails. Although local excess VEGFs might cause angiogenesis and even have the risk for tumor formation, precisely controlling VEGF or VEGF gene release is still a challenge in *in vivo* applications.

5.2.3 ZNF580 gene. The ZNF580 gene (GenBank ID: AF184939), which contains 172 amino acids, was initially cloned by Zhang and coworkers using the differential display reverse transcription PCR technique.[671] As a C2H2 zinc finger protein, the expression of ZNF580 is related on low-density lipoproteins (LDL) in vascular ECs. It is well known that LDL regulates the incidence of coronary artery diseases in a concentration-dependent manner, while atherosclerotic plaque is formed in ECs first. So the expression of the ZNF580 gene plays an important role in the proliferation and migration of ECs. Many results have proven that ZNF580 gene expression can up-regulate the proliferation and migration of ECs,[59,672,673] which can potentially promote endothelialization for revascularization.

By encoding with the green fluorescent protein (GFP), the pGFP–ZNF580 gene can be used as a target gene and reporter gene. More recently, we used this gene as a model gene and ECs as model cells to investigate the transfection efficiency of amphiphilic PEI-based cationic carriers. Their transfection efficiency was as high as Lipofectamine™ 2000 and obvious significant proliferation and migration can be observed after the expression of the pGFP–ZNF580 gene in ECs.[60,61,559] Fig. 32 shows the process of transfection promoted by biodegradable MPs–pEGFP-ZNF580 complexes.[61] The first step or bottleneck for the complexes transported into cells is endocytosis. When the complexes escape from the endolysosome, the pGFP–ZNF580 gene can be expressed in the nucleus. The transfected ECs are beneficial to the formation of a living functional layer of ECs.

5.3 Targeting gene-complexes for the endothelialization of artificial vascular grafts

The RGD peptide is commonly used as a tumor-targeted peptide because of its specific binding ability with the $\alpha_v\beta_3$ or $\alpha_v\beta_5$ integrin, and the RGD targeting gene-complexes have been widely used in recognizing and eradicating tumor cells in cancer therapy.[475,674–676] In addition to tumor cells, the $\alpha_v\beta_3$ and $\alpha_v\beta_5$ integrins also exist in some other cells, which include ECs. These integrins have a high expression level on ECs, which not only facilitates the binding of targeting gene-complexes with ECs, but also improves the expression of relative genes. Hence, RGD targeting gene-complexes can also be used to enhance the endothelialization of artificial vascular grafts.[677,678]

Suh *et al.* developed an angiogenic EC-targeted polymeric gene delivery carrier (PEI-*g*-PEG–RGD) by conjugating the RGD peptide onto the PEI polymer with PEG as a spacer. In transfection experiments with angiogenic ECs, the transfection efficiency of the PEI-*g*-PEG–RGD targeting gene carrier is five times as PEI due to the binding affinity of RGD with the integrins of ECs. Compared with the non-targeting delivery carrier PEI-*g*-PEG–RAE, which is
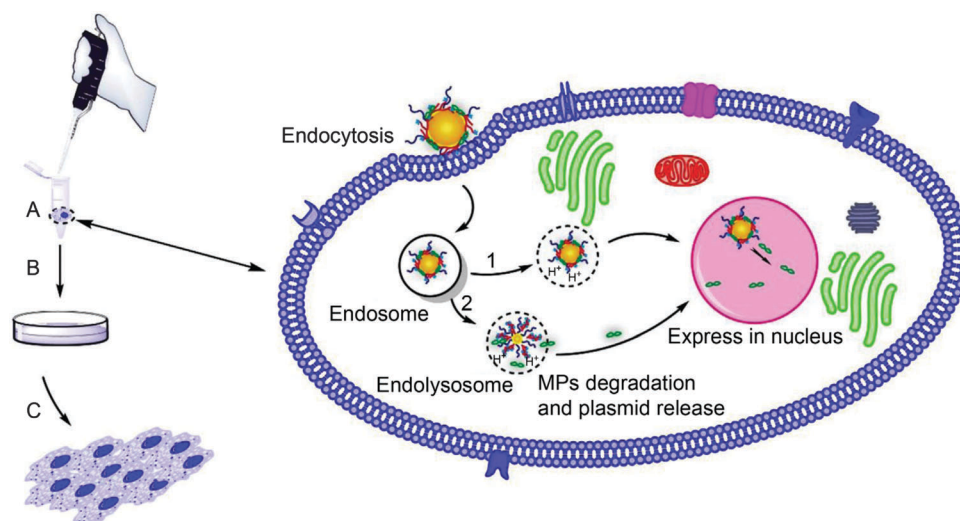
Fig. 32 The process of transfection and proliferation promoted by biodegradable MPs–pEGFP-ZNF580 complexes. (A) MPs–pEGFP-ZNF580 complexes at the N/P ratio of 10 were mixed with ECs in a serum-free medium, then the MPs–pEGFP-ZNF580 complexes was transfected into ECs *via* endocytosis, through path 1 or 2 plasmids of pEGFP-ZNF580 and enter into nucleus, (B) after 4 h, the ECs were cultured with fresh growth medium (10% FBS DMEM), (C) by rapid endothelialization, a living functional layer of ECs was formed. Reproduced with permission from ref. 61. Copyright 2014 Elsevier.

5724 | *Chem. Soc. Rev.*, 2015, **44**, 5680–5742

This journal is © The Royal Society of Chemistry 2015

composed of the RAE (Arg–Ala–Glu) peptide with PEI-*g*-PEG, PEI-*g*-PEG–RGD exhibited a higher binding ability to angiogenic ECs than normal ECs. Their study proved that the gene complexes formed by PEI-*g*-PEG–RGD can be directly delivered into angiogenic ECs *via* the binding ability of the RGD peptide with the $\alpha_v\beta_3$ and $\alpha_v\beta_5$ integrins. Thus, the transfection efficiency of these targeting gene carriers can be improved in angiogenic ECs gene therapy.[679]

Anwer *et al.* synthesized targeting gene delivery systems by conjugating the RGD peptide with liposome–pCMV-Luc plasmid complexes.[680] The transfection efficiency of the targeted complexes was 4-fold higher than the non-targeted liposome–pCMV-Luc complexes under serum-free conditions. More interestingly, in the presence of serum, the RGD targeted transfection complexes yielded a 4-fold higher expression level than the non-targeted transfection complexes, which indicates that the binding affinity of RGD to the $\alpha_v\beta_3$ integrin can also be maintained under serum conditions. However, in *in vivo* transfection experiments of targeted transfection complexes, the plasmid expression level was decreased by 50 times compared with the non-targeted complexes. They inferred that the low transfection efficiency *in vivo* may be induced by the aggregation of these complexes in the blood, and then they are cleared by alveolar macrophages. Thus, further investigations should be done by using different gene-complexes for transfecting ECs and modifying the complexes by PEG for high stability and prolonging the circulation time *in vivo*.

In 2011, Kibria *et al.* prepared PEGylated liposomes (PEG-LP) to obtain a stable gene carrier.[681] The RGD peptide, which has affinity for the $\alpha_v\beta_3$ integrin, was further conjugated with PEG-LP to form RGD–PEG-LP for targeting ECs. More interestingly, they further incorporated stearylated octaarginine (STR-R8) on the surface of RGD–PEG-LP to obtain a dual-ligand R8/RGD–PEG-LP carrier containing the RGD motif in association with STR-R8 as a CPP. As expected, the R8/RGD–PEG-LP–pDNA complexes showed a higher cellular uptake as well as transfection efficiency in $\alpha_v\beta_3$ integrin expression ECs than the PEG-LP–pDNA and RGD–pDNA complexes. They concluded that the dual-ligand (RGD and STR-R8) modified PEG-LP possesses a strong capability for recognition and entrance into ECs. This inspires us to have new insight for targeting delivery in the endothelialization of artificial vascular grafts.

In addition to the RGD peptide, other EC-targeted peptides as discussed in Section 4, such as CAG,[481] REDV and YIGSR,[492] can selectively bind with the integrins of normal vascular ECs. Thus, a novel promising strategy has been developed by incorporating these peptides with gene-complexes for EC transfection. These gene-complexes might have a very promising application in the rapid endothelialization of artificial vascular grafts. More recently, we developed a REDV functionalized polycationic gene carrier for pEGFP-ZNF580 delivery in ECs (Fig. 33).[527] This polycationic gene carrier, mPEG-P(LA-*co*-CL)-PEI-REDV, was prepared by the conjugation of the Cys-Arg–Glu–Asp–Val–Trp (CREDVW) peptide with the amphiphilic block copolymer of methoxy poly(ethylene glycol)ether-poly(L-lactide-*co*-ε-caprolactone)-poly(ethyleneimine) (mPEG-P(LA-*co*-CL)-PEI). mPEG-P(LA-*co*-CL)-PEI-REDV nanoparticles (REDV-NPs) and mPEG-P(LA-*co*-CL)-PEI nanoparticles (control NPs) were formed by the self-assembly of
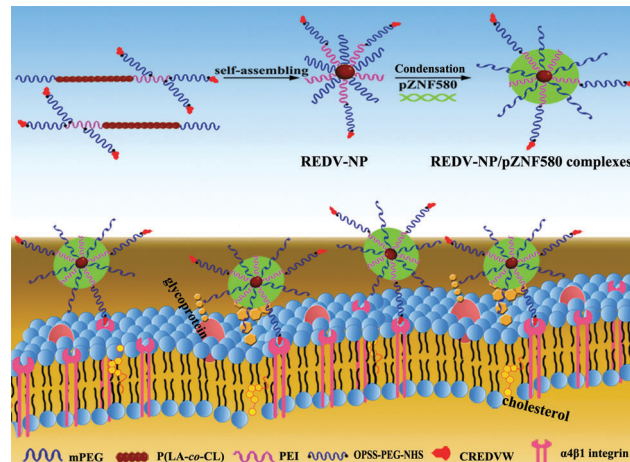

Fig. 33 Schematic illustration of the preparation of REDV-mediated REDV-NP–pZNF580 complexes by the self-assembling method and recognition of REDV-NP–pZNF580 complexes and integrins in ECs. Reproduced with permission from ref. 527. Copyright ©The Royal Society of Chemistry 2015.

the corresponding copolymers. Both NPs could condense pEGFP-ZNF580 plasmids into stable complexes and protect plasmids against DNase I degradation. The REDV-NP–pEGFP-ZNF580 complexes exhibited better cytocompatibility than the control NP–pEGFP-ZNF580 complexes. Moreover, *in vitro* transfection experiments and western blot analysis showed that pEGFP-ZNF580 plasmid expression and key protein expression in the REDV-NP–pEGFP-ZNF580 complexes group were better than the control group. More importantly, cell spreading ability was improved significantly in the targeted gene complexes group. The better results of the targeted complexes in the transfection and migration experiments are mainly ascribed to the REDV biofunction. Due to the specific selectivity between the REDV peptide and the $\alpha_4\beta_1$ integrin in ECs, the targeted complexes have a higher recognition to ECs than the non-targeted complexes. Thus, the REDV-NP–pEGFP-ZNF580 complexes can be efficiently and selectively adsorbed onto the surface of ECs, which is beneficial for complexes to enter into cells by endocytosis. These positive results demonstrated that these copolymers with functional EC-selective peptides can be a type of promising gene carrier with low cytotoxicity and high transfection efficiency.[527] We believe that this method will open a new avenue for the design and synthesis of novel targeting gene carriers for ECs, and will be more widely used in the rapid endothelialization of biomaterial surfaces in the future.

5.4 Biomimetic scaffolds modified with plasmid complexes for enhancing the proliferation of ECs

Biomimetic electrospun scaffolds are particularly beneficial for tissue-engineered vascular grafts and artificial vascular grafts.[245,402,682,683] These scaffolds usually have a large, interconnected porous structure that is ideal for the controlled release of bioactive molecules, growth factors, genes as well as for cell delivery.[647,684] Hadjiargyrou *et al.* first successfully demonstrated plasmid DNA incorporation into a polymer scaffold using electrospinning in 2003.[684] Their interesting results

indicated that plasmid DNA released directly from these electrospun scaffolds was indeed intact, capable of cellular transfection, and successfully encoded the protein β-galactosidase. Another approach involved encapsulating plasmid DNA into core–shell fibers where the shell was composed of PCL and poly(ethylenimine)–hyaluronic acid (PEI–HA), while plasmid DNA containing PEG constituted the core content.[647,685] The transfection efficiency of released plasmid DNA from these scaffolds was sustained up to 60 days. The release kinetics and transfection efficiency can be modulated by changing the electrospinning parameters and by varying the structures and compositions of electrospun scaffolds to meet tissue growth rate.[684] Inspired by DNA incorporation into scaffolds, we recently prepared PLGA/SF nanofibrous scaffolds with a weight ratio of 70/30 by the electrospinning technology to meet the mechanical demands in vascular tissue engineering applications; furthermore, we modified them with MPs–pEGFP-ZNF580 complexes using the electrospraying technique. MPs–pEGFP-ZNF580 complexes were prepared from ZNF580 plasmid and MPs of the amphiphilic copolymer, mPEG-*b*-P(MMD-*co*-GA)-*g*-PEI.[686] Negatively charged PLGA/SF scaffolds adsorbed the positively charged MPs–pEGFP-ZNF580 complexes *via* physical deposition and electrostatic forces. These scaffolds did not change their macroscopic shape and microscopic 3-D structures after the introduction of the MPs–pEGFP-ZNF580 complexes. Importantly, they could significantly enhance the adhesion and proliferation of HUVECs and inhibit SMC proliferation, which is beneficial for the rapid endothelialization of artificial vascular scaffolds. Although a fundamental understanding of gene complex modified scaffolds prepared by the electrospinning process, which include gene release kinetics, transfection properties and effects of electrospinning parameters, has yet to be achieved, this method is a promising approach to enhance the endothelialization of scaffolds. It will open a new avenue to prepare novel tissue-engineering scaffolds for artificial vascular grafts in the future.

The sophisticated processes of endothelialization on artificial vascular grafts involve many complex processes, such as EC adhesion, migration and proliferation, which are regulated by numerous signals. The delivery of growth factors and genes in the same temporal and spatial sequences as in ECs during the endothelialization processes is beneficial for inducing ECs to migrate, proliferate and finally form a new endothelial layer. The gene complexes and growth factor modified scaffolds will be able to deliver a potent combination of genes in a controllable sequence if they are further optimized. Moreover, the transfection efficiency can be improved by new emerging approaches, such as targeting gene carriers with bioactive peptides for selectively promoting the proliferation and migration of ECs. These combination approaches will promisingly develop more efficient gene delivery systems and composite scaffolds for vascular tissue engineering.

6. Conclusion and perspectives

Implantable PET, ePTFE and PU artificial vascular grafts have become one kind of main treatment for vascular diseases; however, thrombosis, restenosis and low long-term patency always limit their usage, especially as small-diameter artificial vascular grafts. In recent years, many strategies have been developed to improve the hemocompatibility and endothelialization of small-diameter artificial vascular grafts. In this review, we have summarized recent research progress in the surface modification and endothelialization of vascular biomaterials.

From the standpoint of anti-nonspecific protein adsorption on artificial vascular graft surfaces, the application of hydrophilic polymers in the modification of graft surfaces has obviously experienced rapid growth during the past few years. Hydrophilic PEG and zwitterionic polymers have been successfully grafted onto biomaterial surfaces by UV polymerization and ATRP. Importantly, the surface should be completely modified by these hydrophilic polymers, namely, the surface must be fully covered by a hydrophilic layer. Otherwise, even only few default areas will cause the adsorption of proteins and platelets from blood plasma and consequently induce thrombosis and restenosis. High graft densities and optimal polymer chain structures are beneficial to modify surfaces without any default. Therefore, through the grafting of poly(PEGMA) chains on biomaterial surfaces with many end hydroxyl groups as functional groups to introduce surface initiators for ATRP, multicomb block copolymers have successfully modified surfaces with high graft density. We believe that this modification strategy opens a new avenue to construct non-default surfaces with the combination of high hydrophilicity and the immobilization of bioactive molecules. While there are some intrinsic limitations of hydrophilic modification, such as poor EC attachment and spreading, it is a tough challenge to specifically enhance the adherence and proliferation of ECs on hydrophilic graft surfaces. Fortunately, these limitations can be overcome by linking EC specifically selective peptides onto the surfaces. The RGD, CAG, REDV, YIGSR and SVVYGLR peptides have been demonstrated to promote the adhesion and proliferation of ECs efficiently.[484] Among these peptides, RGD has been extensively investigated to modify artificial vascular grafts by various approaches. However, RGD can simultaneously enhance EC, platelets as well as SMC adhesion. This non-selectivity for cell types causes the competitive growth of SMCs or other cells on graft surfaces, which interferes with the formation of an endothelial monolayer. The CAG and REDV peptides exhibit high affinity for ECs, but far lower affinity for SMCs than RGD.[47,484] REDV has been demonstrated to have the best ability to enhance EC proliferation and to promote angiogenesis *in vivo*. The *in vivo* competitive ability of ECs over SMCs plays a very important role in the development of a pure confluent layer of ECs and the attainment of a better anti-restenosis effect.[687] Moreover, different peptides mediate different cell signaling pathways, which consequently result in different effects on cell spreading and migration. The surface modification by covalently immobilizing two or more kinds of peptides may be beneficial for optimal EC specific responses and endothelialization of artificial vascular grafts.

In addition to PET, ePTFE and PU non-degradable artificial vascular grafts, biodegradable electrospun scaffolds are beneficial for tissue engineered vascular grafts and blood vessel

5726 | *Chem. Soc. Rev.*, 2015, **44**, 5680–5742

This journal is © The Royal Society of Chemistry 2015

regeneration as well as blood vessel reconstruction. These biodegradable scaffolds can easily be prepared with optimal pore size, multilayer structures, as well as complex structures with nanofibers, microfibers, nanoparticles and gene complexes.[686] In particular, multilayer structure grafts can mimic native arteries with sufficient mechanical strength and elasticity as well as biocompatibility, bioactivity and antithrombotic properties. Furthermore, macroporous PCL scaffolds (~ 30 μm) have been successfully developed by simultaneously using the electrospinning and electrospraying technologies, which overcomes some limitations of electrospun scaffolds such as inadequate pore size and poor cell spreading.[142] These macroporous scaffolds provide cells with enough large pores to grow and also significantly enhance cell migration. Another attractive feature of multilayer scaffolds is the locally sustained release of growth factors and other fragile water soluble bioactive agents. Recent research has demonstrated that multilayered electrospun scaffolds can act as potential artificial vascular grafts with spatio-temporal delivery of growth factors.[651] Although tremendous progress in electrospun vascular grafts has been made *in vitro* during the past decade, they have still not approached the clinical trial stage. In addition, the electrospinning technology can be used to prepare linear tubes easily, but it is not suitable for mimicking the complex macrostructure of native blood vessels. More recently, 3D printing and 3D bioprinting technologies have been developed to reproduce complex configurations other than simple cylindrical structures; therefore, they are able to create patient-specific arterial scaffolds with biodegradable polymers, hydrogels and cells. Moreover, 3D bioprinting technology can print ECs and SMCs in defined spatial locations of scaffolds to mimic native blood vessels.[509] A combination of the electrospinning technology, 3D bioprinting technology, controlled release of growth factors and gene delivery will benefit the development of artificial vascular grafts or scaffolds with complex macrostructures, defined microarchitectures and biofunctions. However, the endothelialization process involves EC adhesion, migration and proliferation and is regulated by numerous signals.

Gene delivery technology has been utilized to promote the endothelialization of artificial vascular grafts; therefore, the development of safe and effective gene carriers is of great demand and importance.[688] As the "golden" standard for gene delivery, high molecular weight PEI is the most effective non-viral gene carrier *in vitro* and *in vivo* because of its unique combination of high charge density and enhanced "proton sponge effect" in endolysosomes, but it is often accompanied with significant cytotoxicity. Recently, micro- and nano-particles with different biodegradable and hydrophobic cores have been developed to overcome the limitations of PEI.[60,61,559] The cores of these micro- and nano-particles are composed of degradable poly(ester amide)s; moreover, several PEG chains as the hydrophilic corona and short PEI chains as the cationic shell are connected with the core. This special structure enables these gene carriers with considerable positive charges, low cytotoxicity and biodegradability. Furthermore, the gene carriers modified by EC selective peptides can be specifically recognized by ECs and efficiently promote EC transfection and migration.[527] The combination of cell-penetrating peptides, cell-adhesion

peptides, hydrophilic polymers (for improved serum stability and low cytotoxicity) and cationic endosomal buffering functionality in one gene carrier seems to serve as a highly efficient transfection agent for ECs.[599,601] In addition to the VEGF gene, the ZNF580 gene also plays an important role in the intervention of atherosclerosis and the process of migration and proliferation of ECs. More importantly, compared with the VEGF gene, the ZNF580 gene not only promotes the proliferation of ECs, but also might inhibit the proliferation of SMCs. We believe that complexes with ZNF580 gene, especially targeted complexes with low cytotoxicity and high transfection efficiency, might be used to enhance the endothelialization of tissue engineering scaffolds and vascular grafts.[60,61,527,559] However, it should be noted that these special selectivity functions of targeted complexes still need more investigations to be proven both *in vitro* and *in vivo*.

In summary, numerous strategies have been explored and developed to improve the performances of small-diameter artificial vascular grafts (diameter <4 mm); however, it is still a major challenge to selectively promote rapid endothelialization and endothelium regeneration at the early stage to enhance the formation of a confluent endothelium layer on graft surfaces, as well as to prevent thrombosis and intimal hyperplasia. This review highly recommends several technologies, methods and their combinations with the aim to develop ideal artificial vascular grafts, such as the synthesis of novel biomaterials, biomaterial processes, multilayer scaffolds, surface modification, targeting peptides and gene delivery.[689] Some multifunctional artificial vascular grafts with hydrophilic polymer modified surfaces, bioactive peptides, spatio-temporal delivery of growth factors and gene complexes, may exhibit great potential in future. However, much more fundamental research must be performed to better understand the mechanisms of the interactions between ECs and material surfaces, growth factors as well as targeting gene delivery systems *in vitro* and *in vivo*. In particular, the release kinetics of growth factors and genes should be controlled precisely, locally and spatio-temporally. Moreover, there remain many major challenges to create an ideal small-diameter artificial vascular graft with all the requirements in terms of mechanical properties and biological functions. In conclusion, considering EC adhesion, migration and proliferation, surface modification by EC selective peptides and targeting gene delivery systems will play a key role in the *in situ* endothelialization process. With future emerging advanced biomaterials and novel strategies for the preparation of small-diameter artificial vascular grafts (diameter <4 mm), we believe that highly performed artificial vascular grafts will be developed in the future.

Acknowledgements

References

1 T. Liu, S. Liu, K. Zhang, J. Chen and N. Huang, *J. Biomed. Mater. Res., Part A*, 2014, **102**, 3754–3772.

2 E. Filova, F. Straka, T. Mirejovsky, J. Masin and L. Bacakova, *Physiol. Res.*, 2009, **58**(suppl 2), S141–S158.

3 B. H. Oh, R. W. Kaligis, Y. Wang, F. E. Punzalan, N. C. Suwanwela, V. L. Nguyen, T. H. Lee, K. H. Sim, Y. Itoh, N. Bahadur and J. Leong, *Int. J. Cardiol.*, 2013, **168**, 2761–2766.

4 K. A. Rocco, M. W. Maxfield, C. A. Best, E. W. Dean and C. K. Breuer, *Tissue Eng., Part B*, 2014, **20**, 628–640.

5 L. Zhang and Y. K. Feng, *Curr. Sci.*, 2014, **106**, 816–822.

6 C. Spadaccio, M. Chello, M. Trombetta, A. Rainer, Y. Toyoda and J. A. Genovese, *J. Cell. Mol. Med.*, 2009, **13**, 422–439.

7 H. Naderi, M. M. Matin and A. R. Bahrami, *J. Biomater. Appl.*, 2011, **26**, 383–417.

8 A. Hasan, A. Memic, N. Annabi, M. Hossain, A. Paul, M. R. Dokmeci, F. Dehghani and A. Khademhosseini, *Acta Biomater.*, 2014, **10**, 11–25.

9 L. Ou, W. Li, Y. Zhang, W. Wang, J. Liu, H. Sorg, D. Furlani, R. Gabel, P. Mark, C. Klopsch, L. Wang, K. Lutzow, A. Lendlein, K. Wagner, D. Klee, A. Liebold, R. K. Li, D. Kong, G. Steinhoff and N. Ma, *J. Cell. Mol. Med.*, 2011, **15**, 1310–1318.

10 C. Devine and C. McCollum, *J. Vasc. Surg.*, 2004, **40**, 924–931.

11 M. J. Smith, M. J. McClure, S. A. Sell, C. P. Barnes, B. H. Walpoth, D. G. Simpson and G. L. Bowlin, *Acta Biomater.*, 2008, **4**, 58–66.

12 N. L'Heureux, N. Dusserre, A. Marini, S. Garrido, L. de la Fuente and T. McAllister, *Nat. Clin. Pract. Cardiovasc. Med.*, 2007, **4**, 389–395.

13 H. Wang, Y. Feng, H. Zhao, Z. Fang, M. Khan and J. Guo, *J. Nanosci. Nanotechnol.*, 2013, **13**, 1578–1582.

14 C. C. Mohan, K. P. Chennazhi and D. Menon, *Acta Biomater.*, 2013, **9**, 9568–9577.

15 W. van Oeveren, *Scientifica*, 2013, **2013**, 392584.

16 B. Nilsson, O. Korsgren, J. D. Lambris and K. N. Ekdahl, *Trends Immunol.*, 2010, **31**, 32–38.

17 B. D. Ratner, *Biomaterials*, 2007, **28**, 5144–5147.

18 A. de Mel, B. G. Cousins and A. M. Seifalian, *Int. J. Biomater.*, 2012, **2012**, 707863.

19 M. Bosiers, K. Deloose, J. Verbist, H. Schroe, G. Lauwers, W. Lansink and P. Peeters, *J. Vasc. Surg.*, 2006, **43**, 313–318.

20 L. C. Hsu, *Perfusion*, 2001, **16**, 417–428.

21 J. J. Wykrzykowska, J. L. Gutierrez-Chico and R. J. van Geuns, *Catheter. Cardiovasc. Interv.*, 2010, **75**, 964–966.

22 W. Zhai, L. J. Qiu, X. M. Mo, S. Wang, Y. F. Xu, B. Peng, M. Liu, J. H. Huang, G. C. Wang and J. H. Zheng, *J. Biomed. Mater. Res., Part B*, 2013, **102**, 203–211.

23 S. Wang, Y. Zhang, H. Wang and Z. Dong, *Int. J. Biol. Macromol.*, 2011, **48**, 345–353.

24 P. K. Shireman and H. P. Greisler, *J. Vasc. Surg.*, 2000, **31**, 936–943.

25 J. P. Chen and C. H. Su, *Acta Biomater.*, 2011, **7**, 234–243.

26 H. Y. Wang, Y. K. Feng, H. Y. Zhao, R. F. Xiao, J. Lu, L. Zhang and J. T. Guo, *Macromol. Res.*, 2012, **20**, 347–350.

27 Y. Chang, W. J. Chang, Y. J. Shih, T. C. Wei and G. H. Hsiue, *ACS Appl. Mater. Interfaces*, 2011, **3**, 1228–1237.

28 P. S. Liu, Q. Chen, S. S. Wu, J. Shen and S. C. Lin, *J. Membr. Sci.*, 2010, **350**, 387–394.

29 J. H. Li, M. Z. Li, J. Miao, J. B. Wang, X. S. Shao and Q. Q. Zhang, *Appl. Surf. Sci.*, 2012, **258**, 6398–6405.

30 S. H. Chen, Y. Chang, K. R. Lee, T. C. Wei, A. Higuchi, F. M. Ho, C. C. Tsou, H. T. Ho and J. Y. Lai, *Langmuir*, 2012, **28**, 17733–17742.

31 B. Gao, Y. Feng, J. Lu, L. Zhang, M. Zhao, C. Shi, M. Khan and J. Guo, *Mater. Sci. Eng., C*, 2013, **33**, 2871–2878.

32 M. Sun, J. Deng, Z. Tang, J. Wu, D. Li, H. Chen and C. Gao, *Colloids Surf., B*, 2014, **122**, 134–142.

33 C. H. Kim, M. S. Khil, H. Y. Kim, H. U. Lee and K. Y. Jahng, *J. Biomed. Mater. Res., Part B*, 2006, **78**, 283–290.

34 L. Bacakova, E. Filova, M. Parizek, T. Ruml and V. Svorcik, *Biotechnol. Adv.*, 2011, **29**, 739–767.

35 R. Ayala, C. Zhang, D. Yang, Y. Hwang, A. Aung, S. S. Shroff, F. T. Arce, R. Lal, G. Arya and S. Varghese, *Biomaterials*, 2011, **32**, 3700–3711.

36 O. F. Khan and M. V. Sefton, *Trends Biotechnol.*, 2011, **29**, 379–387.

37 S. B. Kennedy, N. R. Washburn, C. G. Simon, Jr. and E. J. Amis, *Biomaterials*, 2006, **27**, 3817–3824.

38 R. A. Gittens, L. Scheideler, F. Rupp, S. L. Hyzy, J. Geis-Gerstorfer, Z. Schwartz and B. D. Boyan, *Acta Biomater.*, 2014, **10**, 2907–2918.

39 H. Liu, X. Li, X. Niu, G. Zhou, P. Li and Y. Fan, *Biomacromolecules*, 2011, **12**, 2914–2924.

40 M. A. Cleary, E. Geiger, C. Grady, C. Best, Y. Naito and C. Breuer, *Trends Mol. Med.*, 2012, **18**, 394–404.

41 M. Zhang, Z. Wang, Z. Wang, S. Feng, H. Xu, Q. Zhao, S. Wang, J. Fang, M. Qiao and D. Kong, *Colloids Surf., B*, 2011, **85**, 32–39.

42 M. Avci-Adali, G. Ziemer and H. P. Wendel, *Biotechnol. Adv.*, 2010, **28**, 119–129.

43 Y. M. Shin, Y. B. Lee, S. J. Kim, J. K. Kang, J. C. Park, W. Jang and H. Shin, *Biomacromolecules*, 2012, **13**, 2020–2028.

44 A. de Mel, G. Jell, M. M. Stevens and A. M. Seifalian, *Biomacromolecules*, 2008, **9**, 2969–2979.

45 Z. Zhang, Y. Lai, L. Yu and J. Ding, *Biomaterials*, 2010, **31**, 7873–7882.

46 J. C. Liu and D. A. Tirrell, *Biomacromolecules*, 2008, **9**, 2984–2988.

47 Y. Wei, Y. Ji, L. Xiao, Q. Lin and J. Ji, *Colloids Surf., B*, 2011, **84**, 369–378.

48 W. Zheng, Z. Wang, L. Song, Q. Zhao, J. Zhang, D. Li, S. Wang, J. Han, X. L. Zheng, Z. Yang and D. Kong, *Biomaterials*, 2012, **33**, 2880–2891.

5728 | *Chem. Soc. Rev.*, 2015, **44**, 5680–5742

This journal is © The Royal Society of Chemistry 2015

49 K. Tashiro, G. C. Sephel, B. Weeks, M. Sasaki, G. R. Martin, H. K. Kleinman and Y. Yamada, *J. Biol. Chem.*, 1989, **264**, 16174–16182.

50 M. H. Fittkau, P. Zilla, D. Bezuidenhout, M. P. Lutolf, P. Human, J. A. Hubbell and N. Davies, *Biomaterials*, 2005, **26**, 167–174.

51 A. Andukuri, W. P. Minor, M. Kushwaha, J. M. Anderson and H. W. Jun, *J. Nanomed. Nanotechnol.*, 2010, **6**, 289–297.

52 B. Geiger, J. P. Spatz and A. D. Bershadsky, *Nat. Rev. Mol. Cell Biol.*, 2009, **10**, 21–33.

53 Y. Ji, Y. Wei, X. Liu, J. Wang, K. Ren and J. Ji, *J. Biomed. Mater. Res., Part A*, 2012, **100**, 1387–1397.

54 J. S. Golub, Y. T. Kim, C. L. Duvall, R. V. Bellamkonda, D. Gupta, A. S. Lin, D. Weiss, W. Robert Taylor and R. E. Guldberg, *Am. J. Physiol.: Heart Circ. Physiol.*, 2010, **298**, H1959–H1965.

55 Q. Hao, H. Su, D. Palmer, B. Sun, P. Gao, G. Y. Yang and W. L. Young, *Stroke*, 2011, **42**, 453–458.

56 R. K. Jain, *Semin. Oncol.*, 2002, **29**, 3–9.

57 D. B. Pike, S. Cai, K. R. Pomraning, M. A. Firpo, R. J. Fisher, X. Z. Shu, G. D. Prestwich and R. A. Peattie, *Biomaterials*, 2006, **27**, 5242–5251.

58 H. Zhang, X. Jia, F. Han, J. Zhao, Y. Zhao, Y. Fan and X. Yuan, *Biomaterials*, 2013, **34**, 2202–2212.

59 H. Y. Sun, S. P. Wei, R. C. Xu, P. X. Xu and W. C. Zhang, *Biochem. Biophys. Res. Commun.*, 2010, **395**, 361–366.

60 C. C. Shi, F. L. Yao, J. W. Huang, G. L. Han, Q. Li, M. Khan, Y. K. Feng and W. C. Zhang, *J. Mater. Chem. B*, 2014, **2**, 1825–1837.

61 C. Shi, F. Yao, Q. Li, M. Khan, X. Ren, Y. Feng, J. Huang and W. Zhang, *Biomaterials*, 2014, **35**, 7133–7145.

62 S. Venkatraman, F. Boey and L. L. Lao, *Prog. Polym. Sci.*, 2008, **33**, 853–874.

63 Z. Ma, M. Kotaki, T. Yong, W. He and S. Ramakrishna, *Biomaterials*, 2005, **26**, 2527–2536.

64 M. C. Burrows, V. M. Zamarion, F. B. Filippin-Monteiro, D. C. Schuck, H. E. Toma, A. Campa, C. R. Garcia and L. H. Catalani, *Macromol. Biosci.*, 2012, **12**, 1660–1670.

65 M. J. Moreno, A. Ajji, D. Mohebbi-Kalhori, M. Rukhlova, A. Hadjizadeh and M. N. Bureau, *J. Biomed. Mater. Res., Part B*, 2011, **97**, 201–214.

66 S. Dimitrievska, A. Petit, C. J. Doillon, L. Epure, A. Ajji, L. Yahia and M. N. Bureau, *Macromol. Biosci.*, 2011, **11**, 13–21.

67 D. Pfeiffer, C. Stefanitsch, K. Wankhammer, M. Muller, L. Dreyer, B. Krolitzki, H. Zernetsch, B. Glasmacher, C. Lindner, A. Lass, M. Schwarz, W. Muckenauer and I. Lang, *J. Biomed. Mater. Res., Part A*, 2014, **102**, 4500–4509.

68 Y. Gustafsson, J. Haag, P. Jungebluth, V. Lundin, M. L. Lim, S. Baiguera, F. Ajalloueian, C. Del Gaudio, A. Bianco, G. Moll, S. Sjoqvist, G. Lemon, A. I. Teixeira and P. Macchiarini, *Biomaterials*, 2012, **33**, 8094–8103.

69 M. Dhahri, A. Abed, R. H. Lajimi, M. B. Mansour, V. Gueguen, S. B. Abdesselem, F. Chaubet, D. Letourneur, A. Meddahi-Pelle and R. M. Maaroufi, *J. Biomed. Mater. Res., Part A*, 2011, **98**, 114–121.

70 J. M. van der Bas, P. H. Quax, A. C. van den Berg, M. J. Visser, E. van der Linden and J. H. van Bockel, *J. Vasc. Surg.*, 2004, **39**, 850–858.

71 A. Hadjizadeh, *J. Biomed. Mater. Res., Part B*, 2010, **94**, 11–21.

72 H. Savoji, A. Hadjizadeh, M. Maire, A. Ajji, M. R. Wertheimer and S. Lerouge, *Macromol. Biosci.*, 2014, **14**, 1084–1095.

73 F. Truica-Marasescu and M. R. Wertheimer, *Plasma Processes Polym.*, 2008, **5**, 44–57.

74 A. Gigout, J. C. Ruiz, M. R. Wertheimer, M. Jolicoeur and S. Lerouge, *Macromol. Biosci.*, 2011, **11**, 1110–1119.

75 A. K. Silva, D. Letourneur and C. Chauvierre, *Theranostics*, 2014, **4**, 579–591.

76 T. Indest, J. Laine, L. S. Johansson, K. Stana-Kleinschek, S. Strnad, R. Dworczak and V. Ribitsch, *Biomacromolecules*, 2009, **10**, 630–637.

77 M. Gericke, A. Doliska, J. Stana, T. Liebert, T. Heinze and K. Stana-Kleinschek, *Macromol. Biosci.*, 2011, **11**, 549–556.

78 H. Fasl, J. Stana, D. Stropnik, S. Strnad, K. Stana-Kleinschek and V. Ribitsch, *Biomacromolecules*, 2010, **11**, 377–381.

79 A. P. Zhu, F. Zhao and N. Fang, *J. Biomed. Mater. Res., Part A*, 2008, **86**, 467–476.

80 V. Švorčík, Z. Makajová, N. Slepičková Kasálková, Z. Kolská, P. Žáková, J. Karpíšková, I. Stibor and P. Slepička, *Carbon*, 2014, **69**, 361–371.

81 P. K. Thalla, H. Fadlallah, B. Liberelle, P. Lequoy, G. De Crescenzo, Y. Merhi and S. Lerouge, *Biomacromolecules*, 2014, **15**, 2512–2520.

82 A. Hadjizadeh, A. Ajji, M. Jolicoeur, B. Liberelle and G. De Crescenzo, *J. Biomed. Nanotechnol.*, 2013, **9**, 1195–1209.

83 S. Noel, B. Liberelle, A. Yogi, M. J. Moreno, M. N. Bureau, L. Robitaille and G. De Crescenzo, *J. Mater. Chem. B*, 2013, **1**, 230–238.

84 W. Chaouch, F. Dieval, N. Chakfe and B. Durand, *Int. J. Polym. Mater. Polym. Biomater.*, 2012, **61**, 410–423.

85 M. Modic, I. Junkar, A. Vesel and M. Mozetic, *Surf. Coat. Technol.*, 2012, **213**, 98–104.

86 A. I. Cassady, N. M. Hidzir and L. Grøndahl, *J. Appl. Polym. Sci.*, 2014, **131**, 40533.

87 Y. Farhatnia, A. Tan, A. Motiwala, B. G. Cousins and A. M. Seifalian, *Biotechnol. Adv.*, 2013, **31**, 524–542.

88 H. Takagi, S. N. Goto, M. Matsui, H. Manabe and T. Umemoto, *J. Vasc. Surg.*, 2010, **52**, 232–236.

89 N. R. Barshes, C. K. Ozaki, P. Kougias and M. Belkin, *J. Vasc. Surg.*, 2013, **57**, 1466–1470.

90 S. Liu, C. Dong, G. Lu, Q. Lu, Z. Li, D. L. Kaplan and H. Zhu, *Acta Biomater.*, 2013, **9**, 8991–9003.

91 X. Kapfer, W. Meichelboeck and F. M. Groegler, *Eur. J. Vasc. Endovasc. Surg.*, 2006, **32**, 155–168.

92 B. H. Walpoth, P. Zammaretti, M. Cikirikcioglu, E. Khabiri, M. K. Djebaili, J. C. Pache, J. C. Tille, Y. Aggoun, D. Morel, A. Kalangos, J. A. Hubbell and A. H. Zisch, *J. Thorac. Cardiovasc. Surg.*, 2007, **133**, 1163–1170.

93 T. Hubáček, J. Siegel, R. Khalili, N. Slepičková-Kasálková and V. Švorčík, *Appl. Surf. Sci.*, 2013, **275**, 43–48.

This journal is © The Royal Society of Chemistry 2015

Chem. Soc. Rev., 2015, **44**, 5680–5742 | 5729

94 S. K. Williams, L. B. Kleinert and V. Patula-Steinbrenner, *J. Biomed. Mater. Res., Part A*, 2011, **99**, 67–73.

95 Y. K. Cho, D. Park, H. Kim, H. Lee, H. Park, H. J. Kim and D. Jung, *Appl. Surf. Sci.*, 2014, **296**, 79–85.

96 R. J. van Det, B. H. Vriens, J. van der Palen and R. H. Geelkerken, *Eur. J. Vasc. Endovasc. Surg.*, 2009, **37**, 457–463.

97 X. Xie, R. Guidoin, M. Nutley and Z. Zhang, *J. Biomed. Mater. Res., Part B*, 2010, **93**, 497–509.

98 Y. Feng, S. Zhang, H. Wang, H. Zhao, J. Lu, J. Guo, M. Behl and A. Lendlein, *J. Controlled Release*, 2011, **152**(suppl 1), e20–e21.

99 Y. Feng, S. Zhang, H. Wang, H. Zhao, J. Lu, J. Guo, M. Behl and A. Lendlein, *J. Controlled Release*, 2011, **152**(suppl 1), e21–e23.

100 S. F. Zhang, Y. K. Feng, L. Zhang, J. T. Guo and Y. S. Xu, *J. Appl. Polym. Sci.*, 2010, **116**, 861–867.

101 Y. K. Feng, Y. Xue, J. T. Guo, L. Cheng, L. C. Jiao, Y. Zhang and J. L. Yue, *J. Appl. Polym. Sci.*, 2009, **112**, 473–478.

102 J. T. Guo, J. W. Yin and Y. K. Feng, *Trans. Tianjin Univ.*, 2010, **16**, 317–321.

103 M. T. Khorasani and S. Shorgashti, *J. Biomed. Mater. Res., Part A*, 2006, **77**, 253–260.

104 H. Wang, Y. Feng, M. Behl, A. Lendlein, H. Zhao, R. Xiao, J. Lu, L. Zhang and J. Guo, *Front. Chem. Sci. Eng.*, 2011, **5**, 392–400.

105 Y. Feng, F. Meng, R. Xiao, H. Zhao and J. Guo, *Front. Chem. Sci. Eng.*, 2010, **5**, 11–18.

106 M. G. Jeschke, V. Hermanutz, S. E. Wolf and G. B. Koveker, *J. Vasc. Surg.*, 1999, **29**, 168–176.

107 S. Muller-Hulsbeck, K. P. Walluscheck, M. Priebe, J. Grimm, J. Cremer and M. Heller, *Invest. Radiol.*, 2002, **37**, 314–320.

108 P. Zilla, D. Bezuidenhout and P. Human, *Biomaterials*, 2007, **28**, 5009–5027.

109 R. Y. Kannan, H. J. Salacinski, M. Odlyha, P. E. Butler and A. M. Seifalian, *Biomaterials*, 2006, **27**, 1971–1979.

110 R. Y. Kannan, H. J. Salacinski, J.-E. Ghanavi, A. Narula, M. Odlyha, H. Peirovi, P. E. Butler and A. M. Seifalian, *Plast. Reconstr. Surg.*, 2007, **119**, 1653–1662.

111 M. Ahmed, G. Hamilton and A. M. Seifalian, *Biomaterials*, 2014, **35**, 9033–9040.

112 D. S. Chong, L. A. Turner, N. Gadegaard, A. M. Seifalian, M. J. Dalby and G. Hamilton, *Eur. J. Vasc. Endovasc. Surg.*, 2015, **49**, 335–343.

113 H. W. Jun and J. L. West, *J. Biomed. Mater. Res., Part B*, 2005, **72**, 131–139.

114 L. J. Taite, P. Yang, H. W. Jun and J. L. West, *J. Biomed. Mater. Res., Part B*, 2008, **84**, 108–116.

115 F. Xu, J. C. Nacker, W. C. Crone and K. S. Masters, *Biomaterials*, 2008, **29**, 150–160.

116 A. Ruiz, C. E. Flanagan and K. S. Masters, *J. Biomed. Mater. Res., Part A*, 2013, **101**, 2870–2882.

117 A. Ruiz, K. R. Rathnam and K. S. Masters, *J. Mater. Sci.: Mater. Med.*, 2014, **25**, 487–498.

118 K. Takami, R. Matsuno and K. Ishihara, *Polymer*, 2011, **52**, 5445–5451.

119 Y. K. Feng, D. Z. Yang, H. Y. Zhao, J. T. Guo, Q. L. Chen and J. S. Liu, *Adv. Mater. Res.*, 2011, **306–307**, 1631–1634.

120 J. Guo, Y. Feng, Y. Ye and H. Zhao, *J. Appl. Polym. Sci.*, 2011, **122**, 1084–1091.

121 J. Fang, S. H. Ye, V. Shankarraman, Y. Huang, X. Mo and W. R. Wagner, *Acta Biomater.*, 2014, **10**, 4639–4649.

122 D. S. Tan, Z. Li, X. L. Yao, C. L. Xiang, H. Tan and Q. Fu, *J. Mater. Chem. B*, 2014, **2**, 1344–1353.

123 S. Doppalapudi, A. Jain, W. Khan and A. J. Domb, *Polym. Adv. Technol.*, 2014, **25**, 427–435.

124 D. Zhou, S. Shen, J. Yun, K. Yao and D.-Q. Lin, *Front. Chem. Sci. Eng.*, 2012, **6**, 339–347.

125 X. Ye, L. Lu, M. E. Kolewe, H. Park, B. L. Larson, E. S. Kim and L. E. Freed, *Biomaterials*, 2013, **34**, 10007–10015.

126 X. Kong, B. Han, H. Li, Y. Liang, K. Shao and W. Liu, *J. Biomed. Mater. Res., Part A*, 2012, **100**, 1494–1504.

127 H. Cao, Y. Feng, H. Wang, L. Zhang, M. Khan and J. Guo, *Front. Chem. Sci. Eng.*, 2011, **5**, 409–415.

128 M. C. Serrano, R. Pagani, M. Vallet-Regi, J. Pena, A. Ramila, I. Izquierdo and M. T. Portoles, *Biomaterials*, 2004, **25**, 5603–5611.

129 M. C. Serrano, R. Pagani, M. Manzano, J. V. Comas and M. T. Portoles, *Biomaterials*, 2006, **27**, 4706–4714.

130 S. de Valence, J. C. Tille, D. Mugnai, W. Mrowczynski, R. Gurny, M. Moller and B. H. Walpoth, *Biomaterials*, 2012, **33**, 38–47.

131 J. Shen, X. Fu, L. Ou, M. Zhang, Y. Guan, K. Wang, Y. Che, D. Kong, G. Steinhoff, W. Li, Y. Yu and N. Ma, *Int. J. Artif. Organs*, 2010, **33**, 161–170.

132 E. Luong-Van, L. Grondahl, K. N. Chua, K. W. Leong, V. Nurcombe and S. M. Cool, *Biomaterials*, 2006, **27**, 2042–2050.

133 L. Ye, X. Wu, Q. Mu, B. Chen, Y. Duan, X. Geng, Y. Gu, A. Zhang, J. Zhang and Z. G. Feng, *J. Biomater. Sci., Polym. Ed.*, 2010, **389**, 406.

134 S. J. Lee, J. Liu, S. H. Oh, S. Soker, A. Atala and J. J. Yoo, *Biomaterials*, 2008, **29**, 2891–2898.

135 B. W. Tillman, S. K. Yazdani, S. J. Lee, R. L. Geary, A. Atala and J. J. Yoo, *Biomaterials*, 2009, **30**, 583–588.

136 M. J. McClure, S. A. Sell, D. G. Simpson, B. H. Walpoth and G. L. Bowlin, *Acta Biomater.*, 2010, **6**, 2422–2433.

137 Q. Li, Z. Wang, S. Zhang, W. Zheng, Q. Zhao, J. Zhang, L. Wang, S. Wang and D. Kong, *Mater. Sci. Eng., C*, 2013, **33**, 1646–1653.

138 G. M. Xiong, S. J. Yuan, C. K. Tan, J. K. Wang, Y. Liu, T. T. Y. Tan, N. S. Tan and C. Choong, *J. Mater. Chem. B*, 2014, **2**, 485–493.

139 M. R. Williamson, R. Black and C. Kielty, *Biomaterials*, 2006, **27**, 3608–3616.

140 H. Wang, Y. Feng, H. Zhao, R. Xiao and J. Guo, *Adv. Mater. Res.*, 2011, **306–307**, 1627–1630.

141 K. Wang, M. Zhu, T. Li, W. Zheng, L. Li, M. Xu, Q. Zhao, D. Kong and L. Wang, *J. Biomed. Nanotechnol.*, 2014, **10**, 1588–1598.

142 Z. Wang, Y. Cui, J. Wang, X. Yang, Y. Wu, K. Wang, X. Gao, D. Li, Y. Li, X. L. Zheng, Y. Zhu, D. Kong and Q. Zhao, *Biomaterials*, 2014, **35**, 5700–5710.

5730 | *Chem. Soc. Rev.*, 2015, **44**, 5680–5742

This journal is © The Royal Society of Chemistry 2015

143 D. Narayan and S. S. Venkatraman, *J. Biomed. Mater. Res., Part A*, 2008, **87**, 710–718.

144 Y. Iwasaki, S. Sawada, K. Ishihara, G. Khang and H. B. Lee, *Biomaterials*, 2002, **23**, 3897–3903.

145 Y. K. Feng, H. Y. Zhao, L. C. Jiao, J. Lu, H. Y. Wang and J. T. Guo, *Polym. Adv. Technol.*, 2012, **23**, 382–388.

146 A. Alteheld, Y. K. Feng, S. Kelch and A. Lendlein, *Angew. Chem., Int. Ed.*, 2005, **44**, 1188–1192.

147 E. Bat, T. G. van Kooten, J. Feijen and D. W. Grijpma, *Acta Biomater.*, 2011, **7**, 1939–1948.

148 Y. Song, J. W. Wennink, M. M. Kamphuis, L. M. Sterk, I. Vermes, A. A. Poot, J. Feijen and D. W. Grijpma, *Tissue Eng., Part A*, 2011, **17**, 381–387.

149 Y. K. Feng and S. F. Zhang, *J. Polym. Sci., Polym. Chem.*, 2005, **43**, 4819–4827.

150 B. L. Dargaville, C. Vaquette, F. Rasoul, J. J. Cooper-White, J. H. Campbell and A. K. Whittaker, *Acta Biomater.*, 2013, **9**, 6885–6897.

151 V. Thomas, T. Donahoe, E. Nyairo, D. R. Dean and Y. K. Vohra, *Acta Biomater.*, 2011, **7**, 2070–2079.

152 Y. X. Yin, J. L. Yi, L. J. Xie, Q. J. Yan, H. L. Dai and S. P. Li, *Front. Mater. Sci.*, 2014, **8**, 95–101.

153 Y. Z. Li, J. D. He, G. Z. Cui, W. N. He and Z. Peng, *J. Appl. Polym. Sci.*, 2010, **118**, 2005–2008.

154 J. Zotzmann, M. Behl, Y. K. Feng and A. Lendlein, *Adv. Funct. Mater.*, 2010, **20**, 3583–3594.

155 M. Behl, U. Ridder, Y. Feng, S. Kelch and A. Lendlein, *Soft Matter*, 2009, **5**, 676–684.

156 A. Lendlein, J. Zotzmann, Y. Feng, A. Alteheld and S. Kelch, *Biomacromolecules*, 2009, **10**, 975–982.

157 J. Tian, Y. K. Feng and Y. S. Xu, *J. Polym. Res.*, 2006, **13**, 343–347.

158 J. Tian, Y. K. Feng and Y. S. Xu, *Macromol. Res.*, 2006, **14**, 209–213.

159 A. C. Fonseca, M. H. Gil and P. N. Simões, *Prog. Polym. Sci.*, 2014, **39**, 1291–1311.

160 M. Deng, J. Wu, C. A. Reinhart-King and C. C. Chu, *Acta Biomater.*, 2011, **7**, 1504–1515.

161 Y. Feng and J. Guo, *Int. J. Mol. Sci.*, 2009, **10**, 589–615.

162 Y. Feng, J. Lu, M. Behl and A. Lendlein, *Macromol. Biosci.*, 2010, **10**, 1008–1021.

163 Y. Feng, D. Klee and H. Hocker, *Macromol. Chem. Phys.*, 2001, **202**, 3120–3125.

164 Y. Feng, D. Klee and H. Höcker, *Macromol. Chem. Phys.*, 1999, **200**, 2276–2283.

165 Y. Feng, J. Knüfermann, D. Klee and H. Höcker, *Macromol. Rapid Commun.*, 1999, **20**, 88–90.

166 Y. Feng, J. Knüfermann, D. Klee and H. Höcker, *Macromol. Chem. Phys.*, 1999, **200**, 1506–1514.

167 Y. Feng, D. Klee, H. Keul and H. Höcker, *Macromol. Biosci.*, 2001, **1**, 30–39.

168 Y. Feng, D. Klee and H. Höcker, *e-Polym.*, 2001, **003**, 1–15.

169 Y. Feng, D. Klee, H. Keul and H. Höcker, *Macromol. Chem. Phys.*, 2000, **201**, 2670–2675.

170 Y. Feng, D. Klee and H. Hocker, *J. Appl. Polym. Sci.*, 2002, **86**, 2916–2919.

171 Y. Feng, D. Klee and H. Höcker, *Macromol. Chem. Phys.*, 2002, **203**, 819–824.

172 Y. Feng, D. Klee and H. Höcker, *J. Polym. Sci., Polym. Chem.*, 2005, **43**, 3030–3039.

173 Y. Feng, D. Klee and H. Hocker, *Macromol. Biosci.*, 2004, **4**, 587–590.

174 Y. Feng, D. Klee and H. Höcker, *Macromol. Biosci.*, 2001, **1**, 66–74.

175 Y. Feng, M. Behl, S. Kelch and A. Lendlein, *Macromol. Biosci.*, 2009, **9**, 45–54.

176 Y. Feng, J. Lu, M. Behl and A. Lendlein, *Int. J. Artif. Organs*, 2011, **34**, 103–109.

177 J. Lv, L. Zhang, M. Khan, X. Ren, J. Guo and Y. Feng, *React. Funct. Polym.*, 2014, **82**, 89–97.

178 L. Zhang, Y. K. Feng, H. Tian, M. Zhao, M. Khan and J. T. Guo, *J. Polym. Sci., Polym. Chem.*, 2013, **51**, 3213–3226.

179 L. Zhang, Y. K. Feng, H. Tian, C. C. Shi, M. Zhao and J. T. Guo, *React. Funct. Polym.*, 2013, **73**, 1281–1289.

180 L. Zhang, Y. K. Feng, H. F. Cao, J. T. Guo and M. Khan, *J. Controlled Release*, 2013, **172**, E48–E49.

181 L. Elomaa, Y. Kang, J. V. Seppälä and Y. Yang, *J. Polym. Sci., Polym. Chem.*, 2014, **52**, 3307–3315.

182 S. Yin, J. Li, N. Li, G. Wang and X. Gu, *J. Nanopart. Res.*, 2014, **16**, 2274.

183 D. K. Knight, E. R. Gillies and K. Mequanint, *Acta Biomater.*, 2014, **10**, 3484–3496.

184 A. Battig, B. Hiebl, Y. Feng, A. Lendlein and M. Behl, *Clin. Hemorheol. Microcirc.*, 2011, **48**, 161–172.

185 J. A. Horwitz, K. M. Shum, J. C. Bodle, M. Deng, C. C. Chu and C. A. Reinhart-King, *J. Biomed. Mater. Res., Part A*, 2010, **95**, 371–380.

186 D. J. Munoz-Pinto, A. C. Jimenez-Vergara, T. P. Gharat and M. S. Hahn, *Biomaterials*, 2015, **40**, 32–42.

187 K. K. Sankaran, A. Subramanian, U. M. Krishnan and S. Sethuraman, *Biotechnol. J.*, 2015, **10**, 96–108.

188 V. M. Merkle, D. Martin, M. Hutchinson, P. L. Tran, A. Behrens, S. Hossainy, J. Sheriff, D. Bluestein, X. Wu and M. J. Slepian, *ACS Appl. Mater. Interfaces*, 2015, **7**, 8302–8312.

189 M. F. Elahi, G. Guan, L. Wang, X. Zhao, F. Wang and M. W. King, *Langmuir*, 2015, **31**, 2517–2526.

190 W.-C. Hsieh, J.-J. Liau and Y.-J. Li, *Int. J. Polym. Sci.*, 2014, 935305.

191 S. Yano, M. Mori, N. Teramoto, M. Iisaka, N. Suzuki, M. Noto, Y. Kaimoto, M. Kakimoto, M. Yamada, E. Shiratsuchi, T. Shimasaki and M. Shibata, *Mar. Drugs*, 2015, **13**, 338–353.

192 C. H. Chuang, R. Z. Lin, H. W. Tien, Y. C. Chu, Y. C. Li, J. M. Melero-Martin and Y. C. Chen, *Acta Biomater.*, 2015, **19**, 85–99.

193 M. Zhu, K. Wang, J. Mei, C. Li, J. Zhang, W. Zheng, D. An, N. Xiao, Q. Zhao, D. Kong and L. Wang, *Acta Biomater.*, 2014, **10**, 2014–2023.

194 R. Sridhar, K. Madhaiyan, S. Sundarrajan, A. Góra, J. R. Venugopal and S. Ramakrishna, *J. Mater. Chem. B*, 2014, **2**, 1626–1633.

This journal is © The Royal Society of Chemistry 2015

Chem. Soc. Rev., 2015, **44**, 5680–5742 | 5731

195 G. Fercana, D. Bowser, M. Portilla, E. M. Langan, C. G. Carsten, D. L. Cull, L. N. Sierad and D. T. Simionescu, *Tissue Eng., Part C*, 2014, **20**, 1016–1027.

196 C. Quint, Y. Kondo, R. J. Manson, J. H. Lawson, A. Dardik and L. E. Niklason, *Proc. Natl. Acad. Sci. U. S. A.*, 2011, **108**, 9214–9219.

197 S. Dimitrievska, C. Cai, A. Weyers, J. L. Balestrini, T. Lin, S. Sundaram, G. Hatachi, D. A. Spiegel, T. R. Kyriakides, J. Miao, G. Li, L. E. Niklason and R. J. Linhardt, *Acta Biomater.*, 2015, **13**, 177–187.

198 R. Gauvin, T. Ahsan, D. Larouche, P. Levesque, J. Dube, F. A. Auger, R. M. Nerem and L. Germain, *Tissue Eng., Part A*, 2010, **16**, 1737–1747.

199 V. A. Kumar, S. Shi, B. K. Wang, I. C. Li, A. A. Jalan, B. Sarkar, N. C. Wickremasinghe and J. D. Hartgerink, *J. Am. Chem. Soc.*, 2015, **137**, 4823–4830.

200 J. P. Stegemann, S. N. Kaszuba and S. L. Rowe, *Tissue Eng.*, 2007, **13**, 2601–2613.

201 G. Natasha, A. Tan, B. Gundogan, Y. Farhatnia, L. Nayyer, S. Mahdibeiraghdar, J. Rajadas, P. De Coppi, A. H. Davies and A. M. Seifalian, *Expert Opin. Biol. Ther.*, 2015, **15**, 231–244.

202 R. Sridhar, R. Lakshminarayanan, K. Madhaiyan, V. A. Barathi, K. H. Lim and S. Ramakrishna, *Chem. Soc. Rev.*, 2015, **44**, 790–814.

203 R. M. Nezarati, M. B. Eifert, D. K. Dempsey and E. Cosgriff-Hernandez, *J. Biomed. Mater. Res., Part B*, 2015, **103**, 313–323.

204 B. Marelli, A. Alessandrino, S. Fare, G. Freddi, D. Mantovani and M. C. Tanzi, *Acta Biomater.*, 2010, **6**, 4019–4026.

205 X. Zhang, X. Wang, V. Keshav, X. Wang, J. T. Johanas, G. G. Leisk and D. L. Kaplan, *Biomaterials*, 2009, **30**, 3213–3223.

206 X. Zhang, C. B. Baughman and D. L. Kaplan, *Biomaterials*, 2008, **29**, 2217–2227.

207 L. Li, H. Li, Y. Qian, X. Li, G. K. Singh, L. Zhong, W. Liu, Y. Lv, K. Cai and L. Yang, *Int. J. Biol. Macromol.*, 2011, **49**, 223–232.

208 H. Liu, X. Li, G. Zhou, H. Fan and Y. Fan, *Biomaterials*, 2011, **32**, 3784–3793.

209 F. P. Seib, M. Herklotz, K. A. Burke, M. F. Maitz, C. Werner and D. L. Kaplan, *Biomaterials*, 2014, **35**, 83–91.

210 Z. Li, Q. Liu, H. Wang, L. Song, H. Shao, M. Xie, Y. Xu and Y. Zhang, *ACS Biomater. Sci. Eng.*, 2015, **1**, 238–246.

211 T. Asakura, M. Isozaki, T. Saotome, K.-I. Tatematsu, H. Sezutsu, N. Kuwabara and Y. Nakazawa, *J. Mater. Chem. B*, 2014, **2**, 7375–7383.

212 X. Jing, H. Y. Mi, J. Peng, X. F. Peng and L. S. Turng, *Carbohydr. Polym.*, 2015, **117**, 941–949.

213 W. Zhao, W. Liu, J. Li, X. Lin and Y. Wang, *J. Biomed. Mater. Res., Part A*, 2015, **103**, 807–818.

214 J. M. Rajwade, K. M. Paknikar and J. V. Kumbhar, *Appl. Microbiol. Biotechnol.*, 2015, **99**, 2491–2511.

215 Y. Li, S. Wang, R. Huang, Z. Huang, B. Hu, W. Zheng, G. Yang and X. Jiang, *Biomacromolecules*, 2015, **16**, 780–789.

216 S. Zang, R. Zhang, H. Chen, Y. Lu, J. Zhou, X. Chang, G. Qiu, Z. Wu and G. Yang, *Mater. Sci. Eng., C*, 2015, **46**, 111–117.

217 H. G. D. O. Barud, H. D. S. Barud, M. Cavicchioli, T. S. D. Amaral, O. B. D. O. Junior, D. M. Santos, A. L. D. O. A. Petersen, F. Celes, V. M. Borges, C. I. D. Oliveira, P. F. D. Oliveira, R. A. Furtado, D. C. Tavares and S. J. L. Ribeiro, *Carbohydr. Polym.*, 2015, **128**, 41–51.

218 M. Scherner, S. Reutter, D. Klemm, A. Sterner-Kock, M. Guschlbauer, T. Richter, G. Langebartels, N. Madershahian, T. Wahlers and J. Wippermann, *J. Surg. Res.*, 2014, **189**, 340–347.

219 A. Baah-Dwomoh, A. Rolong, P. Gatenholm and R. V. Davalos, *Appl. Microbiol. Biotechnol.*, 2015, **99**, 4785–4794.

220 E. E. Brown, D. Hu, N. Abu Lail and X. Zhang, *Biomacromolecules*, 2013, **14**, 1063–1071.

221 F. Ahmed, S. Saleemi, Z. Khatri, M. I. Abro and I. S. Kim, *Carbohydr. Polym.*, 2015, **115**, 388–393.

222 M. Ahmed, H. Ghanbari, B. G. Cousins, G. Hamilton and A. M. Seifalian, *Acta Biomater.*, 2011, **7**, 3857–3867.

223 L. Budyanto, Y. Q. Goh and C. P. Ooi, *J. Mater. Sci.: Mater. Med.*, 2009, **20**, 105–111.

224 J. G. Torres-Rendon, T. Femmer, L. De Laporte, T. Tigges, K. Rahimi, F. Gremse, S. Zafarnia, W. Lederle, S. Ifuku, M. Wessling, J. G. Hardy and A. Walther, *Adv. Mater.*, 2015, **27**, 2989–2995.

225 T. Lu, Y. Li and T. Chen, *Int. J. Nanomed.*, 2013, **8**, 337–350.

226 A. Ovsianikov, A. Deiwick, S. Van Vlierberghe, P. Dubruel, L. Moller, G. Drager and B. Chichkov, *Biomacromolecules*, 2011, **12**, 851–858.

227 M. E. Kolewe, H. Park, C. Gray, X. Ye, R. Langer and L. E. Freed, *Adv. Mater.*, 2013, **25**, 4459–4465.

228 X. Zhang and Y. Zhang, *Cell Biochem. Biophys.*, 2015, DOI: 10.1007/s12013-015-0531-x.

229 S. J. Lee, D. N. Heo, J. S. Park, S. K. Kwon, J. H. Lee, J. H. Lee, W. D. Kim, I. K. Kwon and S. A. Park, *Phys. Chem. Chem. Phys.*, 2015, **17**, 2996–2999.

230 K. T. Shalumon, S. Deepthi, M. S. Anupama, S. V. Nair, R. Jayakumar and K. P. Chennazhi, *Int. J. Biol. Macromol.*, 2015, **72**, 1048–1055.

231 X. Gong, H. Liu, X. Ding, M. Liu, X. Li, L. Zheng, X. Jia, G. Zhou, Y. Zou, J. Li, X. Huang and Y. Fan, *Biomaterials*, 2014, **35**, 4782–4791.

232 L. Jia, M. P. Prabhakaran, X. Qin and S. Ramakrishna, *J. Biomater. Appl.*, 2014, **29**, 364–377.

233 H. Daemi and M. Barikani, *Carbohydr. Polym.*, 2014, **112**, 638–647.

234 G. Q. Zhu, F. G. Wang, C. H. Su, Q. C. Gao and Y. Y. Liu, *J. Chem. Soc. Pak.*, 2014, **36**, 198–203.

235 H. S. Park, M. S. Gong, J. H. Park, S. I. Moon, I. B. Wall, H. W. Kim, J. H. Lee and J. C. Knowles, *Acta Biomater.*, 2013, **9**, 8962–8971.

236 M. Zhou, W. C. Wang, Y. G. Liao, W. Q. Liu, M. Yu and C. X. Ouyang, *Front. Mater. Sci.*, 2014, **8**, 63–71.

237 H. Wang, Y. Feng, H. Zhao, J. Lu, J. Guo, M. Behl and A. Lendlein, *J. Controlled Release*, 2011, **152**(suppl 1), e28–e29.

238 J. Kucinska-Lipka, I. Gubanska, H. Janik and M. Sienkiewicz, *Mater. Sci. Eng., C*, 2015, **46**, 166–176.

239 C. S. Wong, X. Liu, Z. Xu, T. Lin and X. Wang, *J. Mater. Sci.: Mater. Med.*, 2013, **24**, 1865–1874.

240 P. H. Blit, K. G. Battiston, M. Yang, J. Paul Santerre and K. A. Woodhouse, *Acta Biomater.*, 2012, **8**, 2493–2503.

241 P. H. Blit, W. G. McClung, J. L. Brash, K. A. Woodhouse and J. P. Santerre, *Biomaterials*, 2011, **32**, 5790–5800.

242 Y. Yao, J. Wang, Y. Cui, R. Xu, Z. Wang, J. Zhang, K. Wang, Y. Li, Q. Zhao and D. Kong, *Acta Biomater.*, 2014, **10**, 2739–2749.

243 J. Han, P. Lazarovici, C. Pomerantz, X. Chen, Y. Wei and P. I. Lelkes, *Biomacromolecules*, 2011, **12**, 399–408.

244 N. Diban, S. Haimi, L. Bolhuis-Versteeg, S. Teixeira, S. Miettinen, A. Poot, D. Grijpma and D. Stamatialis, *Acta Biomater.*, 2013, **9**, 6450–6458.

245 W. Zhou, Y. Feng, J. Yang, J. Fan, J. Lv, L. Zhang, J. Guo, X. Ren and W. Zhang, *J. Mater. Sci.: Mater. Med.*, 2015, DOI: 10.1007/s10856-015-5386-6.

246 L. Yu, X. F. Hao, Q. Li, C. C. Shi and Y. K. Feng, *Adv. Mater. Res.*, 2014, **1015**, 336–339.

247 H. Y. Zhao, Y. K. Feng and J. T. Guo, *J. Appl. Polym. Sci.*, 2011, **122**, 1712–1721.

248 C. L. Feng, D. Zhang and H. Schonherr, *J. Controlled Release*, 2011, **152**(suppl 1), e201–e202.

249 A. de Mel, N. Naghavi, B. G. Cousins, I. Clatworthy, G. Hamilton, A. Darbyshire and A. M. Seifalian, *J. Mater. Sci.: Mater. Med.*, 2014, **25**, 917–929.

250 J. T. Guo, Y. Q. Ye, Y. K. Feng and H. Y. Zhao, *Polym. Adv. Technol.*, 2010, **21**, 759–766.

251 Y. Feng, H. Zhao, J. Lu and J. Guo, *J. Controlled Release*, 2011, **152**(suppl 1), e202–e204.

252 H. Y. Wang, Y. K. Feng, Z. C. Fang, W. J. Yuan and M. Khan, *Mater. Sci. Eng., C*, 2012, **32**, 2306–2315.

253 H. Y. Wang, Y. K. Feng, W. J. Yuan, H. Y. Zhao, Z. C. Fang, K. Musammir and J. T. Guo, *Sci. China: Phys., Mech. Astron.*, 2012, **55**, 1189–1193.

254 Y. Feng, H. Zhao, M. Behl, A. Lendlein, J. Guo and D. Yang, *J. Mater. Sci.: Mater. Med.*, 2013, **24**, 61–70.

255 W. Yuan, Y. Feng, H. Wang, D. Yang, B. An, W. Zhang, M. Khan and J. Guo, *Mater. Sci. Eng., C*, 2013, **33**, 3644–3651.

256 Y. Liu, Y. Inoue, A. Mahara, S. Kakinoki, T. Yamaoka and K. Ishihara, *J. Biomater. Sci., Polym. Ed.*, 2014, **25**, 1514–1529.

257 Y. Liu, Y. Inoue, S. Sakata, S. Kakinoki, T. Yamaoka and K. Ishihara, *J. Biomater. Sci., Polym. Ed.*, 2014, **25**, 474–486.

258 N. Nakabayashi and D. F. Williams, *Biomaterials*, 2003, **24**, 2431–2435.

259 T. Yoneyama, K. Sugihara, K. Ishihara, Y. Iwasaki and N. Nakabayashi, *Biomaterials*, 2002, **23**, 1455–1459.

260 Y. Hong, S. H. Ye, A. Nieponice, L. Soletti, D. A. Vorp and W. R. Wagner, *Biomaterials*, 2009, **30**, 2457–2467.

261 X. Jing, H. Y. Mi, M. R. Salick, T. M. Cordie, X. F. Peng and L. S. Turng, *Mater. Sci. Eng., C*, 2015, **49**, 40–50.

262 J. D. Abraham and K. Wahid, *Focal Controlled Drug Delivery*, Springer, Berlin, 2014.

263 J. Han, S. Farah, A. J. Domb and P. I. Lelkes, *Pharm. Res.*, 2013, **30**, 1735–1748.

264 I. Capila and R. J. Linhardt, *Angew. Chem., Int. Ed.*, 2002, **41**, 390–412.

265 P. K. Qi, M. F. Maitz and N. Huang, *Surf. Coat. Technol.*, 2013, **233**, 80–90.

266 Y. Feng, H. Zhao, L. Zhang and J. Guo, *Front. Chem. Eng. China*, 2010, **4**, 372–381.

267 G. S. Wu, P. H. Li, H. Q. Feng, X. M. Zhang and P. K. Chu, *J. Mater. Chem. B*, 2015, **3**, 2024–2042.

268 J. Zheng, L. Y. Li, S. F. Chen and S. Y. Jiang, *Langmuir*, 2004, **20**, 8931–8938.

269 Y. K. Feng, H. Y. Zhao, S. F. Zhang, L. C. Jiao, J. Lu, H. Y. Wang and J. T. Guo, *Macromol. Symp.*, 2011, **306–307**, 18–26.

270 A. T. Neffe, M. von Ruesten-Lange, S. Braune, K. Luetzow, T. Roch, K. Richau, F. Jung and A. Lendlein, *Macromol. Biosci.*, 2013, **13**, 1720–1729.

271 Y. Feng, H. Tian, M. Tan, P. Zhang, Q. Chen and J. Liu, *Trans. Tianjin Univ.*, 2013, **19**, 58–65.

272 J. Huang and W. Xu, *Appl. Surf. Sci.*, 2010, **256**, 3921–3927.

273 H. Gotz, U. Beginn, C. F. Bartelink, H. J. M. Grunbauer and M. Moller, *Macromol. Mater. Eng.*, 2002, **287**, 223–230.

274 J. Heuts, J. Salber, A. M. Goldyn, R. Janser, M. Moller and D. Klee, *J. Biomed. Mater. Res., Part A*, 2010, **92**, 1538–1551.

275 J. Hoffmann, J. Groll, J. Heuts, H. Rong, D. Klee, G. Ziemer, M. Moeller and H. P. Wendel, *J. Biomater. Sci., Polym. Ed.*, 2006, **17**, 985–996.

276 J. Groll, E. V. Amirgoulova, T. Ameringer, C. D. Heyes, C. Rocker, G. U. Nienhaus and M. Moller, *J. Am. Chem. Soc.*, 2004, **126**, 4234–4239.

277 J. Groll, T. Ameringer, J. P. Spatz and M. Moeller, *Langmuir*, 2005, **21**, 1991–1999.

278 J. Groll, J. Fiedler, E. Engelhard, T. Ameringer, S. Tugulu, H. A. Klok, R. E. Brenner and M. Moeller, *J. Biomed. Mater. Res., Part A*, 2005, **74**, 607–617.

279 X. F. Zhou, T. Z. Zhang, D. W. Guo and N. Gu, *Colloids Surf., A*, 2014, **441**, 34–42.

280 M. Khan, Y. K. Feng, D. Z. Yang, W. Zhou, H. Tian, Y. Han, L. Zhang, W. J. Yuan, J. Zhang, J. T. Guo and W. C. Zhang, *J. Polym. Sci., Part A: Polym. Chem.*, 2013, **51**, 3166–3176.

281 H. Y. Zhao, Y. K. Feng and J. T. Guo, *J. Appl. Polym. Sci.*, 2011, **119**, 3717–3727.

282 W. J. Yuan, Y. K. Feng, H. Y. Wang, D. Z. Yang, Y. Han, J. T. Guo, H. Tian and M. Khan, *J. Controlled Release*, 2013, **172**, E142–E143.

283 T. B. Stachowiak, D. A. Mair, T. G. Holden, L. J. Lee, F. Svec and J. M. J. Fréchet, *J. Sep. Sci.*, 2007, **30**, 1088–1093.

284 Y. K. Joung, J. H. Choi, J. W. Bae and K. D. Park, *Acta Biomater.*, 2008, **4**, 960–966.

285 Z. K. Xu, F. Q. Nie, C. Qu, L. S. Wan, J. Wu and K. Yao, *Biomaterials*, 2005, **26**, 589–598.

286 D. Li, H. Chen, W. Glenn McClung and J. L. Brash, *Acta Biomater.*, 2009, **5**, 1864–1871.

287 X. T. Zhao, Y. L. Su, Y. F. Li, R. N. Zhang, J. J. Zhao and Z. Y. Jiang, *J. Membr. Sci.*, 2014, **450**, 111–123.

288 H. J. Jukarainen, S. J. Clarson, J. V. Seppala, G. S. Retzinger and J. K. Ruohonen, *Silicon*, 2012, **4**, 231–238.

289 K. F. Schilke and J. McGuire, *J. Colloid Interface Sci.*, 2011, **358**, 14–24.

This journal is © The Royal Society of Chemistry 2015

Chem. Soc. Rev., 2015, **44**, 5680–5742 | 5733

290 K. Heintz, K. F. Schilke, J. Snider, W. K. Lee, M. Truong, M. Coblyn, G. Jovanovic and J. McGuire, *J. Biomed. Mater. Res., Part B*, 2014, **102**, 1014–1020.

291 S. Colak and G. N. Tew, *Biomacromolecules*, 2012, **13**, 1233–1239.

292 C. Leng, K. A. Gibney, Y. W. Liu, G. N. Tew and Z. Chen, *ACS Macro Lett.*, 2013, **2**, 1011–1015.

293 L. Mi and S. Jiang, *Angew. Chem., Int. Ed.*, 2014, **53**, 1746–1754.

294 W. Yang, S. J. Liu, T. Bai, A. J. Keefe, L. Zhang, J. R. Ella-Menye, Y. T. Li and S. Y. Jiang, *Nano Today*, 2014, **9**, 10–16.

295 Q. Shao and S. Jiang, *Adv. Mater.*, 2015, **27**, 15–26.

296 P. S. Liu, Q. Chen, L. Li, S. C. Lin and J. Shen, *J. Mater. Chem. B*, 2014, **2**, 7222–7231.

297 T. Goda, K. Ishihara and Y. Miyahara, *J. Appl. Polym. Sci.*, 2015, **132**, 41766.

298 Y. Feng, D. Yang, H. Zhao, J. Guo, Q. Chen and J. Liu, *Emerging Focus on Advanced Materials, Pts 1 and 2*, 2011, vol. 306–307, pp. 1631–1634.

299 X. Cai, J. Yuan, S. Chen, P. Li, L. Li and J. Shen, *Mater. Sci. Eng., C*, 2014, **36**, 42–48.

300 W. Feng, J. L. Brash and S. Zhu, *Biomaterials*, 2006, **27**, 847–855.

301 N. Takahashi, F. Iwasa, Y. Inoue, H. Morisaki, K. Ishihara and K. Baba, *J. Prosthet. Dent.*, 2014, **112**, 194–203.

302 Y. Su, C. Li, W. Zhao, Q. Shi, H. Wang, Z. Jiang and S. Zhu, *J. Membr. Sci.*, 2008, **322**, 171–177.

303 X. Hu, G. Liu, J. Ji, D. Fan and X. Yan, *J. Bioact. Compat. Polym.*, 2010, **25**, 654–668.

304 H. Y. Zhao, Y. K. Feng, D. Z. Yang, J. T. Guo, Q. L. Chen and J. S. Liu, *Emerging Focus on Advanced Materials, Pts 1 and 2*, 2011, vol. 306–307, pp. 3–6.

305 M. Kyomoto, T. Moro, S. Yamane, M. Hashimoto, Y. Takatori and K. Ishihara, *J. Biomed. Mater. Res., Part A*, 2014, **102**, 3012–3023.

306 Z. T. Wang, H. X. Wang, J. D. Liu and Y. T. Zhang, *Desalination*, 2014, **344**, 313–320.

307 M. Kyomoto, T. Moro, S. Yamane, M. Hashimoto, Y. Takatori and K. Ishihara, *Biomaterials*, 2013, **34**, 7829–7839.

308 Y. Iwasaki, K. Shimakata, N. Morimoto and K. Kurita, *J. Polym. Sci., Part A: Polym. Chem.*, 2003, **41**, 68–75.

309 K. Kobayashi, K. Ohuchi, H. Hoshi, N. Morimoto, Y. Iwasaki and S. Takatani, *J. Artif. Organs*, 2005, **8**, 237–244.

310 Y. Asanuma, Y. Inoue, S.-I. Yusa and K. Ishihara, *Colloids Surf., B*, 2013, **108**, 239–245.

311 Y. K. Feng, D. Z. Yang, M. Behl, A. Lendlein, H. Y. Zhao and J. T. Guo, *Macromol. Symp.*, 2011, **309–310**, 6–15.

312 Y. Cao, X. Zhang, L. Tao, K. Li, Z. Xue, L. Feng and Y. Wei, *ACS Appl. Mater. Interfaces*, 2013, **5**, 4438–4442.

313 J. Lu, Y. K. Feng, B. Gao and J. T. Guo, *Macromol. Res.*, 2012, **20**, 693–702.

314 J. Lu, Y. K. Feng, B. Gao and J. T. Guo, *J. Polym. Res.*, 2012, **19**, 9959–9969.

315 W. Gao, Y. K. Feng, J. Lu, M. Khan and J. T. Guo, *Macromol. Res.*, 2012, **20**, 1063–1069.

316 W. Gao, Y. K. Feng, J. Lu and J. T. Guo, *Mater. Res. Soc. Symp. Proc.*, 2012, **1403**, 177–182.

317 E. J. Brisbois, H. Handa and M. E. Meyerhoff, *Recent Advances in Hemocompatible Polymers for Biomedical Applications*, Springer, Switzerland, 2015.

318 J. Yang, J. Lv, B. Gao, L. Zhang, D. Yang, C. Shi, J. Guo, W. Li and Y. Feng, *Front. Chem. Sci. Eng.*, 2014, **8**, 188–196.

319 D. Xiong, Y. Deng, N. Wang and Y. Yang, *Appl. Surf. Sci.*, 2014, **298**, 56–61.

320 N. Wang, A. M. Trunfio-Sfarghiu, D. Portinha, S. Descartes, E. Fleury, Y. Berthier and J. P. Rieu, *Colloids Surf., B*, 2013, **108**, 285–294.

321 P. Liu, Q. Chen, B. Yuan, M. Chen, S. Wu, S. Lin and J. Shen, *Mater. Sci. Eng., C*, 2013, **33**, 3865–3874.

322 D. Z. Yang, Y. K. Feng, M. Behl, A. Lendlein, H. Y. Zhao, M. Khan and J. T. Guo, *MRS Proceedings*, Warrendale, 2012.

323 H. Jiang, X. B. Wang, C. Y. Li, J. S. Li, F. J. Xu, C. Mao, W. T. Yang and J. Shen, *Langmuir*, 2011, **27**, 11575–11581.

324 J. Yang, J. Lv, M. Behl, A. Lendlein, D. Yang, L. Zhang, C. Shi, J. Guo and Y. Feng, *Macromol. Biosci.*, 2013, **13**, 1681–1688.

325 M. Khan, J. Yang, C. Shi, Y. Feng, W. Zhang, K. Gibney and G. N. Tew, *RSC Adv.*, 2015, **5**, 11284–11292.

326 M. Khan, J. Yang, C. Shi, Y. Feng, W. Zhang, K. Gibney and G. N. Tew, *Macromol. Mater. Eng.*, 2015, DOI: 10.1002/mame.201500038.

327 N. Singh, X. Cui, T. Boland and S. M. Husson, *Biomaterials*, 2007, **28**, 763–771.

328 I. Kondyurina, I. Shardakov, G. Nechitailo, V. Terpugov and A. Kondyurin, *Appl. Surf. Sci.*, 2014, **314**, 670–678.

329 J. Gao, J. Y. Yu and Y. Z. Ma, *Surf. Interface Anal.*, 2012, **44**, 578–583.

330 N. Mohd Hidzir, D. J. T. Hill, E. Taran, D. Martin and L. Grøndahl, *Polymer*, 2013, **54**, 6536–6546.

331 S. Lu, P. Zhang, X. Sun, F. Gong, S. Yang, L. Shen, Z. Huang and C. Wang, *ACS Appl. Mater. Interfaces*, 2013, **5**, 7360–7369.

332 U. Hedin, *J. Vasc. Access.*, 2015, **16**(suppl 9), 87–92.

333 Y. K. Gong, L. P. Liu and P. B. Messersmith, *Macromol. Biosci.*, 2012, **12**, 979–985.

334 P. Chevallier, R. Janvier, D. Mantovani and G. Laroche, *Macromol. Biosci.*, 2005, **5**, 829–839.

335 H. S. Sundaram, X. Han, A. K. Nowinski, N. D. Brault, Y. Li, J.-R. Ella-Menye, K. A. Amoaka, K. E. Cook, P. Marek, K. Senecal and S. Jiang, *Adv. Mater. Interfaces*, 2014, **1**, 201400071.

336 B. Cao, Q. Tang and G. Cheng, *J. Biomater. Sci., Polym. Ed.*, 2014, **25**, 1502–1513.

337 S. Jiang and Z. Cao, *Adv. Mater.*, 2010, **22**, 920–932.

338 A. K. Nowinski, A. D. White, A. J. Keefe and S. Jiang, *Langmuir*, 2014, **30**, 1864–1870.

339 S. Chen, Z. Cao and S. Jiang, *Biomaterials*, 2009, **30**, 5892–5896.

340 T. Liu, Z. Zeng, Y. Liu, J. Wang, M. F. Maitz, Y. Wang, S. H. Liu, J. Y. Chen and N. Huang, *ACS Appl. Mater. Interfaces*, 2014, **6**, 8729–8743.

5734 | *Chem. Soc. Rev.*, 2015, **44**, 5680–5742

This journal is © The Royal Society of Chemistry 2015

341 M. Q. Tan, Y. K. Feng, H. Y. Wang, L. Zhang, M. Khan, J. T. Guo, Q. L. Chen and J. S. Liu, *Macromol. Res.*, 2013, **21**, 541–549.

342 Q. Cheng, K. Komvopoulos and S. Li, *J. Biomed. Mater. Res., Part A*, 2014, **102**, 1408–1414.

343 W. Gao, T. Lin, T. Li, M. Yu, X. Hu and D. Duan, *Int. J. Clin. Exp. Med.*, 2013, **6**, 259–268.

344 C. D. Easton, A. J. Bullock, G. Gigliobianco, S. L. McArthur and S. MacNeil, *J. Mater. Chem. B*, 2014, **2**, 5558–5568.

345 M. F. Elahi, G. P. Guan, L. Wang and M. W. King, *J. Appl. Polym. Sci.*, 2014, **131**, 9307–9318.

346 M. Cestari, V. Muller, J. H. Rodrigues, C. V. Nakamura, A. F. Rubira and E. C. Muniz, *Biomacromolecules*, 2014, **15**, 1762–1767.

347 Q. Gao, Y. S. Chen, Y. L. Wei, X. D. Wang and Y. L. Luo, *Surf. Coat. Technol.*, 2013, **228**, S126–S130.

348 T. Sharkawi, V. Darcos and M. Vert, *J. Biomed. Mater. Res., Part A*, 2011, **98**, 80–87.

349 J. H. Jiang, L. P. Zhu, X. L. Li, Y. Y. Xu and B. K. Zhu, *J. Membr. Sci.*, 2010, **364**, 194–202.

350 A. L. Gao, F. Liu and L. X. Xue, *J. Membr. Sci.*, 2014, **452**, 390–399.

351 Z. Yang, J. Wang, R. Luo, M. F. Maitz, F. Jing, H. Sun and N. Huang, *Biomaterials*, 2010, **31**, 2072–2083.

352 J. Li, F. Lin, L. D. Li, J. Li and S. Liu, *Macromol. Chem. Phys.*, 2012, **213**, 2120–2129.

353 R. A. Hoshi, R. Van Lith, M. C. Jen, J. B. Allen, K. A. Lapidos and G. Ameer, *Biomaterials*, 2013, **34**, 30–41.

354 G. Bayramoğlu, M. Yılmaz, E. Batislam and M. Y. Arıca, *J. Appl. Polym. Sci.*, 2008, **109**, 749–757.

355 I. You, S. M. Kang, Y. Byun and H. Lee, *Bioconjugate Chem.*, 2011, **22**, 1264–1269.

356 C. J. Pan, Y. H. Hou, B. B. Zhang, Y. X. Dong and H. Y. Ding, *J. Mater. Chem. B*, 2014, **2**, 892–902.

357 S. Gore, J. Andersson, R. Biran, C. Underwood and J. Riesenfeld, *J. Biomed. Mater. Res., Part B*, 2014, **102**, 1817–1824.

358 S. Beni, J. F. Limtiaco and C. K. Larive, *Anal. Bioanal. Chem.*, 2011, **399**, 527–539.

359 L. Pol-Fachin and H. Verli, *Glycobiology*, 2014, **24**, 97–105.

360 P. H. Lin, R. L. Bush, Q. Yao, A. B. Lumsden and C. Chen, *J. Surg. Res.*, 2004, **118**, 45–52.

361 K. T. Lappegard, G. Bergseth, J. Riesenfeld, A. Pharo, P. Magotti, J. D. Lambris and T. E. Mollnes, *J. Biomed. Mater. Res., Part A*, 2008, **87**, 129–135.

362 H. L. Wei, L. L. Han, J. Ren and L. Y. Jia, *ACS Appl. Mater. Interfaces*, 2013, **5**, 12571–12578.

363 G. Li, F. Zhang, Y. Liao, P. Yang and N. Huang, *Colloids Surf., B*, 2010, **81**, 255–262.

364 W. Wang, J. Hu, C. He, W. Nie, W. Feng, K. Qiu, X. Zhou, Y. Gao and G. Wang, *J. Biomed. Mater. Res., Part A*, 2015, **103**, 1784–1797.

365 J. A. Beamish, L. C. Geyer, N. A. Haq-Siddiqi, K. Kottke-Marchant and R. E. Marchant, *Biomaterials*, 2009, **30**, 6286–6294.

366 J. S. Park, K. Park, D. G. Woo, H. N. Yang, H. M. Chung and K. H. Park, *Small*, 2008, **4**, 1950–1955.

367 T. Liu, Y. Liu, Y. Chen, S. H. Liu, M. F. Maitz, X. Wang, K. Zhang, J. Wang, Y. Wang, J. Y. Chen and N. Huang, *Acta Biomater.*, 2014, **10**, 1940–1954.

368 M. F. Elahi, G. P. Guan, L. Wang and M. W. King, *Materials*, 2014, **7**, 2956–2977.

369 X. F. Ye, X. Hu, H. Z. Wang, J. Liu and Q. Zhao, *Acta Biomater.*, 2012, **8**, 1057–1067.

370 K. Zhou, G. Thouas, C. Bernard and J. S. Forsythe, *Nanomedicine*, 2014, **9**, 1239–1251.

371 K. Zhou, G. Z. Sun, C. C. Bernard, G. A. Thouas, D. R. Nisbet and J. S. Forsythe, *Biointerphases*, 2011, **6**, 189–199.

372 F. Y. Mahlicli and S. A. Altinkaya, *J. Mater. Sci.: Mater. Med.*, 2013, **24**, 533–546.

373 Z. She, C. Wang, J. Li, G. B. Sukhorukov and M. N. Antipina, *Biomacromolecules*, 2012, **13**, 2174–2180.

374 Y. Shu, G. M. Ou, L. Wang, J. C. Zou and Q. L. Li, *J. Nanomater.*, 2011, 8–16.

375 J. Almodovar and M. J. Kipper, *Macromol. Biosci.*, 2011, **11**, 72–76.

376 F. Z. Volpato, J. Almodovar, K. Erickson, K. C. Popat, C. Migliaresi and M. J. Kipper, *Acta Biomater.*, 2012, **8**, 1551–1559.

377 S. Takahashi, T. Sato, N. Haraguchi, B. Z. Wang and J. Anzai, *Int. J. Electrochem. Sci.*, 2012, **7**, 6762–6770.

378 R. Hashide, K. Yoshida, K. Kotaki, T. Watanabe, R. Watahiki, S. Takahashi, K. Sato and J. Anzai, *Polym. Bull.*, 2012, **69**, 229–239.

379 Y. Shu, P. Yin, B. Liang, H. Wang and L. Guo, *ACS Appl. Mater. Interfaces*, 2014, **6**, 15154–15161.

380 Y. Q. Shu, P. G. Yin, B. L. Liang, S. S. Wang, L. C. Gao, H. Wang and L. Guo, *J. Mater. Chem.*, 2012, **22**, 21667–21672.

381 Y. J. Min and P. T. Hammond, *Chem. Mater.*, 2011, **23**, 5349–5357.

382 H. G. Wang, T. Y. Yin, S. P. Ge, Q. Zhang, Q. L. Dong, D. X. Lei, D. M. Sun and G. X. Wang, *J. Biomed. Mater. Res., Part A*, 2013, **101**, 413–420.

383 L. J. De Cock, S. De Koker, B. G. De Geest, J. Grooten, C. Vervaet, J. P. Remon, G. B. Sukhorukov and M. N. Antipina, *Angew. Chem., Int. Ed.*, 2010, **49**, 6954–6973.

384 C. J. Ochs, G. K. Such, Y. Yan, M. P. van Koeverden and F. Caruso, *ACS Nano*, 2010, **4**, 1653–1663.

385 G. K. Such, A. P. Johnston and F. Caruso, *Chem. Soc. Rev.*, 2011, **40**, 19–29.

386 X.-H. Huang, M.-M. Zhang, X.-W. Dou, X. Lu, Y.-J. Qin, P. Zhang, J.-H. Shi and Z.-X. Guo, *Chin. Chem. Lett.*, 2015, DOI: 10.1016/j.cclet.2015.04.005.

387 X. Zhang, C. Jiang, M. Cheng, Y. Zhou, X. Zhu, J. Nie, Y. Zhang, Q. An and F. Shi, *Langmuir*, 2012, **28**, 7096–7100.

388 Q. Lin, J. Yan, F. Qiu, X. Song, G. Fu and J. Ji, *J. Biomed. Mater. Res., Part A*, 2011, **96**, 132–141.

389 C. Wen, L. L. Lu and X. S. Li, *Polym. Int.*, 2014, **63**, 1643–1649.

390 C. Wen, L. L. Lu and X. S. Li, *J. Appl. Polym. Sci.*, 2014, **131**, 40975.

391 C. Wen, L. L. Lu and X. S. Li, *Macromol. Mater. Eng.*, 2014, **299**, 504–513.

392 M. Inoue, M. Sasaki, A. Nakasu, M. Takayanagi and T. Taguchi, *Adv. Healthcare Mater.*, 2012, **1**, 573–581.

393 A. Chetouani, M. Elkolli, M. Bounekhel and D. Benachour, *Polym. Bull.*, 2014, **71**, 2303–2316.

394 B. Gupta, M. Tummalapalli, B. L. Deopura and M. S. Alam, *Carbohydr. Polym.*, 2014, **106**, 312–318.

395 A. Chetouani, M. Elkolli, M. Bounekhel and D. Benachour, *J. Biomater. Tissue Eng.*, 2014, **4**, 465–470.

396 U. Rottensteiner, B. Sarker, D. Heusinger, D. Dafinova, S. N. Rath, J. P. Beier, U. Kneser, R. E. Horch, R. Detsch, A. R. Boccaccini and A. Arkudas, *Materials*, 2014, **7**, 1957–1974.

397 M. Nikkhah, N. Eshak, P. Zorlutuna, N. Annabi, M. Castello, K. Kim, A. Dolatshahi-Pirouz, F. Edalat, H. Bae, Y. Yang and A. Khademhosseini, *Biomaterials*, 2012, **33**, 9009–9018.

398 M. B. Chen, S. Srigunapalan, A. R. Wheeler and C. A. Simmons, *Lab Chip*, 2013, **13**, 2591–2598.

399 R. Z. Lin, Y. C. Chen, R. Moreno-Luna, A. Khademhosseini and J. M. Melero-Martin, *Biomaterials*, 2013, **34**, 6785–6796.

400 Y. Feng, Z. Fang, H. Wang and J. Guo, *Trans. Tianjin Univ.*, 2013, **19**, 182–187.

401 Y. M. Shin, J. Y. Lim, J. S. Park, H. J. Gwon, S. I. Jeong and Y. M. Lim, *Biotechnol. Bioprocess Eng.*, 2014, **19**, 118–125.

402 C. Shi, W. Yuan, M. Khan, Q. Li, Y. Feng, F. Yao and W. Zhang, *Mater. Sci. Eng., C*, 2015, **50**, 201–209.

403 S. H. Park, L. P. Zhu, S. Tada, S. Obuse, Y. Yoshida, M. Nakamura, T. I. Son, S. Tsuneda and Y. Ito, *Polym. Int.*, 2014, **63**, 1616–1619.

404 K. Yoshizawa and T. Taguchi, *Int. J. Mol. Sci.*, 2014, **15**, 2142–2156.

405 H. Y. Wang, Y. K. Feng, Z. C. Fang, R. F. Xiao, W. J. Yuan and M. Khan, *Macromol. Res.*, 2013, **21**, 860–869.

406 V. M. Merkle, L. Zeng, M. J. Slepian and X. Wu, *Biopolymers*, 2013, **101**, 336–346.

407 O. Mahony, S. Yue, C. Turdean-Ionescu, J. V. Hanna, M. E. Smith, P. D. Lee and J. R. Jones, *J. Sol-Gel Sci. Technol.*, 2014, **69**, 288–298.

408 P. Zhao, H. Jiang, H. Pan, K. Zhu and W. Chen, *J. Biomed. Mater. Res., Part A*, 2007, **83**, 372–382.

409 S. Cho, H. Li, C. Chen, J. Jiang, H. Tao and S. Chen, *Int. Orthop.*, 2013, **37**, 507–513.

410 H. Li, C. Chen, S. Zhang, J. Jiang, H. Tao, J. Xu, J. Sun, W. Zhong and S. Chen, *Acta Biomater.*, 2012, **8**, 4007–4019.

411 B. H. Fang, Q. Y. Ling, W. F. Zhao, Y. L. Ma, P. L. Bai, Q. Wei, H. F. Li and C. S. Zhao, *J. Membr. Sci.*, 2009, **329**, 46–55.

412 L. P. Zhu, J. H. Jiang, B. K. Zhu and Y. Y. Xu, *Colloids Surf., B*, 2011, **86**, 111–118.

413 C. M. Li, J. Jin, J. C. Liu, X. D. Xu and J. H. Yin, *RSC Adv.*, 2014, **4**, 24842–24851.

414 C. Zhang, J. Jin, J. Zhao, W. Jiang and J. Yin, *Colloids Surf., B*, 2013, **102**, 45–52.

415 C. J. Pan, Y. H. Hou, B. B. Zhang and L. C. Zhang, *Bio-Med. Mater. Eng.*, 2014, **24**, 781–787.

416 J. Ji, Q. Tan, D. Z. Fan, F. Y. Sun, M. A. Barbosa and J. Shen, *Colloids Surf., B*, 2004, **34**, 185–190.

417 Z. Liu, C. Dong, X. Wang, H. Wang, W. Li, J. Tan and J. Chang, *ACS Appl. Mater. Interfaces*, 2014, **6**, 2393–2400.

418 S. Li and J. J. Henry, *Annu. Rev. Biomed. Eng.*, 2011, **13**, 451–475.

419 H. Chen, Y. Teramura and H. Iwata, *J. Controlled Release*, 2011, **150**, 229–234.

420 E. Arenas, F. F. Castillon and M. H. Farias, *Des. Monomers Polym.*, 2012, **15**, 369–378.

421 S. Absar, Y. M. Kwon and F. Ahsan, *J. Controlled Release*, 2014, **177**, 42–50.

422 Z. Tang, X. Liu, Y. Luan, W. Liu, Z. Wu, D. Li and H. Chen, *Polym. Chem.*, 2013, **4**, 5597–5602.

423 E. G. Fernandes, A. A. de Queiroz, G. A. Abraham and J. San Roman, *J. Mater. Sci.: Mater. Med.*, 2006, **17**, 105–111.

424 W. Liu, Z. Q. Wu, Y. Y. Wang, Z. C. Tang, J. Du, L. Yuan, D. Li and H. Chen, *J. Mater. Chem. B*, 2014, **2**, 4272–4279.

425 K. Knop, R. Hoogenboom, D. Fischer and U. S. Schubert, *Angew. Chem., Int. Ed.*, 2010, **49**, 6288–6308.

426 S. Chen, L. Li, C. Zhao and J. Zheng, *Polymer*, 2010, **51**, 5283–5293.

427 J. Yu, A. Wang, Z. Tang, J. Henry, B. Li-Ping Lee, Y. Zhu, F. Yuan, F. Huang and S. Li, *Biomaterials*, 2012, **33**, 8062–8074.

428 U. Hersel, C. Dahmen and H. Kessler, *Biomaterials*, 2003, **24**, 4385–4415.

429 R. C. Liddington and M. H. Ginsberg, *J. Cell Biol.*, 2002, **158**, 833–839.

430 M. D. Pierschbacher and E. Ruoslahti, *Nature*, 1984, **309**, 30–33.

431 H. B. Lin, W. Sun, D. F. Mosher, C. Garcia-Echeverria, K. Schaufelberger, P. I. Lelkes and S. L. Cooper, *J. Biomed. Mater. Res.*, 1994, **28**, 329–342.

432 S. Jo, P. S. Engel and A. G. Mikos, *Polymer*, 2000, **41**, 7595–7604.

433 P. Banerjee, D. J. Irvine, A. M. Mayes and L. G. Griffith, *J. Biomed. Mater. Res.*, 2000, **50**, 331–339.

434 J. T. Li, J. Carlsson, J. N. Lin and K. D. Caldwell, *Bioconjugate Chem.*, 1996, **7**, 592–599.

435 Y. Y. Wang, L. X. Lu, J. C. Shi, H. F. Wang, Z. D. Xiao and N. P. Huang, *Biomacromolecules*, 2011, **12**, 551–559.

436 F. Shamsi, H. Coster and K. A. Jolliffe, *Surf. Sci.*, 2011, **605**, 1763–1770.

437 M. Mizutani, S. C. Arnold and T. Matsuda, *Biomacromolecules*, 2002, **3**, 668–675.

438 Z. Wang, H. Wang, W. Zheng, J. Zhang, Q. Zhao, S. Wang, Z. Yang and D. Kong, *Chem. Commun.*, 2011, **47**, 8901–8903.

439 W. T. Zheng, D. Guan, Y. X. Teng, Z. H. Wang, S. A. Zhang, L. Y. Wang, D. L. Kong and J. Zhang, *Chin. Sci. Bull.*, 2014, **59**, 2776–2784.

440 C. C. Larsen, F. Kligman, K. Kottke-Marchant and R. E. Marchant, *Biomaterials*, 2006, **27**, 4846–4855.

441 S. Wang, A. S. Gupta, S. Sagnella, P. M. Barendt, K. Kottke-Marchant and R. E. Marchant, *J. Biomater. Sci., Polym. Ed.*, 2009, **20**, 619–635.

442 D. A. Wang, J. Ji, Y. H. Sun, J. C. Shen, L. X. Feng and J. H. Elisseeff, *Biomacromolecules*, 2002, **3**, 1286–1295.

443 R. A. Quirk, W. C. Chan, M. C. Davies, S. J. B. Tendler and K. M. Shakesheff, *Biomaterials*, 2001, **22**, 865–872.

444 Y. Sun, Y. Deng, Z. Ye, S. Liang, Z. Tang and S. Wei, *Colloids Surf., B*, 2013, **111**, 107–116.

445 J. S. Lee, K. Lee, S. H. Moon, H. M. Chung, J. H. Lee, S. H. Um, D. I. Kim and S. W. Cho, *Macromol. Biosci.*, 2014, **14**, 1181–1189.

446 K. Yang, J. S. Lee, J. Kim, Y. B. Lee, H. Shin, S. H. Um, J. B. Kim, K. I. Park, H. Lee and S. W. Cho, *Biomaterials*, 2012, **33**, 6952–6964.

447 J. Park, T. F. Brust, H. J. Lee, S. C. Lee, V. J. Watts and Y. Yeo, *ACS Nano*, 2014, **8**, 3347–3356.

448 E. Ko, K. Yang, J. Shin and S. W. Cho, *Biomacromolecules*, 2013, **14**, 3202–3213.

449 Y. M. Shin, Y. B. Lee and H. Shin, *Colloids Surf., B*, 2011, **87**, 79–87.

450 Y. M. Shin, I. Jun, Y. M. Lim, T. Rhim and H. Shin, *Macromol. Mater. Eng.*, 2013, **298**, 555–564.

451 C. Deng, X. S. Chen, H. J. Yu, J. Sun, T. C. Lu and X. B. Jing, *Polymer*, 2007, **48**, 139–149.

452 H. Yu, X. Guo, X. Qi, P. Liu, X. Shen and Y. Duan, *J. Mater. Sci.: Mater. Med.*, 2008, **19**, 1275–1281.

453 B. R. Coad, M. Jasieniak, S. S. Griesser and H. J. Griesser, *Surf. Coat. Technol.*, 2013, **233**, 169–177.

454 Y. M. Shin, S. Y. Jo, J. S. Park, H. J. Gwon, S. I. Jeong and Y. M. Lim, *Macromol. Biosci.*, 2014, **14**, 1190–1198.

455 F. He, B. W. Luo, S. J. Yuan, B. Liang, C. Choong and S. O. Pehkonen, *RSC Adv.*, 2014, **4**, 105–117.

456 W. F. Tong, X. L. Liu, F. Pan, Z. Q. Wu and W. W. Jiang, *Chin. J. Polym. Sci.*, 2013, **31**, 495–502.

457 W. S. Choi, J. W. Bae, H. R. Lim, Y. K. Joung, J. C. Park, I. K. Kwon and K. D. Park, *Biomed. Mater.*, 2008, **3**, 044104.

458 F. Causa, E. Battista, R. Della Moglie, D. Guarnieri, M. Iannone and P. A. Netti, *Langmuir*, 2010, **26**, 9875–9884.

459 X. Chen, P. Sevilla and C. Aparicio, *Colloids Surf., B*, 2013, **107**, 189–197.

460 P. Koegler, P. Pasic, J. Gardiner, V. Glattauer, P. Kingshott and H. Thissen, *Biomacromolecules*, 2014, **15**, 2265–2273.

461 J. Auernheimer, C. Dahmen, U. Hersel, A. Bausch and H. Kessler, *J. Am. Chem. Soc.*, 2005, **127**, 16107–16110.

462 M. S. Hahn, L. J. Taite, J. J. Moon, M. C. Rowland, K. A. Ruffino and J. L. West, *Biomaterials*, 2006, **27**, 2519–2524.

463 O. I. Bol'shakov and E. O. Akala, *J. Appl. Polym. Sci.*, 2014, **131**, 40385.

464 J. H. Oh, J. S. Lee, K. M. Park, H. T. Moon and K. D. Park, *Macromol. Res.*, 2012, **20**, 1150–1155.

465 H. Lee, J. Rho and P. B. Messersmith, *Adv. Mater.*, 2009, **21**, 431–434.

466 K. M. Park and K. D. Park, *J. Mater. Chem.*, 2011, **21**, 15906–15908.

467 A. Wieckowska, A. B. Braunschweig and I. Willner, *Chem. Commun.*, 2007, 3918–3920.

468 E. Lieb, M. Hacker, J. Tessmar, L. A. Kunz-Schughart, J. Fiedler, C. Dahmen, U. Hersel, H. Kessler, M. B. Schulz and A. Gopferich, *Biomaterials*, 2005, **26**, 2333–2341.

469 W. Kuhlman, I. Taniguchi, L. G. Griffith and A. M. Mayes, *Biomacromolecules*, 2007, **8**, 3206–3213.

470 X. Wang, C. Yan, K. Ye, Y. He, Z. Li and J. Ding, *Biomaterials*, 2013, **34**, 2865–2874.

471 S. V. Graeter, J. Huang, N. Perschmann, M. Lopez-Garcia, H. Kessler, J. Ding and J. P. Spatz, *Nano Lett.*, 2007, **7**, 1413–1418.

472 J. Huang, S. V. Grater, F. Corbellini, S. Rinck, E. Bock, R. Kemkemer, H. Kessler, J. Ding and J. P. Spatz, *Nano Lett.*, 2009, **9**, 1111–1116.

473 M. Arnold, V. C. Hirschfeld-Warneken, T. Lohmuller, P. Heil, J. Blummel, E. A. Cavalcanti-Adam, M. Lopez-Garcia, P. Walther, H. Kessler, B. Geiger and J. P. Spatz, *Nano Lett.*, 2008, **8**, 2063–2069.

474 C. Tao, J. Huang, Y. Lu, H. Zou, X. He, Y. Chen and Y. Zhong, *Colloids Surf., B*, 2014, **122**, 439–446.

475 S. L. Bellis, *Biomaterials*, 2011, **32**, 4205–4210.

476 J. A. Hubbell, S. P. Massia, N. P. Desai and P. D. Drumheller, *Nat. Biotechnol.*, 1991, **9**, 568–572.

477 C. Tang, F. Kligman, C. C. Larsen, K. Kottke-Marchant and R. E. Marchant, *J. Biomed. Mater. Res., Part A*, 2009, **88**, 348–358.

478 J. P. Xiong, T. Stehle, R. Zhang, A. Joachimiak, M. Frech, S. L. Goodman and M. A. Arnaout, *Science*, 2002, **296**, 151–155.

479 J. D. Humphries, J. A. Askari, X. P. Zhang, Y. Takada, M. J. Humphries and A. P. Mould, *J. Biol. Chem.*, 2000, **275**, 20337–20345.

480 Y. Wei, Y. Ji, L. L. Xiao, Q. K. Lin, J. P. Xu, K. F. Ren and J. Ji, *Biomaterials*, 2013, **34**, 2588–2599.

481 K. Kanie, Y. Narita, Y. Zhao, F. Kuwabara, M. Satake, S. Honda, H. Kaneko, T. Yoshioka, M. Okochi, H. Honda and R. Kato, *Biotechnol. Bioeng.*, 2012, **109**, 1808–1816.

482 R. Kato, C. Kaga, K. Kanie, M. Kunimatsu, M. Okochi and H. Honda, *Mini-Rev. Org. Chem.*, 2011, **8**, 171–177.

483 F. Kuwabara, Y. Narita, A. Yamawaki-Ogata, K. Kanie, R. Kato, M. Satake, H. Kaneko, H. Oshima, A. Usui and Y. Ueda, *Ann. Thorac. Surg.*, 2012, **93**, 156–163.

484 M. Khan, J. Yang, C. Shi, J. Lv, Y. Feng and W. Zhang, *Acta Biomater.*, 2015, **20**, 69–81.

485 B. D. Plouffe, M. Radisic and S. K. Murthy, *Lab Chip*, 2008, **8**, 462–472.

486 W. J. Seeto, Y. Tian and E. A. Lipke, *Acta Biomater.*, 2013, **9**, 8279–8289.

487 Y. Wei, Y. Ji, L. L. Xiao and J. A. Jian, *Acta Polym. Sin.*, 2010, 1474–1478.

488 Q. K. Lin, Y. Hou, K. F. Ren and J. Ji, *Thin Solid Films*, 2012, **520**, 4971–4978.

489 W. Wang, L. Guo, Y. Yu, Z. Chen, R. Zhou and Z. Yuan, *J. Biomed. Mater. Res., Part A*, 2015, **103**, 1703–1712.

490 Z. J. Li, K. F. Ren, J. L. Wang and J. Ji, *Acta Polym. Sin.*, 2014, 173–178.

491 Y. Fu, P. Li, Q. Xie, X. Xu, L. Lei, C. Chen, C. Zou, W. Deng and S. Yao, *Adv. Funct. Mater.*, 2009, **19**, 1784–1791.

492 T. Ren, S. Yu, Z. Mao, S. E. Moya, L. Han and C. Gao, *Biomacromolecules*, 2014, **15**, 2256–2264.

493 C. Hundt, J. M. Peyrin, S. Haik, S. Gauczynski, C. Leucht, R. Rieger, M. L. Riley, J. P. Deslys, D. Dormont, C. I. Lasmezas and S. Weiss, *EMBO J.*, 2001, **20**, 5876–5886.

494 S. P. Massia and J. A. Hubbell, *J. Biomed. Mater. Res.*, 1991, **25**, 223–242.

495 H. W. Jun and J. West, *J. Biomater. Sci., Polym. Ed.*, 2004, **15**, 73–94.

496 L. B. Koh, M. M. Islam, D. Mitra, C. W. Noel, K. Merrett, S. Odorcic, P. Fagerholm, W. B. Jackson, B. Liedberg, J. Phopase and M. Griffith, *J. Funct. Biomater.*, 2013, **4**, 162–177.

497 P. Y. Wang, T. H. Wu, W. B. Tsai, W. H. Kuo and M. J. Wang, *Colloids Surf., B*, 2013, **110**, 88–95.

498 J. Yu, A. R. Lee, W. H. Lin, C. W. Lin, Y. K. Wu and W. B. Tsai, *Tissue Eng., Part A*, 2014, **20**, 1896–1907.

499 J. M. Garcia-Garcia, I. Quijada-Garrido, L. Lopez, R. Paris, M. T. Nunez-Lopez, E. D. Zarzuelo and L. Garrido, *Mater. Sci. Eng., C*, 2013, **33**, 362–369.

500 Y. C. Li, Y. T. Liao, H. H. Chang and T. H. Young, *Colloids Surf., B*, 2013, **102**, 53–62.

501 C. Yao, M. Hedrick, G. Pareek, J. Renzulli, G. Haleblian and T. J. Webster, *Int. J. Nanomed.*, 2013, **8**, 3285–3296.

502 T. Dvir, M. R. Banghart, B. P. Timko, R. Langer and D. S. Kohane, *Nano Lett.*, 2010, **10**, 250–254.

503 Y. Yokosaki, N. Matsuura, T. Sasaki, I. Murakami, H. Schneider, S. Higashiyama, Y. Saitoh, M. Yamakido, Y. Taooka and D. Sheppard, *J. Biol. Chem.*, 1999, **274**, 36328–36334.

504 K. Ito, S. Kon, Y. Nakayama, D. Kurotaki, Y. Saito, M. Kanayama, C. Kimura, H. Diao, J. Morimoto, Y. Matsui and T. Uede, *Matrix Biol.*, 2009, **28**, 11–19.

505 H. Egusa, Y. Kaneda, Y. Akashi, Y. Hamada, T. Matsumoto, M. Saeki, D. K. Thakor, Y. Tabata, N. Matsuura and H. Yatani, *Biomaterials*, 2009, **30**, 4676–4686.

506 Y. Hamada, K. Nokihara, M. Okazaki, W. Fujitani, T. Matsumoto, M. Matsuo, Y. Umakoshi, J. Takahashi and N. Matsuura, *Biochem. Biophys. Res. Commun.*, 2003, **310**, 153–157.

507 Y. Lei, M. Remy, C. Labrugere and M. C. Durrieu, *J. Mater. Sci.: Mater. Med.*, 2012, **23**, 2761–2772.

508 S. P. Massia, S. S. Rao and J. A. Hubbell, *J. Biol. Chem.*, 1993, **268**, 8053–8059.

509 E. Hoch, G. E. Tovar and K. Borchers, *Eur. J. Cardiothorac. Surg.*, 2014, **46**, 767–778.

510 Y. B. Lee, Y. M. Shin, J. H. Lee, I. Jun, J. K. Kang, J. C. Park and H. Shin, *Biomaterials*, 2012, **33**, 8343–8352.

511 S. O'Rorke, M. Keeney and A. Pandit, *Prog. Polym. Sci.*, 2010, **35**, 441–458.

512 S. M. Dizaj, S. Jafari and A. Y. Khosroushahi, *Nanoscale Res. Lett.*, 2014, **9**, 252–261.

513 Y. N. Yue and C. Wu, *Biomater. Sci.*, 2013, **1**, 152–170.

514 U. Lächelt and E. Wagner, *Front. Chem. Sci. Eng.*, 2011, **5**, 275–286.

515 Y. He, Y. Nie, G. Cheng, L. Xie, Y. Shen and Z. Gu, *Adv. Mater.*, 2014, **26**, 1534–1540.

516 Q. F. Zhang, Q. Y. Yu, Y. Geng, J. Zhang, W. X. Wu, G. Wang, Z. Gu and X. Q. Yu, *ACS Appl. Mater. Interfaces*, 2014, **6**, 15733–15742.

517 W. J. He, H. Hosseinkhani, R. Mohammadinejad, Z. Roveimiab, D. Y. Hueng, K. L. Ou and A. J. Domb, *Polym. Adv. Technol.*, 2014, **25**, 1216–1225.

518 P. Kos, U. Lachelt, D. He, Y. Nie, Z. Gu and E. Wagner, *J. Pharm. Sci.*, 2015, **104**, 464–475.

519 Y. Zhao, B. Yu, H. Hu, Y. Hu, N. N. Zhao and F. J. Xu, *ACS Appl. Mater. Interfaces*, 2014, **6**, 17911–17919.

520 P. Yan, N. Zhao, H. Hu, X. Lin, F. Liu and F. J. Xu, *Acta Biomater.*, 2014, **10**, 3786–3794.

521 J. J. Nie, X. B. Dou, H. Hu, B. Yu, D. F. Chen, R. X. Wang and F. J. Xu, *ACS Appl. Mater. Interfaces*, 2015, **7**, 553–562.

522 H. Q. Song, X. B. Dou, R. Q. Li, B. R. Yu, N. N. Zhao and F. J. Xu, *Acta Biomater.*, 2015, **12**, 156–165.

523 Y. Zhu, X. F. Zheng, B. R. Yu, W. T. Yang, N. N. Zhao and F. J. Xu, *Macromol. Biosci.*, 2014, **14**, 1135–1148.

524 X. Lin, N. Zhao, P. Yan, H. Hu and F. J. Xu, *Acta Biomater.*, 2015, **11**, 381–392.

525 X. Cai, Y. Li, D. Yue, Q. Yi, S. Li, D. Shi and Z. Gu, *J. Mater. Chem. B*, 2015, **3**, 1507–1517.

526 J. Luo, C. Li, J. Chen, G. Wang, R. Gao and Z. Gu, *Int. J. Nanomed.*, 2015, **10**, 1667–1678.

527 H. Wang, Y. Feng, J. Yang, J. Guo and W. Zhang, *J. Mater. Chem. B*, 2015, **3**, 3379–3391.

528 M. Matsumoto, R. Kishikawa, T. Kurosaki, H. Nakagawa, N. Ichikawa, T. Hamamoto, H. To, T. Kitahara and H. Sasaki, *Int. J. Pharm.*, 2008, **363**, 58–65.

529 P. Resnier, P. LeQuinio, N. Lautram, E. Andre, C. Gaillard, G. Bastiat, J. P. Benoit and C. Passirani, *Biotechnol. J.*, 2014, **9**, 1389–1401.

530 J. P. Behr, B. Demeneix, J. P. Loeffler and J. Perez-Mutul, *Proc. Natl. Acad. Sci. U. S. A.*, 1989, **86**, 6982–6986.

531 H. Hashida, M. Miyamoto, Y. Cho, Y. Hida, K. Kato, T. Kurokawa, S. Okushiba, S. Kondo, H. Dosaka-Akita and H. Katoh, *Br. J. Cancer*, 2004, **90**, 1252–1258.

532 F. C. Tanner, D. P. Carr, G. J. Nabel and E. G. Nabel, *Cardiovasc. Res.*, 1997, **35**, 522–528.

533 H. Dannowski, J. Bednarz, R. Reszka, K. Engelmann and U. Pleyer, *Exp. Eye Res.*, 2005, **80**, 93–101.

534 U. Pleyer, D. Groth, B. Hinz, O. Keil, E. Bertelmann, P. Rieck and R. Reszka, *Exp. Eye Res.*, 2001, **73**, 1–7.

535 C. Boulanger, C. Di Giorgio, J. Gaucheron and P. Vierling, *Bioconjugate Chem.*, 2004, **15**, 901–908.

536 A. Fraix, T. Montier, N. Carmoy, D. Loizeau, L. Burel-Deschamps, T. Le Gall, P. Giamarchi, H. Couthon-Gourves, J. P. Haelters, P. Lehn and P. A. Jaffres, *Org. Biomol. Chem.*, 2011, **9**, 2422–2432.

537 Y. Negishi, Y. Tsunoda, N. Hamano, D. Omata, Y. Endo-Takahashi, R. Suzuki, K. Maruyama, M. Nomizu and Y. Aramaki, *Biopolymers*, 2013, **100**, 402–407.

538 T. Lajunen, K. Hisazumi, T. Kanazawa, H. Okada, Y. Seta, M. Yliperttula, A. Urtti and Y. Takashima, *Eur. J. Pharm. Sci.*, 2014, **62**, 23–32.

539 E. Delyagina, A. Schade, D. Scharfenberg, A. Skorska, C. Lux, W. Li and G. Steinhoff, *Nanomedicine*, 2014, **9**, 999–1017.

540 W. Li, C. Nesselmann, Z. Zhou, L.-L. Ong, F. Öri, G. Tang, A. Kaminski, K. Lützow, A. Lendlein, A. Liebold, C. Stamm,

5738 | *Chem. Soc. Rev.*, 2015, **44**, 5680–5742

This journal is © The Royal Society of Chemistry 2015

J. Wang, G. Steinhoff and N. Ma, *J. Magn. Magn. Mater.*, 2007, **311**, 336–341.

541 A. L. G. Jones, M. Neumann and J. Zomlefer, *J. Org. Chem.*, 1944, **9**, 125–147.

542 B. Brissault, A. Kichler, C. Guis, C. Leborgne, O. Danos and H. Cheradame, *Bioconjugate Chem.*, 2003, **14**, 581–587.

543 S. M. Moghimi, P. Symonds, J. C. Murray, A. C. Hunter, G. Debska and A. Szewczyk, *Mol. Ther.*, 2005, **11**, 990–995.

544 J. Yang, H. Y. Wang, W. J. Yi, Y. H. Gong, X. Zhou, R. X. Zhuo and X. Z. Zhang, *Adv. Healthcare Mater.*, 2013, **2**, 481–489.

545 C. Fortier, Y. Durocher and G. De Crescenzo, *Nanomedicine*, 2014, **9**, 135–151.

546 X. Zhang, S. R. Pan, M. Feng, Z. J. Li, W. Zhang and X. Luo, *Prog. Biochem. Biophys.*, 2007, **34**, 1065–1071.

547 A. Calarco, M. Bosetti, S. Margarucci, L. Fusaro, E. Nicoli, O. Petillo, M. Cannas, U. Galderisi and G. Peluso, *Toxicol. Lett.*, 2013, **218**, 10–17.

548 N. Singh, B. Manshian, G. J. Jenkins, S. M. Griffiths, P. M. Williams, T. G. Maffeis, C. J. Wright and S. H. Doak, *Biomaterials*, 2009, **30**, 3891–3914.

549 K. Luo, B. He, Y. Wu, Y. Shen and Z. Gu, *Biotechnol. Adv.*, 2014, **32**, 818–830.

550 D. Y. Furgeson, W. S. Chan, J. W. Yockman and S. W. Kim, *Bioconjugate Chem.*, 2003, **14**, 840–847.

551 V. Zaric, D. Weltin, P. Erbacher, J. S. Remy, J. P. Behr and D. Stephan, *J. Gene Med.*, 2004, **6**, 176–184.

552 D. Y. Furgeson, J. W. Yockman, M. M. Janat and S. W. Kim, *Mol. Ther.*, 2004, **9**, 837–845.

553 Y. S. Nam, H. S. Kang, J. Y. Park, T. G. Park, S. H. Han and I. S. Chang, *Biomaterials*, 2003, **24**, 2053–2059.

554 M. Turk, S. Dincer, I. G. Yulug and E. Piskin, *J. Controlled Release*, 2004, **96**, 325–340.

555 E. Delyagina, W. Li, A. Schade, A. L. Kuhlo, N. Ma and G. Steinhoff, *AIP Conf. Proc.*, 2010, **1311**, 479–484.

556 M. L. Forrest, J. T. Koerber and D. W. Pack, *Bioconjugate Chem.*, 2003, **14**, 934–940.

557 M. A. Gosselin, W. J. Guo and R. J. Lee, *Bioconjugate Chem.*, 2001, **12**, 989–994.

558 X. Shuai, T. Merdan, F. Unger and T. Kissel, *Bioconjugate Chem.*, 2005, **16**, 322–329.

559 Q. Li, C. Shi, W. Zhang, M. Behl, A. Lendlein and Y. Feng, *Adv. Healthcare Mater.*, 2015, DOI: 10.1002/adhm.201400817.

560 J. Lv, X. F. Hao, J. Yang, Y. K. Feng, M. Behl and A. Lendlein, *Macromol. Chem. Phys.*, 2014, **215**, 2463–2472.

561 S. Sadekar and H. Ghandehari, *Adv. Drug Delivery Rev.*, 2012, **64**, 571–588.

562 J. Guo, H. Hong, G. Chen, S. Shi, Q. Zheng, Y. Zhang, C. P. Theuer, T. E. Barnhart, W. Cai and S. Gong, *Biomaterials*, 2013, **34**, 8323–8332.

563 A. Tschiche, S. Malhotra and R. Haag, *Nanomedicine*, 2014, **9**, 667–693.

564 D. A. Tomalia, A. M. Naylor and W. A. Goddard, *Angew. Chem., Int. Ed. Engl.*, 1990, **29**, 138–175.

565 K. Wada, H. Arima, T. Tsutsumi, F. Hirayama and K. Uekama, *Biol. Pharm. Bull.*, 2005, **28**, 500–505.

566 Y. L. Zhao, Y. L. Chang, S. Liu, Z. Y. Wu, W. Jiang, S. W. Wang, X. X. Fang, Y. P. Li and J. Y. Wang, *J. Lumin.*, 2010, **130**, 576–581.

567 T. Hudde, S. A. Rayner, R. M. Comer, M. Weber, J. D. Isaacs, H. Waldmann, D. F. Larkin and A. J. George, *Gene Ther.*, 1999, **6**, 939–943.

568 J. Haensler and F. C. J. Szoka, *Bioconjugate Chem.*, 1993, **4**, 372–379.

569 H. Y. Nam, K. Nam, H. J. Hahn, B. H. Kim, H. J. Lim, H. J. Kim, J. S. Choi and J. S. Park, *Biomaterials*, 2009, **30**, 665–673.

570 F. Wang, Y. Wang, H. Wang, N. Shao, Y. Chen and Y. Cheng, *Biomaterials*, 2014, **35**, 9187–9198.

571 L. Pu, Y. Geng, S. Liu, J. Chen, K. Luo, G. Wang and Z. Gu, *ACS Appl. Mater. Interfaces*, 2014, **6**, 15344–15351.

572 K. Luo, C. Li, L. Li, W. She, G. Wang and Z. Gu, *Biomaterials*, 2012, **33**, 4917–4927.

573 X. Xu, Y. Jian, Y. Li, X. Zhang, Z. Tu and Z. Gu, *ACS Nano*, 2014, **8**, 9255–9264.

574 N. Wimmer, R. J. Marano, P. S. Kearns, E. P. Rakoczy and I. Toth, *Bioorg. Med. Chem. Lett.*, 2002, **12**, 2635–2637.

575 Q. Hu, J. Wang, J. Shen, M. Liu, X. Jin, G. Tang and P. K. Chu, *Biomaterials*, 2012, **33**, 1135–1145.

576 Y. B. Lim, C. H. Kim, K. Kim, S. W. Kim and J. S. Park, *J. Am. Chem. Soc.*, 2000, **122**, 6524–6525.

577 P. Nydert, A. Dragomir and L. Hjelte, *Biotechnol. Appl. Biochem.*, 2008, **51**, 153–157.

578 J. Chang, X. Xu, H. Li, Y. Jian, G. Wang, B. He and Z. Gu, *Adv. Funct. Mater.*, 2013, **23**, 2691–2699.

579 S. H. Pun, N. C. Bellocq, A. Liu, G. Jensen, T. Machemer, E. Quijano, T. Schluep, S. Wen, H. Engler, J. Heidel and M. E. Davis, *Bioconjugate Chem.*, 2004, **15**, 831–840.

580 C. Yang, H. Li, S. H. Goh and J. Li, *Biomaterials*, 2007, **28**, 3245–3254.

581 X. Zhao, Z. Li, H. Pan, W. Liu, M. Lv, F. Leung and W. W. Lu, *Acta Biomater.*, 2013, **9**, 6694–6703.

582 L. H. Peng, W. Wei, X. T. Qi, Y. H. Shan, F. J. Zhang, X. Chen, Q. Y. Zhu, L. Yu, W. Q. Liang and J. Q. Gao, *Mol. Pharmaceutics*, 2013, **10**, 3090–3102.

583 T. Azzam, A. Raskin, A. Makovitzki, H. Brem, P. Vierling, M. Lineal and A. J. Domb, *Macromolecules*, 2002, **35**, 9947–9953.

584 H. Eliyahu, A. Makovitzki, T. Azzam, A. Zlotkin, A. Joseph, D. Gazit, Y. Barenholz and A. J. Domb, *Gene Ther.*, 2005, **12**, 494–503.

585 P. Calvo, B. Gouritin, H. Chacun, D. Desmaele, J. D'Angelo, J. P. Noel, D. Georgin, E. Fattal, J. P. Andreux and P. Couvreur, *Pharm. Res.*, 2001, **18**, 1157–1166.

586 M. Zheng, Z. Zhong, L. Zhou, F. Meng, R. Peng and Z. Zhong, *Biomacromolecules*, 2012, **13**, 881–888.

587 Y. T. Ko, R. Bhattacharya and U. Bickel, *J. Controlled Release*, 2009, **133**, 230–237.

588 H. Tian, Z. Guo, L. Lin, Z. Jiao, J. Chen, S. Gao, X. Zhu and X. Chen, *J. Controlled Release*, 2014, **174**, 117–125.

589 J. M. Benns, J. S. Choi, R. I. Mahato, J. S. Park and S. W. Kim, *Bioconjugate Chem.*, 2000, **11**, 637–645.

This journal is © The Royal Society of Chemistry 2015

Chem. Soc. Rev., 2015, **44**, 5680–5742 | 5739

590 P. Midoux and M. Monsigny, *Bioconjugate Chem.*, 1999, **10**, 406–411.

591 J. Y. Cherng, P. van de Wetering, H. Talsma, D. J. Crommelin and W. E. Hennink, *Pharm. Res.*, 1996, **13**, 1038–1042.

592 A. Mathew, W. X. Wang and A. Pandit, *Pharm. Nanotechnol.*, 2014, **2**, 35–41.

593 H. L. Cao, Y. X. Dong, A. Aied, T. Y. Zhao, X. Chen, W. X. Wang and A. Pandit, *Chem. Commun.*, 2014, **50**, 15565–15568.

594 J. Zhang, Z. Wang, W. Lin and S. Chen, *Biomaterials*, 2014, **35**, 7909–7918.

595 K. Miyata, Y. Kakizawa, N. Nishiyama, A. Harada, Y. Yamasaki, H. Koyama and K. Kataoka, *J. Am. Chem. Soc.*, 2004, **126**, 2355–2361.

596 S. Park and K. E. Healy, *Bioconjugate Chem.*, 2003, **14**, 311–319.

597 A. Sinclair, T. Bai, L. R. Carr, J.-R. Ella-Menye, L. Zhang and S. Jiang, *Biomacromolecules*, 2013, **14**, 1587–1593.

598 L. R. Carr and S. Jiang, *Biomaterials*, 2010, **31**, 4186–4193.

599 F. Wang, Y. Wang, X. Zhang, W. Zhang, S. Guo and F. Jin, *J. Controlled Release*, 2014, **174**, 126–136.

600 D. M. Copolovici, K. Langel, E. Eriste and U. Langel, *ACS Nano*, 2014, **8**, 1972–1994.

601 W. Qu, S. Y. Qin, S. Ren, X. J. Jiang, R. X. Zhuo and X. Z. Zhang, *Bioconjugate Chem.*, 2013, **24**, 960–967.

602 H. N. He, Q. L. Liang, M. C. Shin, K. Lee, J. B. Gong, J. X. Ye, Q. Liu, J. K. Wang and V. Yang, *Front. Chem. Sci. Eng.*, 2013, **7**, 496–507.

603 H. He, J. Ye, J. Sheng, J. Wang, Y. Huang, G. Chen, J. Wang and V. C. Yang, *Front. Chem. Sci. Eng.*, 2013, **7**, 9–19.

604 S. Chen, K. Han, J. Yang, Q. Lei, R. X. Zhuo and X. Z. Zhang, *Pharm. Res.*, 2013, **30**, 1968–1978.

605 Y. T. Ko, W. C. Hartner, A. Kale and V. P. Torchilin, *Gene Ther.*, 2009, **16**, 52–59.

606 L. Yin, H. Tang, K. H. Kim, N. Zheng, Z. Song, N. P. Gabrielson, H. Lu and J. Cheng, *Angew. Chem., Int. Ed.*, 2013, **52**, 9182–9186.

607 W. J. Yi, J. Yang, C. Li, H. Y. Wang, C. W. Liu, L. Tao, S. X. Cheng, R. X. Zhuo and X. Z. Zhang, *Bioconjugate Chem.*, 2012, **23**, 125–134.

608 M. Lavu, S. Gundewar and D. J. Lefer, *J. Mol. Cell. Cardiol.*, 2011, **50**, 742–750.

609 R. Khurana and M. Simons, *Trends Cardiovasc. Med.*, 2003, **13**, 116–122.

610 A. S. Pandit, D. J. Wilson, D. S. Feldman and J. A. Thompson, *J. Biomater. Appl.*, 2000, **14**, 229–242.

611 M. K. Furue, J. Na, J. P. Jackson, T. Okamoto, M. Jones, D. Baker, R. Hata, H. D. Moore, J. D. Sato and P. W. Andrews, *Proc. Natl. Acad. Sci. U. S. A.*, 2008, **105**, 13409–13414.

612 T. Miao, K. S. Rao, J. L. Spees and R. A. Oldinski, *J. Controlled Release*, 2014, **192**, 57–66.

613 S. S. Chang, H. Yokomise, N. Matsuura, M. Gotoh and Y. Tabata, *Surg. Today*, 2014, **44**, 1536–1541.

614 O. Khanna, M. L. Moya, E. C. Opara and E. M. Brey, *J. Biomed. Mater. Res., Part A*, 2010, **95**, 632–640.

615 O. Khanna, M. L. Moya, H. P. Greisler, E. C. Opara and E. M. Brey, *Am. J. Surg.*, 2010, **200**, 655–658.

616 O. Khanna, J. J. Huang, M. L. Moya, C. W. Wu, M. H. Cheng, E. C. Opara and E. M. Brey, *Microvasc. Res.*, 2013, **90**, 23–29.

617 P. S. Gungor-Ozkerim, T. Balkan, G. T. Kose, A. S. Sarac and F. N. Kok, *J. Biomed. Mater. Res., Part A*, 2014, **102**, 1897–1908.

618 Y. Cho, J. B. Lee and J. Hong, *Chem. Eng. J.*, 2013, **221**, 32–36.

619 J. H. Park and J. Hong, *Integr. Biol.*, 2014, **6**, 1196–1200.

620 L. P. Brewster, C. Washington, E. M. Brey, A. Gassman, A. Subramanian, J. Calceterra, W. Wolf, C. L. Hall, W. H. Velander, W. H. Burgess and H. P. Greisler, *Biomaterials*, 2008, **29**, 327–336.

621 V. Z. Erzurum, J. F. Bian, V. A. Husak, J. Ellinger, L. Xue, W. H. Burgess and H. P. Greisler, *J. Vasc. Surg.*, 2003, **37**, 1075–1081.

622 E. Jeon, Y. R. Yun, H. W. Kim and J. H. Jang, *J. Biomed. Mater. Res., Part A*, 2013, **102A**, 1–7.

623 J. Safi Jr., A. F. DiPaula Jr., T. Riccioni, J. Kajstura, G. Ambrosio, L. C. Becker, P. Anversa and M. C. Capogrossi, *Microvasc. Res.*, 1999, **58**, 238–249.

624 H. K. Hammond and M. D. McKirnan, *Cardiovasc. Res.*, 2001, **49**, 561–567.

625 B. S. Lewis, M. Y. Flugelman, A. Weisz, I. Keren-Tal and W. Schaper, *Cardiovasc. Res.*, 1997, **35**, 490–497.

626 B. S. Conklin, H. Wu, P. H. Lin, A. B. Lumsden and C. Chen, *Artif. Organs*, 2004, **28**, 668–675.

627 Y. Bai, Y. Leng, G. Yin, X. Pu, Z. Huang, X. Liao, X. Chen and Y. Yao, *Cell Tissue Res.*, 2014, **356**, 109–121.

628 J. Zhang and Y. Li, *Drug Discovery Today*, 2014, **19**, 579–589.

629 C. Nesselmann, W. Li, N. Ma and G. Steinhoff, *Ther. Adv. Cardiovasc. Dis.*, 2010, **4**, 27–42.

630 W. Risau, H. Sariola, H. G. Zerwes, J. Sasse, P. Ekblom, R. Kemler and T. Doetschman, *Development*, 1988, **102**, 471–478.

631 I. Flamme and W. Risau, *Development*, 1992, **116**, 435–439.

632 F. Shalaby, J. Rossant, T. P. Yamaguchi, M. Gertsenstein, X. F. Wu, M. L. Breitman and A. C. Schuh, *Nature*, 1995, **376**, 62–66.

633 I. Baumgartner and J. M. Isner, *Annu. Rev. Physiol.*, 2001, **63**, 427–450.

634 Q. Liu, Z. Lu, W. Zhang and J. Yan, *J. Tongji Med. Univ.*, 2000, **20**, 186–189.

635 S. Banai, M. T. Jaklitsch, M. Shou, D. F. Lazarous, M. Scheinowitz, S. Biro, S. E. Epstein and E. F. Unger, *Circulation*, 1994, **89**, 2183–2189.

636 K. G. Shyu, M. T. Wang, B. W. Wang, C. C. Chang, J. G. Leu, P. L. Kuan and H. Chang, *Cardiovasc. Res.*, 2002, **54**, 576–583.

637 S. H. Kim, J. H. Jeong, S. H. Lee, S. W. Kim and T. G. Park, *J. Controlled Release*, 2008, **129**, 107–116.

638 E. R. Schwarz, M. T. Speakman, M. Patterson, S. S. Hale, J. M. Isner, L. H. Kedes and R. A. Kloner, *J. Am. Coll. Cardiol.*, 2000, **35**, 1323–1330.

639 R. C. Hendel, T. D. Henry, K. Rocha-Singh, J. M. Isner, D. J. Kereiakes, F. J. Giordano, M. Simons and R. O. Bonow, *Circulation*, 2000, **101**, 118–121.

640 T. D. Henry, B. H. Annex, G. R. McKendall, M. A. Azrin, J. J. Lopez, F. J. Giordano, P. K. Shah, J. T. Willerson, R. L. Benza, D. S. Berman, C. M. Gibson, A. Bajamonde, A. C. Rundle, J. Fine and E. R. McCluskey, *Circulation*, 2003, **107**, 1359–1365.

641 S. M. Eppler, D. L. Combs, T. D. Henry, J. J. Lopez, S. G. Ellis, J. H. Yi, B. H. Annex, E. R. McCluskey and T. F. Zioncheck, *Clin. Pharmacol. Ther.*, 2002, **72**, 20–32.

642 H. K. Awada, N. R. Johnson and Y. Wang, *Macromol. Biosci.*, 2014, **14**, 679–686.

643 P. H. Kim, H. G. Yim, Y. J. Choi, B. J. Kang, J. Kim, S. M. Kwon, B. S. Kim, N. S. Hwang and J. Y. Cho, *J. Controlled Release*, 2014, **187**, 1–13.

644 W. Mulyasasmita, L. Cai, R. E. Dewi, A. Jha, S. D. Ullmann, R. H. Luong, N. F. Huang and S. C. Heilshorn, *J. Controlled Release*, 2014, **191**, 71–81.

645 G. Fontana, A. Srivastava, D. Thomas, P. Lalor, P. Dockery and A. Pandit, *Bioconjugate Chem.*, 2014, DOI: 10.1021/bc5004247.

646 D. G. Belair, A. S. Khalil, M. J. Miller and W. L. Murphy, *Biomacromolecules*, 2014, **15**, 2038–2048.

647 H. Jiang, L. Wang and K. Zhu, *J. Controlled Release*, 2014, **193**, 296–303.

648 M. T. Poldervaart, H. Gremmels, K. van Deventer, J. O. Fledderus, F. C. Oner, M. C. Verhaar, W. J. Dhert and J. Alblas, *J. Controlled Release*, 2014, **184**, 58–66.

649 H. J. Lai, C. H. Kuan, H. C. Wu, J. C. Tsai, T. M. Chen, D. J. Hsieh and T. W. Wang, *Acta Biomater.*, 2014, **10**, 4156–4166.

650 F. X. Han, X. L. Jia, D. D. Dai, X. L. Yang, J. Zhao, Y. H. Zhao, Y. B. Fan and X. Y. Yuan, *Biomaterials*, 2013, **34**, 7302–7313.

651 B. Duan, L. Wu, X. Yuan, Z. Hu, X. Li, Y. Zhang, K. Yao and M. Wang, *J. Biomed. Mater. Res., Part A*, 2007, **83**, 868–878.

652 T. Simon-Yarza, F. R. Formiga, E. Tamayo, B. Pelacho, F. Prosper and M. J. Blanco-Prieto, *Int. J. Pharm.*, 2013, **440**, 13–18.

653 X. Chang, H. Wang, Z. H. Wu, X. J. Lian, F. Z. Cui, X. S. Weng, B. Yang, G. X. Qiu and B. Z. Zhang, *Int. J. Polym. Sci.*, 2014, **2014**, 236259.

654 M. Y. Zhang, S. L. Ding, S. J. Tang, H. Yang, H. F. Shi, X. Z. Shen and W. Q. Tan, *Tissue Eng., Part A*, 2014, **20**, 2273–2282.

655 Q. Tan, H. Tang, J. Hu, Y. Hu, X. Zhou, Y. Tao and Z. Wu, *Int. J. Nanomed.*, 2011, **6**, 929–942.

656 S. Takeshita, T. Isshiki, H. Mori, E. Tanaka, A. Tanaka, K. Umetani, K. Eto, Y. Miyazawa, M. Ochiai and T. Sato, *Cardiovasc. Res.*, 1997, **35**, 547–552.

657 X. Guo, T. Xia, H. Wang, F. Chen, R. Cheng, X. Luo and X. Li, *Pharm. Res.*, 2014, **31**, 874–886.

658 L. V. Christensen, C. W. Chang, J. W. Yockman, R. Conners, H. Jackson, Z. Zhong, J. Feijen, D. A. Bull and S. W. Kim, *J. Controlled Release*, 2007, **118**, 254–261.

659 H. J. Jung, Y. H. Jeon, K. K. Bokara, B. N. Koo, W. T. Lee, K. A. Park and J. E. Lee, *Life Sci.*, 2013, **92**, 42–50.

660 J. A. Ware, G. Dalziel, J. Y. Jin, J. D. Pellett, G. S. Smelick, D. A. West, L. Salphati, X. Ding, R. Sutton, J. Fridyland, M. J. Dresser, G. Morrisson and S. N. Holden, *Mol. Pharmaceutics*, 2013, **10**, 4074–4081.

661 Y. Y. Tian, C. J. Tang, J. N. Wang, Y. Feng, X. W. Chen, L. Wang, X. Qiao and S. G. Sun, *Neurosci. Lett.*, 2007, **421**, 239–244.

662 Y. Zhang, W. Li, L. Ou, W. Wang, E. Delyagina, C. Lux, H. Sorg, K. Riehemann, G. Steinhoff and N. Ma, *PLoS One*, 2012, **7**, e39490.

663 M. J. Kwon, S. An, S. Choi, K. Nam, H. S. Jung, C. S. Yoon, J. H. Ko, H. J. Jun, T. K. Kim, S. J. Jung, J. H. Park, Y. Lee and J. S. Park, *J. Gene Med.*, 2012, **14**, 272–278.

664 Z. Huang, W. Teng, L. Liu, L. Wang, Q. Wang and Y. Dong, *Nanotechnology*, 2013, **24**, 265104.

665 W. Teng, Z. Huang, Y. Chen, L. Wang, Q. Wang and H. Huang, *Nanotechnology*, 2014, **25**, 065702.

666 S. O. Han, R. I. Mahato and S. W. Kim, *Bioconjugate Chem.*, 2001, **12**, 337–345.

667 D. A. Wang, A. S. Narang, M. Kotb, A. O. Gaber, D. D. Miller, S. W. Kim and R. I. Mahato, *Biomacromolecules*, 2002, **3**, 1197–1207.

668 C. R. Ozawa, A. Banfi, N. L. Glazer, G. Thurston, M. L. Springer, P. E. Kraft, D. M. McDonald and H. M. Blau, *J. Clin. Invest.*, 2004, **113**, 516–527.

669 L. Ye, W. Zhang, L. P. Su, H. K. Haider, K. K. Poh, M. J. Galupo, G. Songco, R. W. Ge, H. C. Tan and E. K. Sim, *Biomaterials*, 2011, **32**, 2424–2431.

670 C. B. Zhang, H. L. Cao, Q. Li, J. Tu, X. Guo, Z. Liu and D. Zhang, *Ultrasound Med. Biol.*, 2013, **39**, 161–171.

671 D. Ren, H. Wang, J. Liu, M. Zhang and W. Zhang, *Mol. Cell. Biochem.*, 2012, **359**, 183–191.

672 S. Zhang, Y. Wu, B. He, K. Luo and Z. Gu, *Sci. China: Chem.*, 2014, **57**, 461–475.

673 Y. Luo, W. Hu, R. Xu, B. Hou, L. Zhang and W. Zhang, *Cell Biol. Int.*, 2011, **35**, 1153–1157.

674 Y. Tomiyama, E. Brojer, Z. M. Ruggeri, S. J. Shattil, J. Smiltneck, J. Gorski, A. Kumar, T. Kieber-Emmons and T. J. Kunicki, *J. Biol. Chem.*, 1992, **267**, 18085–18092.

675 P. Joshi, C. Y. Chung, I. Aukhil and H. P. Erickson, *J. Cell Sci.*, 1993, **106**, 389–400.

676 B. K. Wacker, S. K. Alford, E. A. Scott, M. D. Thakur, G. D. Longmore and D. L. Elbert, *Biophys. J.*, 2008, **94**, 273–285.

677 T. W. Chung, Y. F. Lu, H. Y. Wang, W. P. Chen, S. S. Wang, Y. S. Lin and S. H. Chu, *Artif. Organs*, 2003, **27**, 155–161.

678 W. J. Kim, J. W. Yockman, M. Lee, J. H. Jeong, Y. H. Kim and S. W. Kim, *J. Controlled Release*, 2005, **106**, 224–234.

679 W. Suh, S. O. Han, L. Yu and S. W. Kim, *Mol. Ther.*, 2002, **6**, 664–672.

680 K. Anwer, G. Kao, A. Rolland, W. H. P. Driessen and S. M. Sullivan, *J. Drug Targeting*, 2004, **12**, 215–221.

681 G. Kibria, H. Hatakeyama, N. Ohga, K. Hida and H. Harashima, *J. Controlled Release*, 2011, **153**, 141–148.

682 J. Chen, C. Peng, J. Nie, J. F. Kennedy and G. Ma, *Carbohydr. Polym.*, 2014, **102**, 8–11.

683 J. L. Lowery, N. Datta and G. C. Rutledge, *Biomaterials*, 2010, **31**, 491–504.

This journal is © The Royal Society of Chemistry 2015

Chem. Soc. Rev., 2015, **44**, 5680–5742 | 5741

684 Y. K. Luu, K. Kim, B. S. Hsiao, B. Chu and M. Hadjiargyrou, *J. Controlled Release*, 2003, **89**, 341–353.

685 A. Saraf, L. S. Baggett, R. M. Raphael, F. K. Kasper and A. G. Mikos, *J. Controlled Release*, 2010, **143**, 95–103.

686 L. Yu, Y. Feng, Q. Li, X. Hao, W. Liu, W. Zhou, C. Shi, X. Ren and W. Zhang, *React. Funct. Polym.*, 2015, **91–92**, 19–27.

687 Y. Liang, Y. Lai, D. Li, B. He and Z. Gu, *Mater. Lett.*, 2013, **97**, 4–7.

688 A. Aied, U. Greiser, A. Pandit and W. Wang, *Drug Discovery Today*, 2013, **18**, 1090–1098.

689 S. Browne and A. Pandit, *J. Mater. Chem. B*, 2014, **2**, 6692–6707.